<u>Bukti Korespondensi Artikel Jurnal</u>

Nama: Asep Yoyo Wardaya
Mathematical Modelling of Engineering Problems (MMEP 16795)
Q2, SJR 2021 : 0,31
Vol. 9, No. 5, October, 2022, pp. 1161-1171
Usulan :
Pangkat/Gol : Pembina TkI/IV b
Jabatna: Lektor Kepala

No	Aktivitas Korespondensi
1.	Draf Manuscript yang disubmit
2.	Permintaan Revisi dari Editor
3.	Materi Revisi dari Reviewer
4.	Permintaan Perpanjangan Waktu Untuk Revisi
5.	Permintaan Perpanjangan Waktu Disetujui oleh Fihak Editor
6.	Penyerahan Koreksi dari Manuskript
7.	List of reviewer's corrections
8.	Revised Manuscript
9.	Accept Submission
10.	Acceptance Letter
11.	INVOICE
12.	Pembayaran Jurnal
13.	Bukti Pembayaran Jurnal
14.	Permintaan Mengisi Copyright Transfer
15.	Copyright Transfer Agreement
16.	List of corrections
17.	Permintaan Check the Final Proof
18.	Pernyataan sudah mengecek Final Proof
19.	Koreksi Final
29.	Jurnal Publish

Draft Manuscript

Mathematical Modelling of Engineering Problems
Vol., No., Month, Year, pp. **-**
Journal homepage: http://iieta.org/journals/mmep

Capacitance Calculation Model in Corona Discharge Case

Asep Yoyo Wardaya[1,*], Zaenul Muhlisin[1], Jatmiko Endro Suseno[1], Charis Munajib[1], Susilo Hadi[2], Heri Sugito[1], Jaka Windarta[3]

[1] Department of Physics, Faculty of Science and Mathematics, Diponegoro University, Semarang Indonesia
[2] M1 Physique, Faculté de sciences, Université d'Aix-Marseille, Marseille, France
[3] Department of Electrical Engineering, Faculty of Engineering, Diponegoro University, Semarang Indonesia

Corresponding Author Email: asepyoyowardayafisika@gmail.com

https://doi.org/10.18280/mmep.xxxxxx

Received:
Accepted:

Keywords:
Corona discharge, (I-V) characteristics, CEM-P, shape sharpness factor, Python GUI Programming

ABSTRACT

In this study, we use a capacitance calculation model for positive dc corona discharge in air, especially in calculating the (*I-V*) current-voltage characteristics of an electrode configuration model, often referred to as capacitively coupled plasma (CCP). The configuration model comprises active and passive electrodes, with the active electrode in the form of a pentagonal with the sharp end (in the middle) facing downwards in an upright position. The passive electrode under the active electrode has a large rectangular shape in a lying place. This configuration model is named The Chisel Eye and Midpoint-Plane (CEM-P). The analytical calculation of the (*I-V*) characteristics uses the geometric properties of the active electrode, which will produce a large corona current flow at the pointed electrode. These properties in analytical calculation manifest with the emergence of the corona flow multiplication factor at the sharp active electrode's integration boundary condition called the shape sharpness factor k. The Python GUI Programming simulation program makes graphic simulations, Standard Deviation (*SD*), t-tests, and calculating the factor *k* (fitting curve value) between numerical calculations and research data. The values of the *SD*, the t-tests, and the Percentage of tangent points meet the requirements for a high level of accuracy for the four CEM-P configuration models of the (*I-V*) characteristics simulation graph with the graph has a relatively large percentage of tangent points values (82.35 % – 94.44 %).

1. INTRODUCTION

The development of cold plasma technology had a positive impact on the industry, especially for use in electronic equipment with plasma temperatures that are not too high but produce a high enough technological leap through an equipment model called capacitively coupled plasma (CCP) [1]. The CCP model uses the concept of corona plasma discharge with an electrode configuration consisting of an active electrode in a vertical position and a passive electrode in a horizontal position (under the active electrode). The active electrode has a sharp-shaped surface towards the bottom. The passive electrode has a large surface to accommodate all the plasma flow from the active electrode. The CCP equipment is similar to the capacitance equipment with the position of the two electrodes perpendicular to each other [2]. If the CCP equipment connects to a dc voltage source, it can produce a corona plasma discharge under the appropriate voltage conditions.

The (*I-V*) current-voltage characteristic in the corona plasma discharge is an exciting research topic. This topic involves a variety of physical properties that cause Townsend's low current to appear, followed by a reasonably high current increase in corona discharge and arc discharge events [3]. Various studies explain the characteristic current-voltage phenomenon in the corona discharge, including the coaxial cylinders model [4,5], the electro-hydrodynamics model [6], and the Electric Wind model [7]. Similarly, the application of CCP equipment has helped the development of research in other fields or used for industries such as ultra-large-scale integrated circuit (ULSI) fabrication [8], surface modification of polymeric materials [9], Large-area coating [10], lens-shaped electrodes [11], AC dielectric barrier discharges [12], etc.

In 2020, [13] make another form of the (I-V) characteristic related to the geometric function of the CCP electrode model. The geometric part has also been discussed by [7] to compare the corona current function and the voltage's square function. In the research [13,14], the geometric part comes from the modified capacitance function by adding a multiplier factor k to the sharp surface of the active electrode. The value of factor *k* came from the suitability factor between the analytical formulation and the experimental results (curve fitting value). The factor k is the shape sharpness factor, which came from calculating the capacitance through the insertion of the integration limit on the part of the active electrode with a sharp surface. The ideal value of k will be higher if the shape of the active electrode is more tapered. The presence of the factor k came from the research results from [15], who proved that the pointed tip of the active electrode (with a variety of sharpness angles and different materials) would look the plasma discharge brighter and more significant.

This research discusses the calculation of the (*I-V*) characteristic of positive dc corona discharge in the air (the CCP model) using The Chisel Eye and Midpoint-Plane (CEM-P) electrodes configuration models. These electrodes model consists of a pair of electrodes positioned perpendicular to each other in the air. These electrodes couple consist of an active electrode shaped like a Pentagonal thin plate, and the mid-sharp end is directed downward in a vertical position. In contrast, a passive electrode is horizontally shaped under the active electrode.

2. MATHEMATICAL MODELS

The (*I-V*) characteristic model in the case of corona plasma discharge expressed in terms of the current function as a function of the square of *V* has two equations. The first form of this model is as follows,

$$I = CV\left(V - V_i\right), \tag{1}$$

where *I* is the corona plasma current, *V* is the applied voltage, V_i is the initial voltage, and *C* is the constant. Some of the proponents of the Eq. (1) model include [4,7,16,17,18]. According to [7], the form of the constant *C* in Eq. (1) is a function of geometry. The next model of the (*I-V*) characteristic, as proposed by [6,13,14,19], has the equation form as.

$$I = C\left(V - V_i\right)^2. \tag{2}$$

This study will use the Eq. (2) model as a reference in the calculation of the (*I-V*) characteristic model, with constant *C* being a geometric function of the capacitance as proposed by [13,14]. The electrode active of the CEM-P configuration has a pentagonal shape. The width and length of the rectangular plate are *a* and *b*, respectively, while the width and sharp angle of the triangular plate are *d* and 2θ, respectively. In comparison, the thickness of the electrode active is skinny ($\delta \cong$ 0.00015 meters). The distance between the lower end of electrode active and electrode passive is equal to *c*. The Electrode passive has a rectangular plane configuration with a big area to accommodate all the flow of electric plasma flux from the electrode active to the electrode passive. If a dc voltage difference of *V* between the two electrodes is attached, then a corona plasma discharge event can be created, producing an electric current. The electrode scheme with the CEM-P configuration is found in Figure 1.a.

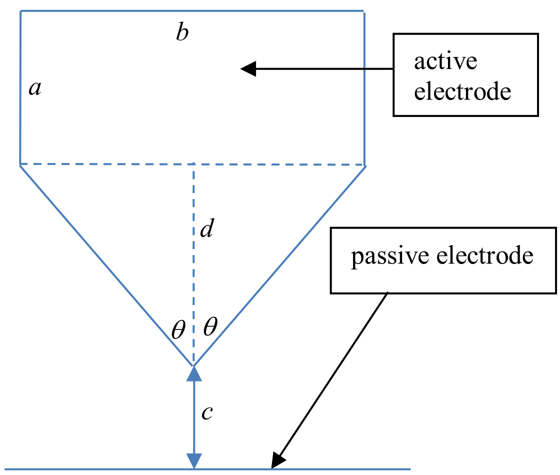

(a)

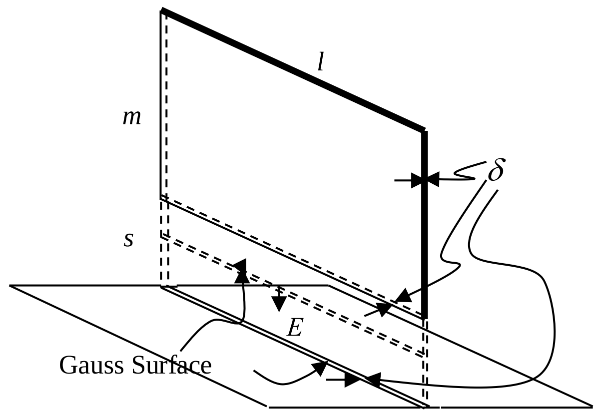

(b)

Figure 1. The electrode model Illustration for (a) the CEM-P configuration and (b) the L-P Configuration [13,14].

Before calculating the capacitance value of the electrode model with the CEM-P configuration, a simpler electrode model is needed as the basis for calculating the CEM-P configuration model, namely the electrode model with the Line-Plane (L-P) configuration [13,14]. This electrode model consists of two rectangular plates in a mutually perpendicular position in the air. The active electrode has the area of the rectangle as *lm* (*l* and *m* are the lengths and width values of the plate, respectively) in a vertical position above the passive electrode, which is in a horizontal position. These plates have a thin thickness δ, and the distance between the two plates is *s*, as shown in Figure 1.b.

The total capacitance value of the electrode model with the L-P configuration, according to [13,14], can be written as,

$$C_{LP} = \varepsilon_0 \, l \ln\left|\frac{m+s}{s}\right|, \tag{3}$$

where ε_0 is the vacuum permittivity. By using formulation (3), we can derive the formulation of the capacitance element from the electrode model with the CEM-P configuration as shown in Figure 2.a,

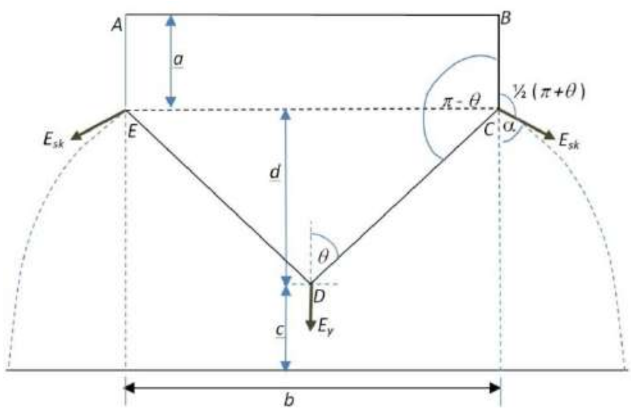

(a)

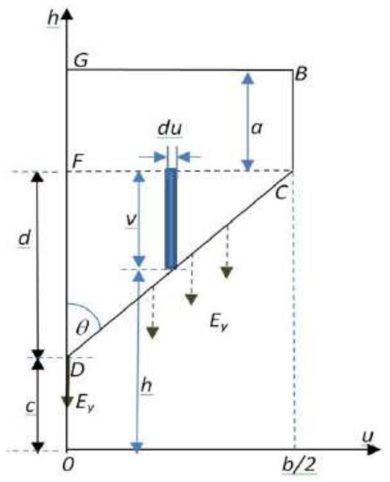

(b)

Figure 2. (a) Calculation of the corona plasma discharge electrode's capacitance with the CEM-P configuration has three plasma flows: the lower oblique of the right and left; and straight downward, (b). The plasma flows are calculated straight down, taking only half the right part of the plate. The enormous plasma flow is the one coming out of point *D*.

Figure 2.a shows the CEM-P electrode configuration model with plate 1 in the shape of an *ABCDE* five-angle plate in an upright position to plate 2, lying horizontally. In this study, the plasma flow was thought to have multiple flow directions that were visible out of some of the sharp surfaces of the electrodes. The flow direction is straight down (seen clearly out of point *D*) and towards the left oblique (seen at point *E*), and oblique to the right (seen at point *C*). Figure 2.b shows the calculation model of the plasma flow, which is specifically directed downward by taking half part of the electrode because it has a symmetrical character between the right and left sides of the *ABCDE* five-angle plate.

The *ABCDE* five-angle plate can be divided into two symmetrical plate areas, where half of the *ABCDE* plate consists of a *GBCF* rectangular plate and an *FDC* triangle. By adopting the Eq. (3) in Figure 2.b, the capacitance calculation of the *GBCF* rectangular plate electrode will produce a value,

$$C_{1A} = \varepsilon_0 \left(\frac{b}{2}\right) \ln\left|\frac{a+c+d}{c+d}\right| . \qquad (4)$$

To calculate the electrode capacitance value of the *FDC* triangular plate, we can make a comparison of the *FDC* triangular plate elements with the Eq. (3) so that the value of the capacitance element along with the boundary condition of variable *u* is obtained as,

$$dC_{1B} = \varepsilon_0 \, du \ln\left|\frac{v+h}{h}\right| \; ; \qquad 0 \le u \le \tfrac{1}{2} b \; , \qquad (5)$$

where there is a relationship

$$d + c = v + h \qquad \text{and} \qquad v = \frac{2ud}{b} \; . \qquad (6)$$

The variables v and h in Eq. (5) can be made as a function of u using Eq. (6). The capacitance value calculating results of the FDC triangle plate in Eq. (5) through the concept of integration is

$$C_{1B} = \left\{ \varepsilon_0 \frac{b}{2d}(c+d) - \varepsilon_0 \frac{bc}{2d} \ln|c+d| \right\} + \left\{ c\varepsilon_0 \frac{b}{2d} \ln|c| - c\varepsilon_0 \frac{b}{2d} \right\}. \qquad (7)$$

From the comparison of Figures 2.a and 2.b, the *ABCDE* plate's capacitance value is two times that of the *GBCDF* plate. However, if the multiplier factor k is entered in the sharp surface around point *D* or at the limit condition $u = 0$ in Figure 2.b, then the capacitance value involving the *ABCDE* plate in the plasma flow downward is

$$C_1 = \varepsilon_0 \, b \ln\left|\frac{a+c+d}{c+d}\right| + \frac{\varepsilon_0 b}{d}\left[c+d - c\ln|c+d|\right] + \lim_{k \to \text{big value}} k \frac{\varepsilon_0 bc}{d}\left[\ln|c| - 1\right]. \qquad (8)$$

In the case of plasma flow out of the left and right oblique directions (points *E* and *C*) from the *ABCDE* plate in Figure 2.a, then plasma flow depiction for the case half the portion of the total *ABCDE* plate (i.e., *GBCDF* plate) is shown in Figure 3.a. From point *C* in the *GBCDF* plate, we assumed that there is a plasma flow that is curved at an angle of 60^0 (considered the mean angle of the observations) so that in the end, the plasma flow reaches the second plate (the passive electrode). The concept of plasma flow from the *GBCDF* plate in Figure 3.a will be easier to calculate if a simplification is made with the plate position on the *u-h* coordinate axis, respectively, on the horizontal and vertical coordinate axes as shown in Figure 3.b. Point *C* on the *GBCDF* plate is the tip of the sharp electrode surface that delivers a more significant amount of plasma than any other surface.

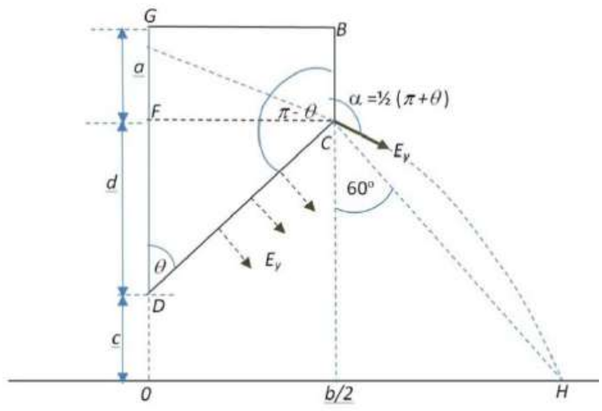

(a)

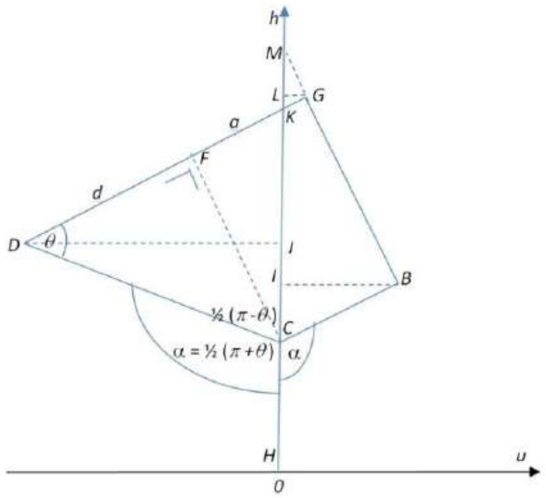

(b)

Figure 3. (a). The plasma outflows right obliquely from point C. The horizontal length of the plasma path on plate 2 is l sin 60^0, where l is the straight distance from the plasma path that exits from point C to the end of the H line, and the angle 60^0 is the mean angle of the observations. (b). The capacitance calculation model with a curved path CH is considered a straight line and functions as the vertical coordinate axis of variable h with the horizontal coordinate axis of variable u.

In the case of the CCP electrode, the sharper the electrode shape (the angle is getting taper), the plasma flow is also more excellent (which is indicated by the increasing value of k), so there is a relationship as $k \cong 1/\phi$, where ϕ is the acute angle at the end of the CCP electrode emitting plasma flow. If at point C which has an acute angle of 2θ and the multiplier factor of shape sharpness is k, then the magnitude of the shape sharpness factor at point C or E is equal to $k_1 = 2\theta k/(\pi-\theta)$.

The total capacitance in the case of plasma flow coming out of the right oblique electrode in Figure 3.a (with the depiction of the capacitance triangle in Figure 3.b) is,

$$C_2 = \left(\frac{2\theta}{\pi-\theta}\right)k\ C_{CBI} + \left(\frac{2\theta}{\pi-\theta}\right)k\ C_{CDJ} + C_{JDK} + C_{IBM} - C_{KGL} - C_{LGM}. \tag{9}$$

The multiplier factor k_1 is added to the capacitance-capacitance values of C_{CBI} and C_{CDJ} because the two electrodes are at the sharp end of the electrode at point C. The calculation of capacitance from C_{CBI} is based on the concept of the image in Figure 4,

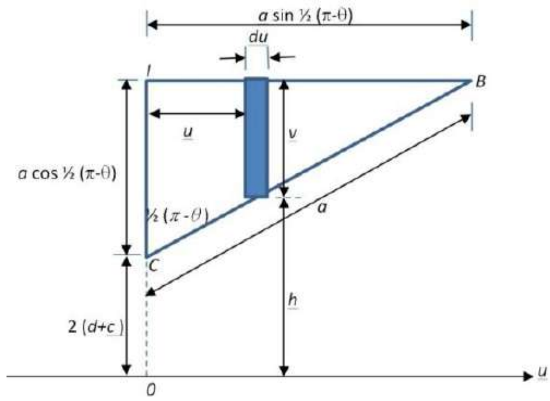

Figure 4. The concept of calculating the capacitance of an electrode C_{CBI}.

By comparing the triangles and the same height limit from Figure 4, the values of v and h are obtained as,

$$v = \tan\left(\tfrac{1}{2}\theta\right)\left[d\sec\theta\cos\left(\tfrac{1}{2}\theta\right) - u\right],$$
$$h = 2(d+c) + u\tan\left(\tfrac{1}{2}\theta\right). \tag{10}$$

Through the formulation of the capacitance element and the boundary conditions of the variable u as,

$$dC_{CBI} = \varepsilon_0\ du \ln\left|\frac{v+h}{h}\right|, \quad 0 \le u \le a\cos\left(\tfrac{1}{2}\theta\right). \tag{11}$$

Table 1. Some capacitance boundary conditions for the triangular electrodes indexes name CDJ, JDK, IBM, KGL and LGM.

No.	Indexes name	v	h	boundary conditions of u
1.	CDJ	$d\sec\theta\sin\left(\tfrac{1}{2}\theta\right) - \tan\left(\tfrac{1}{2}\theta\right)u$	$2(d+c) + u\tan\left(\tfrac{1}{2}\theta\right)$	$-d\sec\theta\cos\left(\frac{1}{2}\theta\right) \le u \le 0$
2.	JDK	$d\sec\theta\sin\left(\tfrac{1}{2}\theta\right) - \tan\left(\tfrac{1}{2}\theta\right)u$	$2(d+c) + d\sec\theta\sin\left(\tfrac{1}{2}\theta\right)$	$-d\sec\theta\cos\left(\tfrac{1}{2}\theta\right) \le u \le 0$
3.	IBM	$a\cot\left(\tfrac{1}{2}\theta\right)\cos\left(\tfrac{1}{2}\theta\right) - u\cot\left(\tfrac{1}{2}\theta\right)$	$2(d+c) + a\sin\left(\tfrac{1}{2}\theta\right)$	$0 \le u \le a\cos\left(\tfrac{1}{2}\theta\right)$
4.	KGL	$(a+d-d\sec\theta)\sin\left(\tfrac{1}{2}\theta\right)$ $-u\tan\left(\tfrac{1}{2}\theta\right)$	$2(d+c) + u\tan\left(\tfrac{1}{2}\theta\right)$ $+2d\sec\theta\sin\left(\tfrac{1}{2}\theta\right)$	$0 \le u \le 2(d+c) + 2d\sec\theta\sin\left(\tfrac{1}{2}\theta\right)$
5.	LGM	$\left[a\cos\left(\tfrac{1}{2}\theta\right) - u\right]\cot\left(\tfrac{1}{2}\theta\right)$ $-(d+d\sec\theta)\sin\left(\tfrac{1}{2}\theta\right)$	$2(d+c)+$ $(a+d+d\sec\theta)\sin\left(\tfrac{1}{2}\theta\right)$	$2(d+c) + a\sin\left(\tfrac{1}{2}\theta\right) + a\cos\left(\tfrac{1}{2}\theta\right)\cot\left(\tfrac{1}{2}\theta\right)$ $\le u \le 2(d+c) + (a+d+d\sec\theta)\sin\left(\tfrac{1}{2}\theta\right)$

Table 2. Some capacitance values for the triangular electrodes.

No.	Indexes name	The triangle capacitance value
1.	CDJ	$\varepsilon_0 d\sec\theta\cos\frac{1}{2}(\theta)\ln\left\lvert\frac{2(d+c)+d\sec\theta\sin\frac{1}{2}(\theta)}{2(d+c)-d\sec\theta\sin\frac{1}{2}(\theta)}\right\rvert+\frac{2\varepsilon_0(d+c)}{\tan\frac{1}{2}(\theta)}\ln\left\lvert\frac{2(d+c)-d\sec\theta\sin\frac{1}{2}(\theta)}{2(d+c)}\right\rvert$ $+\varepsilon_0 d\sec\theta\cos\frac{1}{2}(\theta)$
2.	JDK	$2\varepsilon_0 d\sec\theta\cos\frac{1}{2}(\theta)\ln\left\lvert 3d\sec\theta\sin\left(\frac{1}{2}\theta\right)+2(d+c)\right\rvert-\varepsilon_0 d\sec\theta\cos\frac{1}{2}(\theta)\ln\left\lvert 2d\sec\theta\sin\left(\frac{1}{2}\theta\right)+2(d+c)\right\rvert$ $+\left[2\varepsilon_0(d+c)\cot\left(\frac{1}{2}\theta\right)+\varepsilon_0 d\sec\theta\cos\left(\frac{1}{2}\theta\right)\right]\ln\left\lvert\frac{2d\sec\theta\sin\left(\frac{1}{2}\theta\right)+2(d+c)+d\sec\theta\sin\frac{1}{2}(\theta)}{d\sec\theta\sin\left(\frac{1}{2}\theta\right)+2(d+c)+d\sec\theta\sin\frac{1}{2}(\theta)}\right\rvert$ $-\varepsilon_0 d\sec\theta\cos\frac{1}{2}(\theta)\ln\left\lvert d\sec\theta\sin\frac{1}{2}(\theta)+2(d+c)\right\rvert-\varepsilon_0 d\sec\theta\cos\frac{1}{2}(\theta)$
3.	IBM	$\varepsilon_0\left[a\sin\frac{1}{2}(\theta)+2(d+c)\tan\frac{1}{2}(\theta)+a\sin\frac{1}{2}(\theta)\tan\frac{1}{2}(\theta)\right]\ln\left\lvert a\cos\frac{1}{2}(\theta)\cot\frac{1}{2}(\theta)+2(d+c)+a\sin\frac{1}{2}(\theta)\right\rvert$ $-\varepsilon_0\left[2(d+c)\tan\frac{1}{2}(\theta)+a\sin\frac{1}{2}(\theta)\tan\frac{1}{2}(\theta)\right]\ln\left\lvert 2(d+c)+a\sin\frac{1}{2}(\theta)\right\rvert$ $-\varepsilon_0 a\cos\frac{1}{2}(\theta)\ln\left\lvert 2(d+c)+a\sin\frac{1}{2}(\theta)\right\rvert-\varepsilon_0 a\cos\frac{1}{2}(\theta)$
4.	KGL	$\varepsilon_0\left[2(d+c)+2d\sec\theta\sin\frac{1}{2}\theta\right]\ln\left\lvert(a+d)\sin\left(\frac{1}{2}\theta\right)+2(d+c)+d\sec\theta\sin\left(\frac{1}{2}\theta\right)\right\rvert$ $+\left[2\varepsilon_0(d+c)\cot\left(\frac{1}{2}\theta\right)+2\varepsilon_0 d\sec\theta\cos\left(\frac{1}{2}\theta\right)\right]\ln\left\lvert 2(d+c)+2d\sec\theta\sin\left(\frac{1}{2}\theta\right)\right\rvert$ $-\begin{bmatrix}2\varepsilon_0(d+c)\cot\left(\frac{1}{2}\theta\right)+2\varepsilon_0 d\sec\theta\cos\left(\frac{1}{2}\theta\right)\\+2\varepsilon_0(d+c)+2\varepsilon_0 d\sec\theta\sin\frac{1}{2}\theta\end{bmatrix}\ln\begin{vmatrix}2d\sec\theta\sin\left(\frac{1}{2}\theta\right)+2(d+c)\tan\left(\frac{1}{2}\theta\right)\\+2d\sec\theta\sin\frac{1}{2}\theta\tan\left(\frac{1}{2}\theta\right)+2(d+c)\end{vmatrix}$ $+2\varepsilon_0(d+c)+2\varepsilon_0 d\sec\theta\sin\frac{1}{2}\theta$
5.	LGM	$\varepsilon_0\begin{bmatrix}2(d+c)\tan\left(\frac{1}{2}\theta\right)+a\cos\left(\frac{1}{2}\theta\right)\\+a\sin\left(\frac{1}{2}\theta\right)\tan\left(\frac{1}{2}\theta\right)\end{bmatrix}\ln\left\lvert\frac{2(d+c)+a\sin\left(\frac{1}{2}\theta\right)+a\cos\left(\frac{1}{2}\theta\right)\cot\left(\frac{1}{2}\theta\right)}{2(d+c)+(a+d+d\sec\theta)\sin\left(\frac{1}{2}\theta\right)}\right\rvert$ $+\varepsilon_0(d+d\sec\theta)\tan\left(\frac{1}{2}\theta\right)\sin\left(\frac{1}{2}\theta\right)-\varepsilon_0 a\cos\left(\frac{1}{2}\theta\right)$

We get the value of the capacitance C_{CBI} as,

$$C_{CBI}=\varepsilon_0 a\cos\left(\tfrac{1}{2}\theta\right)-2\varepsilon_0(d+c)\cot\left(\tfrac{1}{2}\theta\right)\ln\left\lvert\frac{2(d+c)+a\sin\left(\frac{1}{2}\theta\right)}{2(d+c)}\right\rvert. \quad (12)$$

The calculation of units along with other capacitance values from Eq. (9) can be seen in tables 1 and 2. Using Eqs. (9), (12) and table 2, then the capacitance part value is obtained in the case of plasma flow coming out of the right oblique direction of the electrode, as

$$\begin{aligned}C_2=&\left(\frac{2\theta}{\pi-\theta}\right)k\left\{\begin{matrix}\varepsilon_0 d\sec\theta\cos\frac{1}{2}(\theta)\ln\left\lvert\frac{2(d+c)+d\sec\theta\sin\frac{1}{2}(\theta)}{2(d+c)-d\sec\theta\sin\frac{1}{2}(\theta)}\right\rvert+\varepsilon_0 a\cos\left(\frac{1}{2}\theta\right)\\+2\varepsilon_0(d+c)\cot\left(\frac{1}{2}\theta\right)\ln\left\lvert\frac{2(d+c)-d\sec\theta\sin\frac{1}{2}(\theta)}{2(d+c)+a\sin\left(\frac{1}{2}\theta\right)}\right\rvert+\varepsilon_0 d\sec\theta\cos\frac{1}{2}(\theta)\end{matrix}\right\}\\&-\varepsilon_0\left[2(d+c)\tan\tfrac{1}{2}(\theta)+a\sin\tfrac{1}{2}(\theta)\tan\tfrac{1}{2}(\theta)+a\cos\tfrac{1}{2}(\theta)\right]\ln\left\lvert 2(d+c)+a\sin\tfrac{1}{2}(\theta)\right\rvert\\&-\varepsilon_0\left[4(d+c)\cot\left(\tfrac{1}{2}\theta\right)+4d\sec\theta\cos\left(\tfrac{1}{2}\theta\right)\right]\ln\left\lvert 2d\sec\theta\sin\left(\tfrac{1}{2}\theta\right)+2(d+c)\right\rvert\\&+\varepsilon_0\left[2(d+c)\cot\left(\tfrac{1}{2}\theta\right)+3d\sec\theta\cos\tfrac{1}{2}(\theta)\right]\ln\left\lvert 3d\sec\theta\sin\left(\tfrac{1}{2}\theta\right)+2(d+c)\right\rvert\\&-\varepsilon_0 d\sec\theta\cos\tfrac{1}{2}(\theta)\ln\left\lvert d\sec\theta\sin\tfrac{1}{2}(\theta)+2(d+c)\right\rvert\\&+\varepsilon_0\begin{bmatrix}2(d+c)\tan\left(\frac{1}{2}\theta\right)+a\sin\left(\frac{1}{2}\theta\right)\tan\left(\frac{1}{2}\theta\right)\\+a\cos\left(\frac{1}{2}\theta\right)-2(d+c)-2d\sec\theta\sin\frac{1}{2}\theta\end{bmatrix}\ln\left\lvert 2(d+c)+(a+d+d\sec\theta)\sin\left(\tfrac{1}{2}\theta\right)\right\rvert\end{aligned}$$

$$+\varepsilon_0\left[a\sin\tfrac{1}{2}(\theta)-a\cos\left(\tfrac{1}{2}\theta\right)\right]\ln\left|a\cos\tfrac{1}{2}(\theta)\cot\tfrac{1}{2}(\theta)+2(d+c)+a\sin\tfrac{1}{2}(\theta)\right|$$

$$+\varepsilon_0\begin{bmatrix}2(d+c)\cot\left(\tfrac{1}{2}\theta\right)+2d\sec\theta\cos\left(\tfrac{1}{2}\theta\right)\\+2(d+c)+2d\sec\theta\sin\tfrac{1}{2}\theta\end{bmatrix}\ln\begin{vmatrix}2(d+c)+2d\sec\theta\sin\left(\tfrac{1}{2}\theta\right)+2(d+c)\tan\left(\tfrac{1}{2}\theta\right)\\+2d\sec\theta\sin\tfrac{1}{2}\theta\tan\left(\tfrac{1}{2}\theta\right)\end{vmatrix}$$

$$-\varepsilon_0\left(d+d\sec\theta\right)\tan\left(\tfrac{1}{2}\theta\right)\sin\left(\tfrac{1}{2}\theta\right)-\varepsilon_0 d\sec\theta\cos\left(\tfrac{1}{2}\theta\right)-2\varepsilon_0\left(d+c\right)+2\varepsilon_0 d\sec\theta\sin\left(\tfrac{1}{2}\theta\right). \quad (13)$$

By using the depiction symmetrical nature of the plasma flow of part half electrodes in the downward direction (Figure 2.b) and the right oblique direction (Figure 3.a) to the depiction total of the electrodes in Figure 2.a, then we get the total capacitance value of the electrode model with the CEM-P configuration is

$$C_{tot}=C_1+2C_2\ , \quad (14)$$

where C_1 and C_2 are the capacitance values in Eqs. (8) and (13), respectively.

The classical Gauss law concept is used to determine the electric current value of the electrode model with the CEM-P configuration. The amount of electric charge flowing between the two electrodes is equal to $q = C_{tot}\ \Delta V$. The magnitude of the electric field in the air that is perpendicular downward (along the y axis) between two thin plates (plate thickness $\delta \cong 0.00015$ meters) at the position of the plates that are perpendicular to each other, as shown in Figure 1.a, can be written as

$$E_y=\frac{q}{\varepsilon_0\left(\Delta A\right)}=\frac{C_{tot}\ \Delta V}{\varepsilon_0\ \left(b\delta+\delta^2\right)}, \quad (15)$$

where the Gauss area is defined as $\Delta A = (b\delta + \delta^2)$ and the notation δ is defined as the thickness value of plate 1. The voltage difference $\Delta V = V - V_i$, where V is the applied voltage and V_i is the threshold voltage of the corona.

The total value of the electric current that leaves the electrode system with the CEM-P configuration using the concept of geometric calculations can be defined as

$$I=-\frac{\mu_0}{\Delta V}\left(qE_y{}^2\right)_{tot}=-\frac{\mu_0\left\{C_{tot}\right\}^3}{\varepsilon_0{}^2\left(b\delta+\delta^2\right)^2}\left(V-V_i\right)^2, \quad (16)$$

where $\varepsilon_0 = 8.854 \times 10^{-12}$ F m^{-1} and $\mu_0 = 4\pi \times 10^{-7}$ Hm^{-1}. Eq. (16) is the formulation of the electric current function I as a function of the voltage V that will characterize the (I-V) theoretical curve at the corona plasma discharge case. This study compared the (I-V) curve and the experimental data points. The sharpness factor of geometric shapes k (contained in the formula of C_{tot}), which is obtained fittingly through a comparison of the theory and experiment results, is the multiplication factor of the current in the corona plasma discharges concept when compared to the ordinary electronic circuit's.

3. EXPERIMENT TECHNIQUE

The electronic circuit arrangement of the corona plasma discharge equipment is shown in Figures 2.a and 2.b and consists of

1. The HV high-voltage source in the DC generator equipment (voltage 4 kV and frequency 25 kHz) is connected to the electrodes with the CEM-P configuration.
2. The electric current measuring instrument uses an analog Multimeter with SANWA brand (type YX-360TREB, voltage 220 V, and frequency 50/60 Hz), arranged in series with the main circuit.
3. The potential difference measuring instrument uses a digital multimeter with SANWA brand CD771.
4. HV probe equipment can convert the potential difference in kV into volts. The electric current that goes to the Voltmeter was passed through the HV probe (Maximum Voltage DC 40 kV DC, model number: AC 28 kV PD-28, serial number: 01605733).

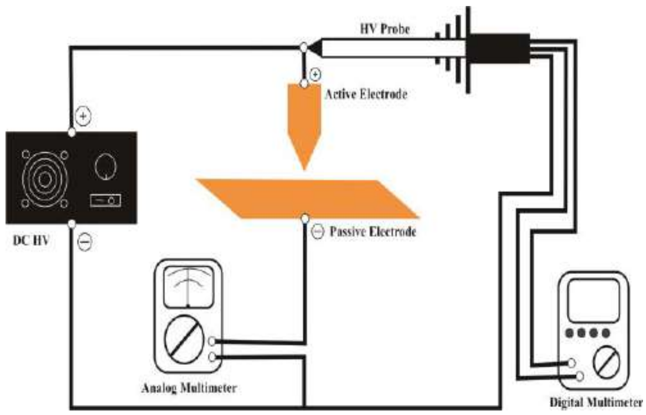

(a)

(b)

Figure 5. (a) and (b) show the circuit schematic and photos of the plasma discharge generator equipment for the CEM-P configuration model, respectively.

4. RESULTS OF SIMULATION AND EXPERIMENT

In the plasma discharge experiment of the CEM-P configuration model, the lower triangular ends of the active electrode have four different angle variations. In Figure 2.a, an active electrode section has several lengths and angles from the pentagon plate. There are several sizes of the same length of the active electrode variations, namely a = 0.01 meters, b = 0.01 meters and δ = 0.00015 meters. While the different sizes (variations) lie in the values of the length d and a half- acute angle θ is,

a. The Electrode Model 1: d = 0.010 meters and θ = 26,57^o
b. The Electrode Model 2: d = 0.015 meters and θ = 18.44 ^{o}
c. The Electrode Model 3: d = 0.025 meters and θ = 11.31 ^{o}
d. The Electrode Model 4: d = 0.030 meters and θ = 9.46 ^{o}

Plasma discharge photos of the four electrode models can be seen in Figure 6,

Model 1

Model 2

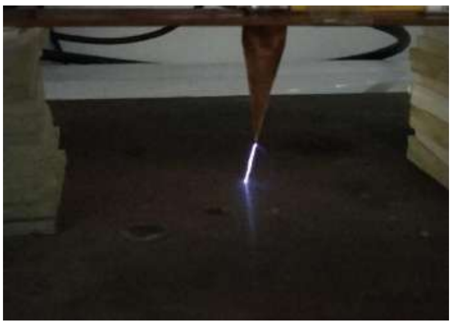

Model 3

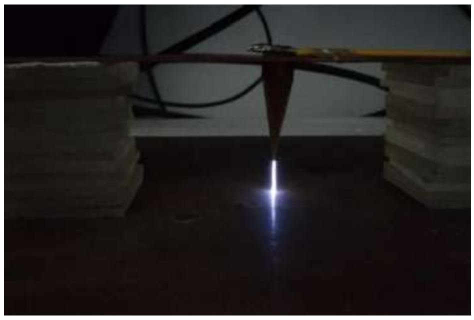

Model 4

Figure 6. The corona discharge photos of four electrode models.

The (I-V) characteristic graph of the corona discharge case for the CEM-P configuration model was made using the Python Graphical User Interface (GUI) Programming [20]. The graph is obtained from the numerical calculations in Eq. (16) for the appropriate value of k. Besides describing graphs and calculating the proper k value, this GUI program can also calculate graph error values consisting of standard deviation (SD) and t-tests. The explanation of the t-test and SD values in this study is

- The t-test value is a parameter that shows the degree of correspondence between the numerical simulation curve and the research data [20] for the (I-V) characteristic graph. The smaller the t-test value (which should be less than 0.05), the higher the level of conformity/accuracy between the two functions (simulation curve and research data).
- The value of SD (standard deviation) σ_I in the GUI program for this research comes from the distribution of the measured data up to order of power two of functions V in the polynomials [21]:

$$I = a_1 + a_2 V + a_3 V^2 \quad ; \quad \sigma_I = \sqrt{\frac{\sum_j \left(I - A_1 - A_2 V_j - A_3 V_j^2\right)^2}{\left(N-2\right)}}, \qquad (17)$$

where a_1, a_2, and a_3 are constants that can be calculated. The values of A_1, A_2, and A_3 are obtained through equation (18),

$$\begin{bmatrix} N & \sum V_j & \sum V_j^2 \\ \sum V_j & \sum V_j^2 & \sum V_j^3 \\ \sum V_j^2 & \sum V_j^3 & \sum V_j^4 \end{bmatrix} \begin{bmatrix} A_1 \\ A_2 \\ A_3 \end{bmatrix} = \begin{bmatrix} \sum I_j \\ \sum V_j I_j \\ \sum V_j^2 I_j \end{bmatrix}. \qquad (18)$$

The SD formula in Eq. (17) is compatible with formula (16) to determine the degree of compatibility between the numerical simulation formula and the research data.

Two (I-V) characteristic graphs for each model (with the same angle of θ) are obtained from two variations of c values. The k factor value, SD value, and t-test value are also included in each graph. The display of the (I-V) characteristic graphs for the four-electrode models is presented in Figure 7.

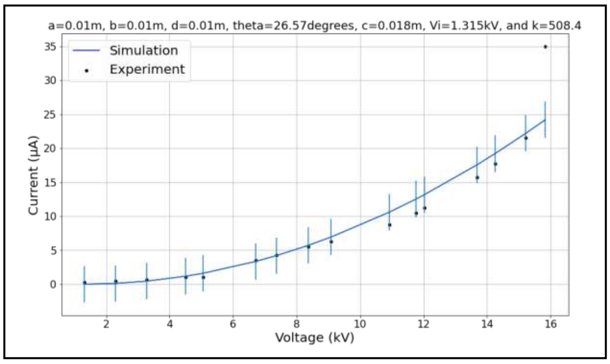

(a)

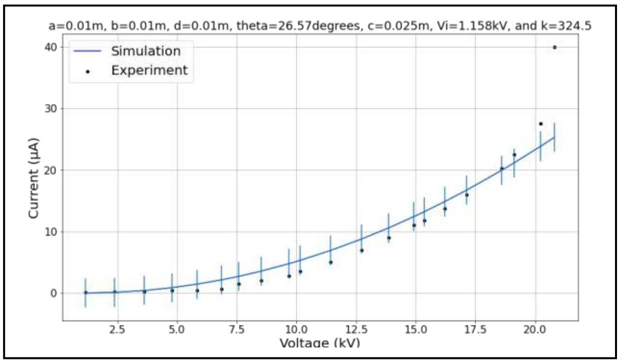

(b)

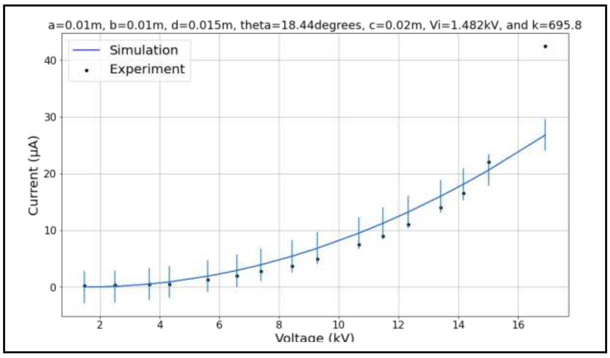

(c)

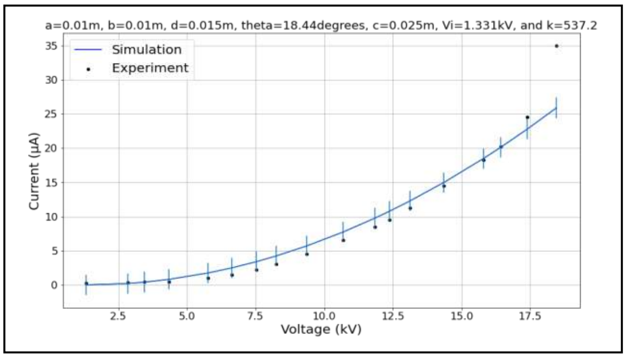

(d)

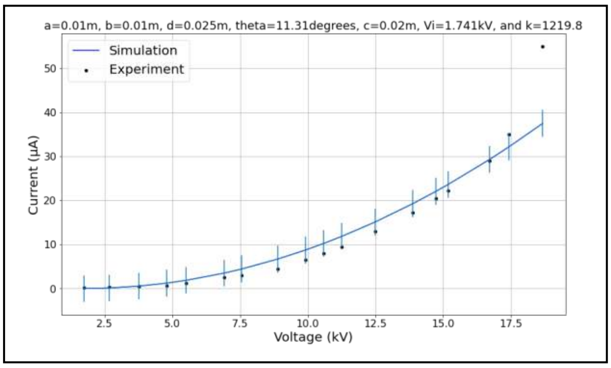

(e)

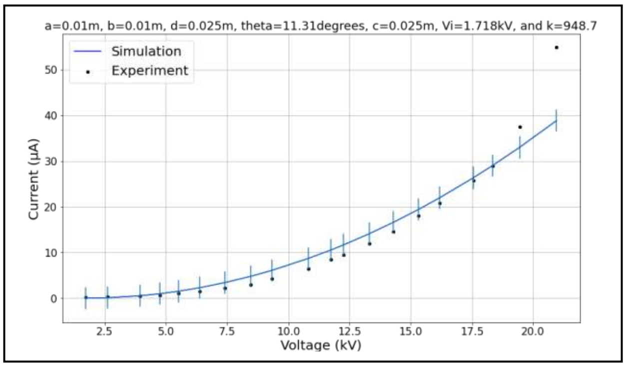

(f)

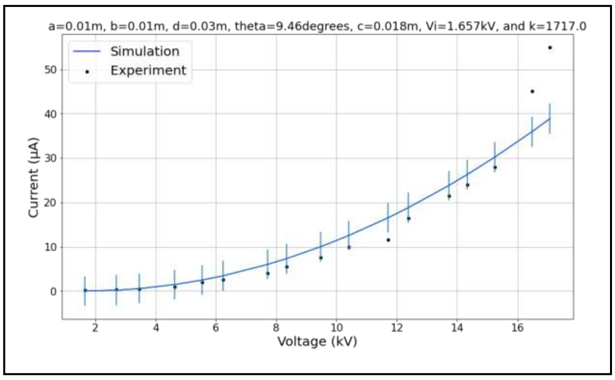

(g)

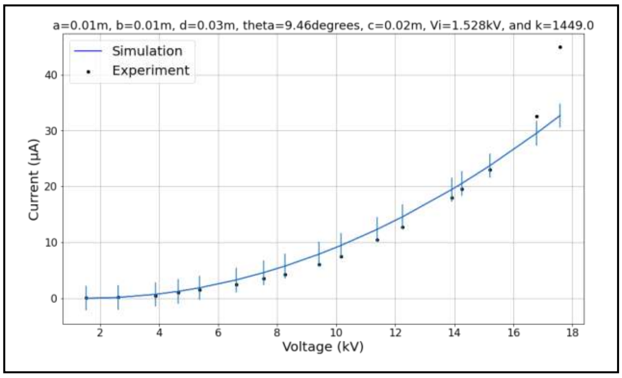

(h)

Figure 7. The (*I*-*V*) Characteristic graph of the corona plasma discharges with the CEM-P configuration at various angles θ and different distances c. (a) and (b) are graphs for Model 1 of distances c = 0.018 m and c = 0.025 m, respectively. (c) and (d) are graphs for Model 2 of distances c = 0.020 m and c = 0.025 m, respectively. (e) and (f) are graphs for Model 3 of distances c = 0.020 m and c = 0.025 m, respectively. (g) and (h) are graphs for Model 4 of distances c = 0.018 m and c = 0.020 m, respectively.

The calculation data for the factor *k*, the *SD* values, and the t-test values in Figure 7 are written in Table 3. On each graph in Figure 7, short vertical lines (*SVL*) connect the data points with the simulation curves. In Figure 7 also, we can manually calculate the values of the number of data points (*NDP*) and the number of tangent points (*NTP*) which is defined as the number of data points that intersect the simulation curve through the *SVL*, and the percentage of tangent points (*PTP*) which is the ratio between *NDP* to *NTP*. A list of the values of *NDP*, *NTP*, and *PTP* is also presented in table 3.

Table 3. Values of the factor *k*, *SD*, and t-test of the (*I-V*) characteristic functions graphs in Figure 7 for different values of *c*.

Model		*c* (m)	*k*	*SD*	t-test	Number of tangent points	Number of data points	Percentage of tangent points
1	$\theta = 26{,}57^{o}$	0.018	508.4	2.6831	0.0468	15	16	93.75 %
		0.025	324.5	2.3665	0.0399	19	21	90.48 %
2	$\theta = 18.44^{o}$	0.020	695.8	2.8317	0.0496	15	16	93.75 %
		0.025	537.2	1.4871	0.0448	17	18	94.44 %
3	$\theta = 11.31^{o}$	0.020	1219.8	3.0485	0.0475	17	18	94.44 %
		0.025	948.7	2.4341	0.0482	18	20	90.00 %
4	$\theta = 9.46^{o}$	0.018	1717.0	3.3546	0.0481	14	17	82.35 %
		0.020	1449.0	2.1841	0.0500	15	17	88.24 %

From the (*I-V*) characteristic graph in Figure 7 and from Table 3, which shows the *SD* and the t-test values, as well as from the calculation of the factor *k* based on the variation of the distance between the two electrodes of the *c*, turned out to produce several trends in cases that arise in this study including:

i. The fit between the line simulated curves with the experimental data points occurs in the low-current portion of the corona plasma discharge.
ii. The *SD* values are relatively large for all graphs, whose values vary between 1.4871-3.3546, and the t-test values for almost all graphs are still below 0.5 (except for the case of θ = 9.46° with c = 0.020). Similarly, the whole graph has relatively large *PTP* values (82.35 % – 94.44 %).
iii. For all variations of the electrodes model, we will see that if the models have a sharper half- acute angle θ, the values of the factor *k* will be greater.
iv. For the case of the same electrodes model, we get research results that the farther the distance between the two electrodes (the greater the value *c*), the values of the factor *k* will be smaller.

5. DISCUSSION

From various research results on the (*I-V*) characteristics of corona discharge such as [4,5,16] etc., the level of match between corona current vs voltage occurred only in the case of low current, not in the case of the sharply increasing current. So this study is the same as many cases of previous studies on the (*I-V*) characteristics of corona discharge.

We concluded that the degree of correspondence between the data points and the simulation curve (representing numerical calculation on the Eq. (16)) is relatively high. The statement is based on several measurable categories (use GUI programming result) for all graphs in Figure 7, such as

i. The values of PTP are relatively large (between 82.35 % – 94.44 %).
ii. The values of the t-test are almost less than 0.5.
iii. Although some factors do not support it, the *SD* values are relatively large (between 1.4871-3.3546). The large enough *SD* values mean that the *SVL* sizes are quite long [14].

The best graph in Figure 7 is a combination of low *SD* and t-test values and has a high PTP value, which is suitable for the case of Model 2 (θ= 18.44°) at c = 0.025 m.

The conclusion from the research results [15] is that the sharper the tip of the active electrode used in the case of corona discharge, the larger and brighter the flow of corona current will be. The factor *k* in this study is a multiplier factor of the corona current magnitude that emerges from the lower end of the sharp surface of the active electrode. The concept of the factor *k* is clear based on the research [15]. We conclude that the sharper the tip of the active electrode, the greater the value of the factor *k*.

Another result obtained in this study (in table 3) is that the greater the value of *c*, the smaller the value of the factor *k*. Figure 6 shows that this study's largest corona current is derived from the corona current coming out of the lower end of the active electrode or out of point *D* in Figure 2.a. The capacitance value of the area (ΔEDC) = 2 × area (ΔFDC) in Figure 2, which contains the current multiplier factor *k*, is part of the formulation of Eq. (8) is

$$C_{EDC} = \lim_{k \to \text{big value}} k \frac{\varepsilon_0 bc}{d}\left[\ln|c| - 1\right]. \tag{19}$$

The values of *b* and *d* in Eq. (18) are constant on the change variation of distance *c*. Suppose it is considered that the C_{EDC} capacitance value is close to a constant on the difference in the value of *c*. In Eq. (18), there is a tendency if the value of *c* is getting bigger it will make the value of *k* tend to be smaller, or vice versa if the value of *c* is getting smaller, then the value of *k* tends to be bigger.

6. CONCLUSION

The calculation results of the values of the fitting factor *k*, *SD* errors, and t-test in table 2 for the (*I-V*) characteristics case conclude that there is a high degree of conformity between numerical calculations and research data. This high degree of the agreement indicates that Eq. (16) is suitable as a general formulation of the (*I-V*) characteristics for the corona plasma discharge model with the Chisel Eye and Midpoint-Plane (CEM-P) electrode configuration. However, there may be deviations from the research results stemming from the negligence of the researchers' observations, the imprecision and asymmetry of the shape and position of the active electrode installation, energy leakage, and other problems that may occur from the physical properties of the corona discharge case.

ACKNOWLEDGMENT

The financials in this work get supported by non-tax revenue (PNBP), Diponegoro University, Semarang, Indonesia, with the schema of International Publication Research (RPI) in 2022. (No. 569-100/UN7.D2/PP/VII/2022).

REFERENCES

[1] Stambouli, A.B., Benallal, R., Oudini, N., Mesli, S.M., Tadjine, R. (2017). Control of Dual Frequency Capacitively Coupled Plasma via blocking capacitor and phase angle. European Physical Journal Applied Physics, 80: 10802. https://doi.org/10.1051/epjap/2017170180

[2] Saikia, P., Bhuyan, H., Escalona, M., Favre, M., Wyndham, E., Maze, J., Schulze, J. (2018). Study of dual radio frequency capacitively coupled plasma: an analytical treatment matched to an experiment. Plasma Sources Science and Technology, 27(1): 015014. https://doi.org/10.1088/1361-6595/aaa565

[3] Townsend, J.S. (1914) The potentials requires to maintain currents between coaxial cylinders. The London, Edinburgh, and Dublin Philosophical Magazine and Journal of Science, 28: 83-90. https://doi.org/10.1080/14786440708635186

[4] Robinson, M. (1967). The Corona Threshold for Coaxial Cylinders in Air at High Pressures. IEEE Transactions on Power Apparatus and Systems, Pas-86:185-189.

[5] Zheng, Y., Zhang, B., He, J. (2015). Current-voltage characteristics of dc corona discharges in air between coaxial cylinders. Physics of Plasmas, 22: 023501. https://doi.org/10.1063/1.4907234

[6] Guan, Y., Vaddi, R.S., Aliseda, A., Novosselov, I. (2018). Analytical model of electrohydrodynamic flow in corona discharge. Physics of Plasmas, 25: 083507. https://doi.org/10.1063/1.5029403

[7] Robinson, M. (1961) Movement of Air in the Electric Wind of the Corona Discharge. Transactions of the American Institute of Electrical Engineers, 80: 143-150. https://doi.org/10.1109/TCE.1961.6373091

[8] Abe, H., Yoneda, M., Fujiwara, N. (2008). Developments of Plasma Etching Technology for Fabricating Semiconductor Devices. Japanese Journal of Applied Physics, 47(3): 1435-1455. https://doi.org/10.1143/JJAP.47.1435

[9] Vidaurre, E.F.C., Achete, C.A., Gallo, F., Garciam D., Simão, R.A., Habert, A.C. (2002). Surface Modification of Polymeric Materials by Plasma Treatment. Materials Research, 5(1): 37-41. https://doi.org/10.1590/S1516-14392002000100006

[10] Anders, A. (2005). Plasma and Ion Sources in Large Area Coatings: A review. Surface and Coatings Technology, 200: 1893-1906. https://doi.org/10.1016/j.surfcoat.2005.08.018

[11] Schmidt, H., Sansonnens, L., Howling, A.A., Hollenstein, C., Elyaakoubi, M., Schmitt, J.P.M. (2004). Improving plasma uniformity using lens-shaped electrodes in a large area very high frequency reactor. Journal of Applied Physics, 95: 4559-4564. https://doi.org/10.1063/1.1690096

[12] Bouremel, Y., Li, J.M., Zhao, Z., Debiasi, M. (2013). Effects of AC Dielectric Barrier Discharge Plasma Actuator Location on Flow Separation and Airfoil Performance. Procedia Engineering, 67: 270-278. https://doi.org/10.1016/j.proeng.2013.12.026

[13] Wardaya, A.Y., Muhlisin, Z., Hudi, A., Suseno, J.E., Nur, M., Kinandana, A.W., Windarta, J. (2020). A study of line-plane configuration in the Corona discharge theory. The European Physical Journal Applied Physics, 89: 30801. https://doi.org/10.1051/epjap/2020200011

[14] Wardaya, A.Y., Muhlisin, Z., Suseno, J.E., Nur, M., Triadyaksa, P., Khumaeni, A., Sarwoko, E.A., Windarta, J., Hadi, S. (2022). The Current-Voltage Characteristics for Electrode Geometry Model of Positive DC Corona Discharge in Air. Gazi University Journal of Science, 35: 1140-1150. https://doi.org/10.35378/gujs.885345

[15] Dobranszky, J., Bernath, A., Marton, H.Z. (2008). Characterisation of the plasma shape of the TIG welding arc. International Journal of Microstructure and Materials Properties 3(1): 126-140. https://doi.org/10.1504/IJMMP.2008.016949

[16] Moreau, E., Benard, N., Alicalapa, F., Douyere, A. (2015). Electrohydrodynamic force produced by a corona discharge between a wire active electrode and several cylinder electrodes-Application to electric propulsion. Journal of Electrostatics, 76: 194-200. https://doi.org/10.1016/j.elstat.2015.05.025

[17] Giubbilini, P. (1988). The current ‐ voltage characteristics of point ‐ to ‐ ring corona. Journal of Applied Physics, 64: 3730-3732. https://doi.org/10.1063/1.341368

[18] Yamada, K. (2004). An empirical formula for negative corona discharge current in point-grid electrode geometry. Journal of Applied Physics, 96: 2472. https://doi.org/10.1063/1.1775301

[19] Ferreira, G.F.L., Oliveira Jr., O.N., Giacometti, J.A. (1986). Point ‐ to ‐ plane corona: Current ‐ voltage characteristics for positive and negative polarity with evidence of an electronic component. Journal of Applied Physics, 59: 3045-3049. https://doi.org/10.1063/1.336926

[20] Boslaugh, S. (2012). Statistics in a nutshell: A desktop quick reference, Second Edition. O'Reilly Media, Inc., USA. ISBN-13: 978-1449316822, ISBN-10: 1449316824.

[21] Taylor, J.R. (1997). An introduction to error analysis, the study of uncertainties in physical measurements, second edition. University Science Books, USA. ISBN 0-935702-42-3. ISBN 0-935702-75-X.

NOMENCLATURE

I	Electric current, Ampere
V	Voltage, Volt
a, b	width and length of the rectangular plate, meters.
d	width of the triangular plate, meters.
c	distance between the lower end of electrode active and electrode passive, meters.
SD	Standard Deviation
k, k_1	shape sharpness factor (dimensionless)
C	constant (the geometric function)
C_1, C_2, .. ,C_{tot}	Capacitance, Coulomb/Volt
q	electrical charge, Coulomb
$\boldsymbol{E}$	electric field, N/C
ΔA	area, m^2

Greek symbols

θ	half- acute angle, radian
δ	plate thickness, meters
σ	standard deviation
ε_0	vacuum permittivity, 8.854×10^{-12} F m^{-1}
μ_0	vacuum permeability, $4\pi \times 10^{-7}$ Hm^{-1}
ϕ	acute angle at the end of the CCP electrode emitting plasma flow

Subscripts

i	threshold/initial
j	sum index
tot	total
CBI, CDJ, JDK, IBM, KGL, LGM	triangular electrodes indexes name

Permintaan Revisi dari Editor

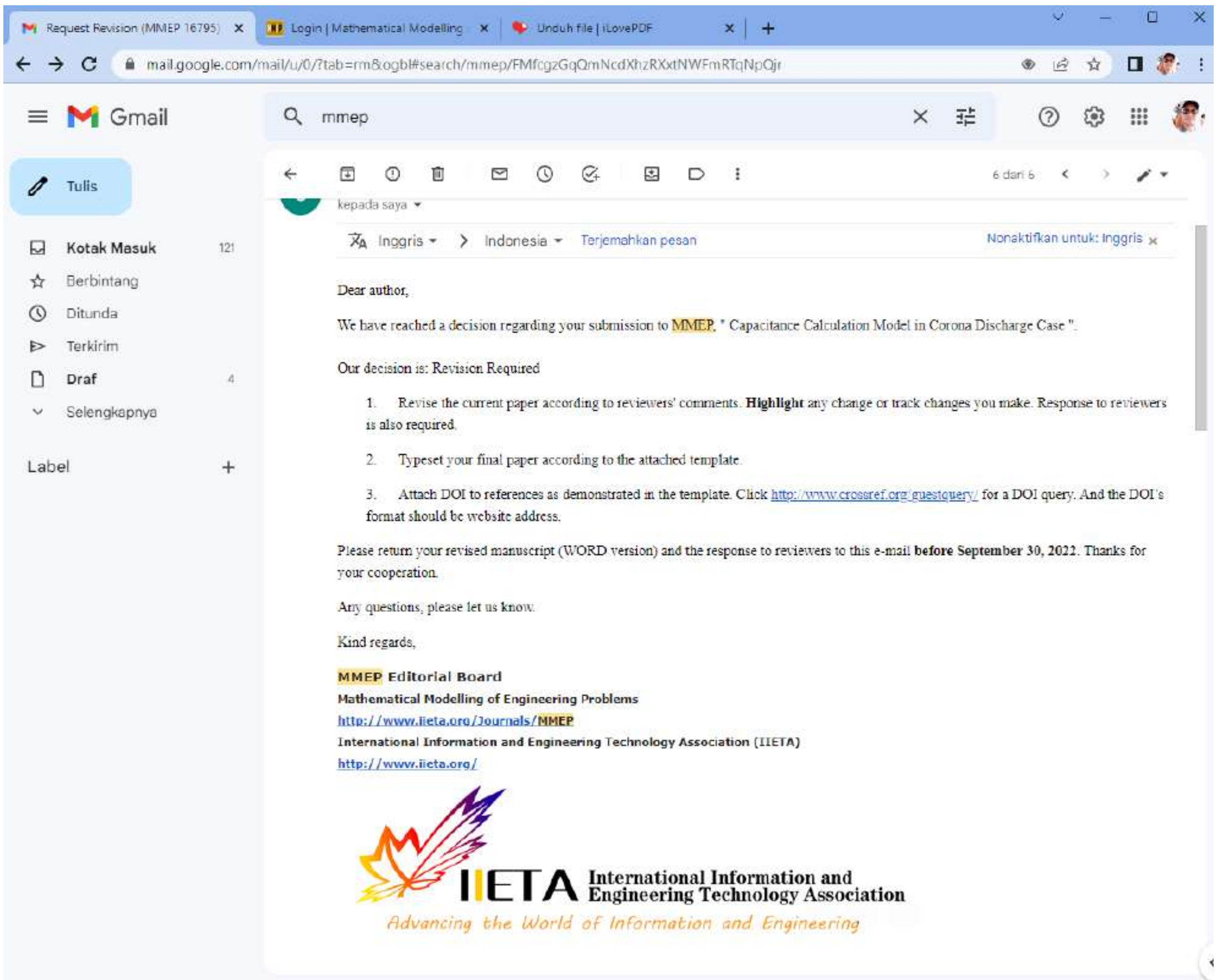

Dear author,

We have reached a decision regarding your submission to MMEP, " Capacitance Calculation Model in Corona Discharge Case ".

Our decision is: Revision Required

1. Revise the current paper according to reviewers' comments. **Highlight** any change or track changes you make. Response to reviewers is also required.
2. Typeset your final paper according to the attached template.
3. Attach DOI to references as demonstrated in the template. Click http://www.crossref.org/guestquery/ for a DOI query. And the DOI's format should be website address.

Please return your revised manuscript (WORD version) and the response to reviewers to this e-mail **before September 30, 2022**. Thanks for your cooperation.

Any questions, please let us know.

Kind regards,

MMEP Editorial Board
Mathematical Modelling of Engineering Problems
http://www.iieta.org/Journals/MMEP
International Information and Engineering Technology Association (IIETA)
http://www.iieta.org/

IIETA International Information and Engineering Technology Association
Advancing the World of Information and Engineering

M

Materi Revisi dari Reviewer

Capacitance Calculation Model in Corona Discharge Case

Overall, this manuscript reads well and has the potential to provide us some useful implications for future direction. However, there are some important issues that the authors have to address in order to make this manuscript better. My major comments to this manuscript are as follows:

1. “In this study, we use a capacitance calculation model for positive dc corona discharge in air, especially in calculating the (I-V) current-voltage characteristics of an electrode configuration model, often referred to as capacitively coupled plasma (CCP).” the author begins the abstract with this sentence directly. It is suggested to add a brief research background before this.
2. “The development of cold plasma technology had a positive impact on the industry, especially for use in electronic equipment with plasma temperatures that are not too high but produce a high enough technological leap through an equipment model called capacitively coupled plasma” The importance of cold plasma technology should be emphasized in the introduction.
3. “This research discusses the calculation of the (*I*-*V*) characteristic of positive dc corona discharge in the air (the CCP model) using The Chisel Eye and Midpoint-Plane (CEM-P) electrodes configuration models.” The research aim is very clear, but the research gap has not been clearly defined. Why does the author want to conduct this study? The research motivation is not sufficient.
4. The findings or research results should be introduced briefly in the introduction part, so as to readers can get a whole view of this paper when they just finish reading the introduction.
5. “In contrast, a passive electrode is horizontally shaped under the active electrode.” After this, it is suggested to add the whole structure or the paper’s layout at the end of the introduction.
6. “The (*I*-*V*) characteristic model in the case of corona plasma discharge expressed in terms of the current function as a function of the square of V has two equations. The first form of this model is as follows,” The author listed a number of equations in this paper, however, most of them are not noted the quotations, please add them to make this paper more convinced.
7. “The electrode scheme with the CEM-P configuration is found in Figure 1.a.” please give more explanation about the information in Figure 1.a. in the text.
8. Good research needs to explain what it means in practice, so the managerial implications should be stressed in this study.

Permintaan Perpanjangan Waktu Untuk Revisi

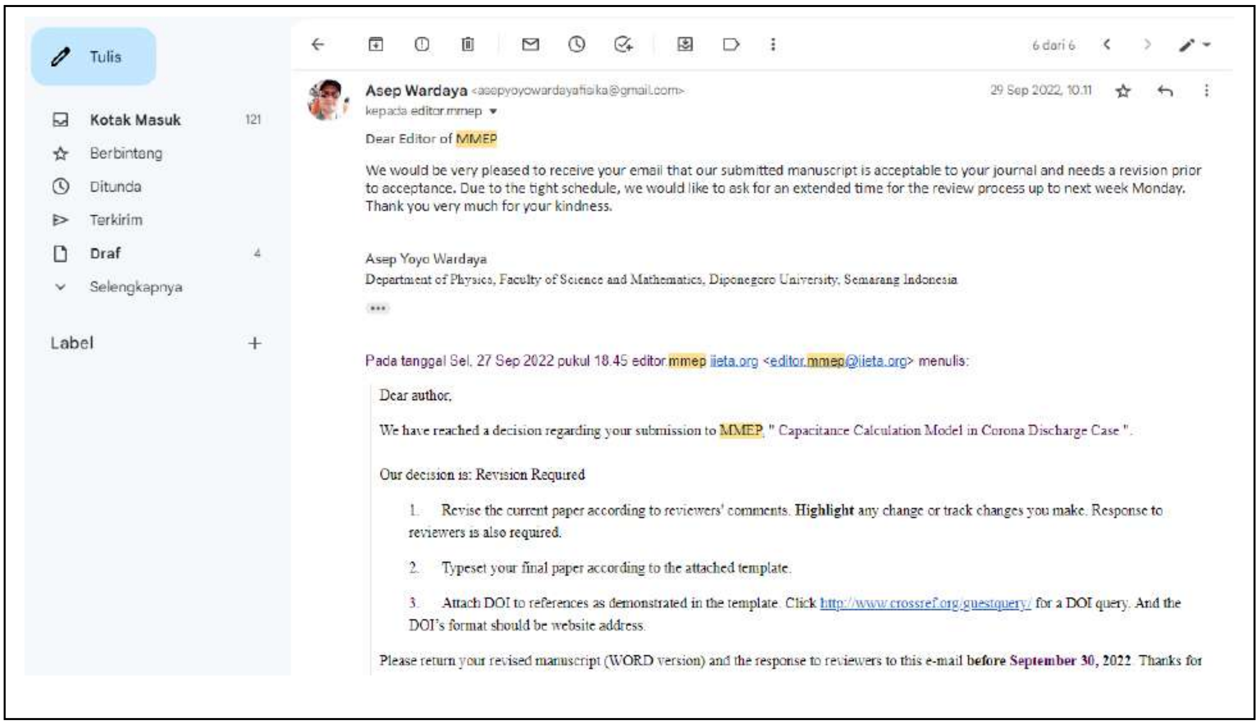

Tulis

Kotak Masuk 121

Berbintang

Ditunda

Terkirim

Draf 4

Selengkapnya

Label

6 dari 6

Asep Wardaya <asepyoyowardayafisika@gmail.com> 29 Sep 2022, 10.11

kepada editor mmep

Dear Editor of MMEP

We would be very pleased to receive your email that our submitted manuscript is acceptable to your journal and needs a revision prior to acceptance. Due to the tight schedule, we would like to ask for an extended time for the review process up to next week Monday. Thank you very much for your kindness.

Asep Yoyo Wardaya

Department of Physics, Faculty of Science and Mathematics, Diponegoro University, Semarang Indonesia

Pada tanggal Sel, 27 Sep 2022 pukul 18.45 editor mmep iieta.org <editor.mmep@iieta.org> menulis:

> Dear author,
>
> We have reached a decision regarding your submission to MMEP, " Capacitance Calculation Model in Corona Discharge Case ".
>
> Our decision is: Revision Required
>
> 1. Revise the current paper according to reviewers' comments. **Highlight** any change or track changes you make. Response to reviewers is also required.
> 2. Typeset your final paper according to the attached template.
> 3. Attach DOI to references as demonstrated in the template. Click http://www.crossref.org/guestquery/ for a DOI query. And the DOI's format should be website address.
>
> Please return your revised manuscript (WORD version) and the response to reviewers to this e-mail **before September 30, 2022**. Thanks for

Permintaan Perpanjangan Waktu Disetujui oleh Fihak Editor

editor.mmep iieta.org <editor.mmep@iieta.org> 29 Sep 2022, 10.18

kepada saya

Inggris > Indonesia Terjemahkan pesan Nonaktifkan untuk: Inggris

Dear author\

Noted, you can return your revision and responses next week, thank you.

Best regards

Penyerahan Koreksi dari Manuskript

Asep Wardaya <asepyoyowardayafisika@gmail.com> 2 Okt 2022, 20.54

kepada editor.mmep

Dear Editor of MMEP

We sent a correction to our manuscript entitled "Capacitance Calculation Model in Corona Discharge Case", according to the reviewer's advice. The submitted file consists of a List of reviewer's corrections and a revised manuscript. Thank you very much for your kindness.

Asep Yoyo Wardaya

Department of Physics, Faculty of Science and Mathematics, Diponegoro University, Semarang Indonesia

3 Lampiran • Dipindai dengan Gmail

- MMEP 16795-202...
- MMEP 16795-202...
- List of reviewer's ...

Balas Teruskan

List of reviewer's corrections

No	Sugestion	Correction	chapter and paragraph (revised manuscript)
1.	"In this study, we use a capacitance calculation model for positive dc corona discharge in air, especially in calculating the (I-V) current-voltage characteristics of an electrode configuration model, often referred to as capacitively coupled plasma (CCP)." the author begins the abstract with this sentence directly. It is suggested to add a brief research background before this.	The (*I-V*) characteristic pattern of the corona discharge case is very different from the pattern of ordinary electric circuits, so it is interesting to investigate. Several previous studies involved the concept of Maxwell's equations on several physical case models such as coaxial cylinder, electrohydrodynamic, and the electric wind.	Abstract
2.	"The development of cold plasma technology had a positive impact on the industry, especially for use in electronic equipment with plasma temperatures that are not too high but produce a high enough technological leap through an equipment model called capacitively coupled plasma" The importance of cold plasma technology should be emphasized in the introduction.	Cold plasma is characterised by the temperature of the heavy species (particles and neutral ions) close to room temperature (25°C - 100°C). This condition becomes important when irradiating materials sensitive to high temperatures [2], such as those used in CCP equipment or materials radiated by the CCP equipment.	Introduction, first paragraph.
3.	"This research discusses the calculation of the (I-V) characteristic of positive dc corona discharge in the air (the CCP model) using The Chisel Eye and Midpoint-Plane (CEM-P) electrodes configuration models." The research aim is very clear,but the research gap has not been clearly defined. Why does the author want to conduct this study? The research	Research [6-8] uses the electric field concept from Maxwell's equation applied to the coaxial cylinder model, the continuity equation of electrohydrodynamic, and the electric wind, respectively. This study does not use a physical approach from Maxwell's equations but a geometric approach from the active electrode tip of the capacitor, which gives rise to the shape sharpness factor of k [14, 15]. The study [14] used an active electrode tip approach in the form of a sharp line,	Introduction, 5th paragraph

	motivation is not sufficient.	[15] using a sharp semicircular active electrode shape with pointed left and right sides. This study uses the tip of the active electrode as a sharp and pointed triangle. The pointed angle at the tip of the active electrode is $\phi = 2\theta$. This study uses variations in the angle θ not found in [14,15] and variations in the distance between the two electrodes.	
		This study is significant. We will be able to calculate the variation of electric current and plasma discharge required from the electrode model (CCP equipment) only by using the given voltage variation and variations in the length and angle of sharpness of the active electrode at a specific value of k. This method is more practical than considering physical effects, such as the effect of using Maxwell's equations on plasma discharge.	
4	The findings or research results should be introduced briefly in the introduction part, so as to readers can get a whole view of this paper when they just finish reading the introduction.	The research results are a graph of the current-voltage characteristics of the corona plasma discharge with a high degree of correspondence between numerical calculations and experimental data (82.35% - 94.44%). The value of the research errors includes standard deviation values between 1.4871-3.3546 and t-test values which are almost all below the value of 0.5 (only one research data with a t-test value = 0.5). This (CEM-P) electrode configuration model uses four variations of the sharp angle at the tip of the active electrode ($\phi = 2\theta$) and two variations of the distance between the active and passive electrodes for any given θ value. The value of the resulting corona discharge current is a function of the voltage difference ΔV, the angle and geometric size of the active electrode, and the distance between the active and passive electrodes.	Introduction, 7th paragraph

5	“In contrast, a passive electrode is horizontally shaped under the active electrode.” After this, it is suggested to add the whole structure or the paper’s layout at the end of the introduction.	The paper's layout has a structure through the following chapters: a. Abstract contains a brief explanation of the background, research objectives, research methods, and research results. b. Introduction contains the background and importance of this research on technological and industrial developments, the background of previous research, research methods, research objectives, research gaps, reasons, and motivations for research. c. Mathematical model contains a detailed explanation physically and mathematically that relates the concept of electric current formulation from plasma discharge with other variables such as voltage and capacitance value. The capacitance value is determined by the length measurements of the electrode components and the value of *k*. d. The technical experiment explains the electronic circuits and equipment used in this research. e. Results of Simulation and Experiments explain the study of four different sizes of electrode models through the depiction of the (I-V) characteristic graphs and their uncertainty errors related to the degree of correspondence between numerical calculations and research data. f. Discussion contains a discussion of the analysis of the (I-V) characteristic graph and the value of the error based on physical and mathematical reasons. g. Conclusion contains a discussion about the feasibility level of this study based on the research results and discussions that have been presented previously. h. Acknowledgment and References.	Introduction, 9th paragraph
6	“The (I-V) characteristic model	Eq. (1) is quoted from [5,8,19,20,21]	Mathematical Models; first

	in the case of corona plasma discharge expressed in terms of the current function as a function of the square of V has two equations. The first form of this model is as follows," The author listed a number of equations in this paper, however, most of them are not noted the quotations, please add them to make this paper more convinced.		paragraph
		Eq. (2) is quoted from [7,14,15,22]	Mathematical Models; first paragraph
		Eq. (3) is quoted from [14,15]	Mathematical Models; 5th paragraph
		Eq.(4) is derived from eq. (3)	-
		Eq. (5) is the capacitance element form of eq. (3)	-
		Eq. (7) is the solution of the capacitance value derived from eq. (5) for FDC plate case	-
		Eq. (8) is the solution of the capacitance value derived from eq. (5) for the *ABCDE* plate case, by adding the factor *k* to the integration in the sharp region (point *D* in Figure 2). Eq. (8) holds for the downward flow of plasma	-
		Eq. (9) is the geometric form of the total capacitance from Figure 2.a using the calculation method in Figures 3.a and 3.b. Eq. (9) applies to the active electrode's plasma flow from the left and right sides (forming an angle with the vertical line).	-
		Eq. (11) is the solution of the capacitance value derived from eq. (5) for *CBI* plate case	-
		Eq. (13) is the solution of the capacitance value derived from eq. (5)	-

		for the plates case in eq. (9)	
		Equations (15) and (16) comes from [14,15], although there is a difference in the value of the Gaussian area with the article [14,15].	Mathematical Models, The penultimate and last paragraphs
		Eqs. (17) and (18) is quoted from [24]	Results Of Simulation And Experiment; Second paragraph
7	"The electrode scheme with the CEM-P configuration is found in Figure 1.a." please give more explanation about the information in Figure 1.a. in the text.	Figure 1. a. is a two-dimensional representation of the CEM-P electrode configuration model. According to geometric calculations, the most significant plasma flow will come out from the lower center end of the pointed active electrode. Furthermore, a smaller stream of plasma will come out of the pointed end of the electrode on both sides of the active electrode. In comparison, the most negligible flow will come out of the sharp lower triangular surface of the active electrode. A passive electrode will accommodate all the plasma flow under the active electrode. For the calculation of the capacitance model of the active electrode system, it has two conditions, namely: a. For plasma flow straight down, the pentagon-shaped capacitance calculation is transformed into rectangular and triangular capacitances. b. For the plasma flow coming out of the left and right sides of the active electrode, the capacitance value will be calculated using the integration technique of the capacitance elements.	Mathematical Models; 3rd paragraph
8.	Good research needs to explain what it means in practice, so the managerial implications should	The CEM-P electrode produces corona plasma under atmospheric conditions. Corona plasma is a form of cold plasma that produces reactive oxygen-nitrogen species (RONS) in atmospheric	Introduction, 6th paragraph

	be stressed in this study.	conditions. In industrial interests, RONS can be used to improve post-harvest quality [17], food quality and safety management [18] and so on.	

Mathematical Modelling of Engineering Problems
Vol., No., Month, Year, pp. **-**
Journal homepage: http://iieta.org/journals/mmep

Capacitance Calculation Model in Corona Discharge Case

Asep Yoyo Wardaya[1,]* , Zaenul Muhlisin[1], Jatmiko Endro Suseno[1], Charis Munajib[1], Susilo Hadi[2], Heri Sugito[1], Jaka Windarta[3]

[1] Department of Physics, Faculty of Science and Mathematics, Diponegoro University, Semarang Indonesia
[2] M1 Physique, Faculté de sciences, Université d'Aix-Marseille, Marseille, France
[3] Department of Electrical Engineering, Faculty of Engineering, Diponegoro University, Semarang Indonesia

Corresponding Author Email: asepyoyowardayafisika@gmail.com

https://doi.org/10.18280/mmep.xxxxxx

Received:
Accepted:

Keywords:
Corona discharge, (I-V) characteristics, CEM-P, shape sharpness factor, Python GUI Programming

Revised Manuscript

ABSTRACT

The (*I-V*) characteristic pattern of the corona discharge case is very different from the pattern of ordinary electric circuits, so it is interesting to investigate. Several previous studies involved the concept of Maxwell's equations on several physical case models such as coaxial cylinder, electrohydrodynamic, and the electric wind. In this study, we use a capacitance calculation model for positive dc corona discharge in air, especially in calculating the (*I-V*) current-voltage characteristics of an electrode configuration model, often referred to as capacitively coupled plasma (CCP). The configuration model comprises active and passive electrodes, with the active electrode in the form of a pentagonal with the sharp end (in the middle) facing downwards in an upright position. The passive electrode under the active electrode has a large rectangular shape in a lying place. This configuration model is named The Chisel Eye and Midpoint-Plane (CEM-P). The analytical calculation of the (*I-V*) characteristics uses the geometric properties of the active electrode, which will produce a large corona current flow at the pointed electrode. These properties in analytical calculation manifest with the emergence of the corona flow multiplication factor at the sharp active electrode's integration boundary condition called the shape sharpness factor k. The Python GUI Programming simulation program makes graphic simulations, Standard Deviation (*SD*), t-tests, and calculating the factor *k* (fitting curve value) between numerical calculations and research data. The values of the *SD*, the t-tests, and the Percentage of tangent points meet the requirements for a high level of accuracy for the four CEM-P configuration models of the (*I-V*) characteristics simulation graph with the graph has a relatively large percentage of tangent points values (82.35 % – 94.44 %).

1. INTRODUCTION

The development of cold plasma technology had a positive impact on the industry, especially for use in electronic equipment with plasma temperatures that are not too high but produce a high enough technological leap through an equipment model called capacitively coupled plasma (CCP) [1]. Cold plasma is characterised by the temperature of the heavy species (particles and neutral ions) close to room temperature (25°C-100°C). This condition becomes important when irradiating materials sensitive to high temperatures [2], such as those used in CCP equipment or materials radiated by the CCP equipment.

The CCP model uses the concept of corona plasma discharge with an electrode configuration consisting of an active electrode in a vertical position and a passive electrode in a horizontal position (under the active electrode). The active electrode has a sharp-shaped surface towards the bottom. The passive electrode has a large surface to accommodate all the plasma flow from the active electrode. The CCP equipment is similar to the capacitance equipment with the position of the two electrodes perpendicular to each other [3]. If the CCP equipment connects to a dc voltage source, it can produce a corona plasma discharge under the appropriate voltage conditions.

The (*I-V*) current-voltage characteristic in the corona plasma discharge is an exciting research topic. This topic involves a variety of physical properties that cause Townsend's low current to appear, followed by a reasonably high current increase in corona discharge and arc discharge events [4]. Various studies explain the characteristic current-voltage phenomenon in the corona discharge, including the coaxial cylinders model [5,6], the electro-hydrodynamics model [7], and the Electric Wind model [8]. Similarly, the application of CCP equipment has helped the development of research in other fields or used for industries such as ultra-large-scale integrated circuit (ULSI) fabrication [9], surface modification of polymeric materials [10], Large-area coating [11], lens-shaped electrodes [12], AC dielectric barrier discharges [13], etc.

In 2020, [14] make another form of the (I-V) characteristic related to the geometric function of the CCP electrode model. The geometric part has also been discussed by [8] to compare the corona current function and the voltage's square function. In the research [14,15], the geometric part comes from the modified capacitance function by adding a multiplier factor *k* to the sharp surface of the active electrode. The value of factor k came from the suitability factor between the analytical formulation and the experimental results (curve fitting value). The factor k is the shape sharpness factor, which came from calculating the capacitance through the insertion of the integration limit on the part of the active electrode with a sharp surface. The ideal value of k will be higher if the shape of the active electrode is more tapered. The presence of the factor k came from the research results from [16], who proved that the pointed tip of the active electrode (with a variety of sharpness angles and different materials) would look the plasma discharge brighter and more significant.

This research discusses the calculation of the (*I-V*) characteristic of positive dc corona discharge in the air (the CCP model) using The Chisel Eye and Midpoint-Plane (CEM-P) electrodes configuration models. Research [6-8] uses the electric field concept from Maxwell's equation applied to the coaxial cylinder model, the continuity equation of electrohydrodynamic, and the electric wind, respectively. This study does not use a physical approach from Maxwell's equations but a geometric approach from the active electrode tip of the capacitor, which gives rise to the shape sharpness factor of k [14,15]. The study [14] used an active electrode tip approach in the form of a sharp line, [15] using a sharp semicircular active electrode shape with pointed left and right sides. This study uses the tip of the active electrode as a sharp and pointed triangle. The pointed angle at the tip of the active electrode is $\phi = 2\theta$. This study uses variations in the angle θ not found in [14,15] and variations in the distance between the two electrodes. This study is significant. We will be able to calculate the variation of electric current and plasma discharge required from the electrode model (*CCP* equipment) only by using the given voltage variation and variations in the length and angle of sharpness of the active electrode at a specific value of k. This method is more practical than considering physical effects, such as the effect of using Maxwell's equations on plasma discharge.

The CEM-P electrode produces corona plasma under atmospheric conditions. Corona plasma is a form of cold plasma that produces reactive oxygen-nitrogen species (RONS) in atmospheric conditions. In industrial interests, RONS can be used to improve post-harvest quality [17], food quality and safety management [18] and so on.

The research results are a graph of the current-voltage characteristics of the corona plasma discharge with a high degree of correspondence between numerical calculations and experimental data (82.35% - 94.44%). The value of the research errors includes standard deviation values between 1.4871-3.3546 and t-test values which are almost all below the value of 0.5 (only one research data with a t-test value = 0.5). This (CEM-P) electrode configuration model uses four variations of the sharp angle at the tip of the active electrode ($\phi = 2\theta$) and two variations of the distance between the active and passive electrodes for any given θ value. The value of the resulting corona discharge current is a function of the voltage difference ΔV, the angle and geometric size of the active electrode, and the distance between the active and passive electrodes.

These electrodes model consists of a pair of electrodes positioned perpendicular to each other in the air. These electrodes couple consist of an active electrode shaped like a Pentagonal thin plate, and the mid-sharp end is directed downward in a vertical position. In contrast, a passive electrode is horizontally shaped under the active electrode.

The paper's layout has a structure through the following chapters:

a. Abstract contains a brief explanation of the background, research objectives, research methods, and research results.
b. Introduction contains the background and importance of this research on technological and industrial developments, the background of previous research, research methods, research objectives, research gaps, reasons, and motivations for research.
c. Mathematical model contains a detailed explanation physically and mathematically that relates the concept of electric current formulation from plasma discharge with other variables such as voltage and capacitance value. The capacitance value is determined by the length measurements of the electrode components and the value of k.
d. The technical experiment explains the electronic circuits and equipment used in this research.
e. Results of Simulation and Experiments explain the study of four different sizes of electrode models through the depiction of the (*I-V*) characteristic graphs and their uncertainty errors related to the degree of correspondence between numerical calculations and research data.
f. Discussion contains a discussion of the analysis of the (*I-V*) characteristic graph and the value of the error based on physical and mathematical reasons.
g. Conclusion contains a discussion about the feasibility level of this study based on the research results and discussions that have been presented previously.
h. Acknowledgment and References.

2. MATHEMATICAL MODELS

The (*I-V*) characteristic model in the case of corona plasma discharge expressed in terms of the current function as a function of the square of V has two equations. The first form of this model is as follows,

$$I = CV\left(V - V_i\right), \tag{1}$$

where I is the corona plasma current, V is the applied voltage, V_i is the initial voltage, and C is the constant. Some of the proponents of the Eq. (1) model include [5,8,19,20,21]. According to [8], the form of the constant C in Eq. (1) is a function of geometry. The next model of the (*I-V*) characteristic, as proposed by [7,14,15,22], has the equation form as.

$$I = C\left(V - V_i\right)^2. \tag{2}$$

This study will use the Eq. (2) model as a reference in the calculation of the (*I-V*) characteristic model, with constant C being a geometric function of the capacitance as proposed by [14,15]. The electrode active of the CEM-P configuration has a pentagonal shape. The width and length of the rectangular plate are a and b, respectively, while the width and sharp angle of the triangular plate are d and 2θ, respectively. In comparison, the thickness of the electrode active is skinny ($\delta \cong 0.00015$ meters). The distance between the lower end of electrode active and electrode passive is equal to c. The Electrode passive has a rectangular plane configuration with a big area to accommodate all the flow of electric plasma flux from the electrode active to the electrode passive. If a dc voltage difference of V between the two electrodes is attached, then a corona plasma discharge event can be created, producing an electric current. The electrode scheme with the CEM-P configuration is found in Figure 1.a.

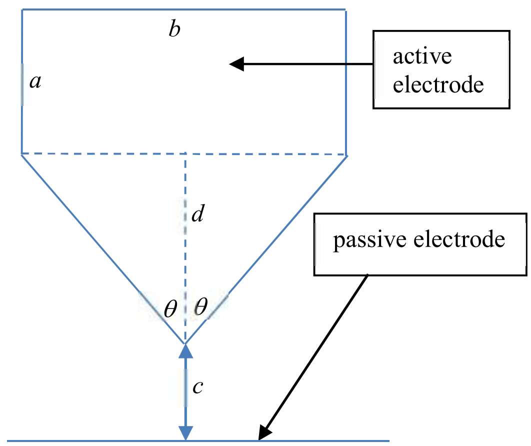

(a)

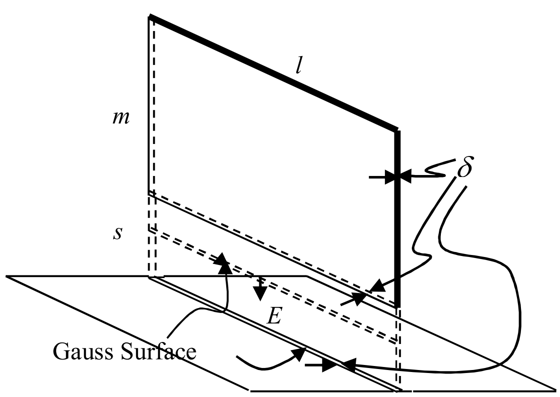

(b)

Figure 1. The electrode model Illustration for (a) the CEM-P configuration and (b) the L-P Configuration [14,15].

Figure 1.a. is a two-dimensional representation of the CEM-P electrode configuration model. According to geometric calculations, the most significant plasma flow will come out from the lower center end of the pointed active electrode. Furthermore, a smaller stream of plasma will come out of the pointed end of the electrode on both sides of the active electrode. In comparison, the most negligible flow will come out of the sharp lower triangular surface of the active electrode. A passive electrode will accommodate all the plasma flow under the active electrode. For the calculation of the capacitance model of the active electrode system, it has two conditions, namely:

a. For plasma flow straight down, the pentagon-shaped capacitance calculation is transformed into rectangular and triangular capacitances.
b. For the plasma flow coming out of the left and right sides of the active electrode, the capacitance value will be calculated using the integration technique of the capacitance elements.

Before calculating the capacitance value of the electrode model with the CEM-P configuration, a simpler electrode model is needed as the basis for calculating the CEM-P configuration model, namely the electrode model with the Line-Plane (*L-P*) configuration [14,15]. This electrode model consists of two rectangular plates in a mutually perpendicular position in the air. The active electrode has the area of the rectangle as lm (l and m are the lengths and width values of the plate, respectively) in a vertical position above the passive electrode, which is in a horizontal position. These plates have a thin thickness δ, and the distance between the two plates is s, as shown in Figure 1.b.

The total capacitance value of the electrode model with the *L-P* configuration, according to [14,15], can be written as,

$$C_{LP} = \varepsilon_0 \, l \ln\left|\frac{m+s}{s}\right| , \tag{3}$$

where ε_0 is the vacuum permittivity. By using formulation (3), we can derive the formulation of the capacitance element from the electrode model with the CEM-P configuration as shown in Figure 2.a,

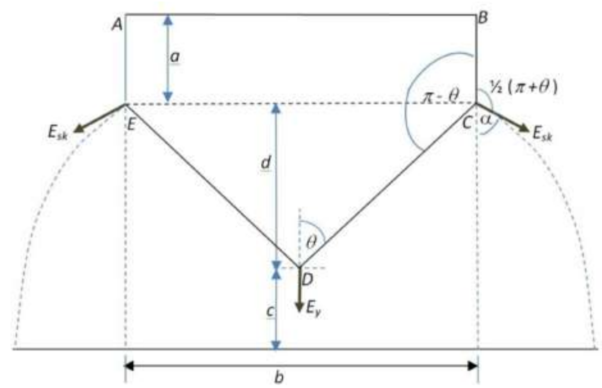

(a)

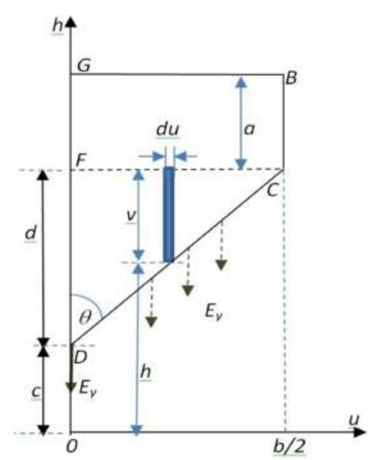

(b)

Figure 2. (a) Calculation of the corona plasma discharge electrode's capacitance with the CEM-P configuration has three plasma flows: the lower oblique of the right and left; and straight downward, (b). The plasma flows are calculated straight down, taking only half the right part of the plate. The enormous plasma flow is the one coming out of point *D*.

Figure 2.a shows the CEM-P electrode configuration model with plate 1 in the shape of an *ABCDE* five-angle plate in an upright position to plate 2, lying horizontally. In this study, the plasma flow was thought to have multiple flow directions that were visible out of some of the sharp surfaces of the electrodes. The flow direction is straight down (seen clearly out of point *D*) and towards the left oblique (seen at point *E*), and oblique to the right (seen at point *C*). Figure 2.b shows the calculation model of the plasma flow, which is specifically directed downward by taking half part of the electrode because it has a symmetrical character between the right and left sides of the *ABCDE* five-angle plate.

The *ABCDE* five-angle plate can be divided into two symmetrical plate areas, where half of the *ABCDE* plate consists of a *GBCF* rectangular plate and an *FDC* triangle. By adopting the Eq. (3) in Figure 2.b, the capacitance calculation of the *GBCF* rectangular plate electrode will produce a value,

$$C_{1A} = \varepsilon_0 \left(\frac{b}{2}\right) \ln \left| \frac{a+c+d}{c+d} \right| . \qquad (4)$$

To calculate the electrode capacitance value of the *FDC* triangular plate, we can make a comparison of the *FDC* triangular plate elements with the Eq. (3) so that the value of the capacitance element along with the boundary condition of variable *u* is obtained as,

$$dC_{1B} = \varepsilon_0 \, du \ln \left| \frac{v+h}{h} \right| ; \qquad 0 \le u \le \tfrac{1}{2} b \ , \qquad (5)$$

where there is a relationship

$$d + c = v + h \qquad \text{and} \qquad v = \frac{2ud}{b} \ . \qquad (6)$$

The variables *v* and *h* in Eq. (5) can be made as a function of *u* using Eq. (6). The capacitance value calculating results of the FDC triangle plate in Eq. (5) through the concept of integration is

$$\begin{aligned} C_{1B} = &\left\{ \varepsilon_0 \frac{b}{2d}(c+d) - \varepsilon_0 \frac{bc}{2d} \ln|c+d| \right\} \\ &+ \left\{ c\varepsilon_0 \frac{b}{2d} \ln|c| - c\varepsilon_0 \frac{b}{2d} \right\}. \end{aligned} \qquad (7)$$

From the comparison of Figures 2.a and 2.b, the *ABCDE* plate's capacitance value is two times that of the *GBCDF* plate. However, if the multiplier factor *k* is entered in the sharp surface around point *D* or at the limit condition $u = 0$ in Figure 2.b, then the capacitance value involving the *ABCDE* plate in the plasma flow downward is

$$\begin{aligned} C_1 = \varepsilon_0 \, b \ln &\left| \frac{a+c+d}{c+d} \right| + \frac{\varepsilon_0 b}{d} \Big[c + d - c \ln|c+d| \Big] \\ &+ \lim_{k \to \text{big value}} k \frac{\varepsilon_0 bc}{d} \Big[\ln|c| - 1 \Big]. \end{aligned} \qquad (8)$$

In the case of plasma flow out of the left and right oblique directions (points *E* and *C*) from the *ABCDE* plate in Figure 2.a, then plasma flow depiction for the case half the portion of the total *ABCDE* plate (i.e., *GBCDF* plate) is shown in Figure 3.a. From point *C* in the *GBCDF* plate, we assumed that there is a plasma flow that is curved at an angle of 60^0 (considered the mean angle of the observations) so that in the end, the plasma flow reaches the second plate (the passive electrode). The concept of plasma flow from the *GBCDF* plate in Figure 3.a will be easier to calculate if a simplification is made with the plate position on the *u-h* coordinate axis, respectively, on the horizontal and vertical coordinate axes as shown in Figure 3.b. Point *C* on the *GBCDF* plate is the tip of the sharp electrode surface that delivers a more significant amount of plasma than any other surface.

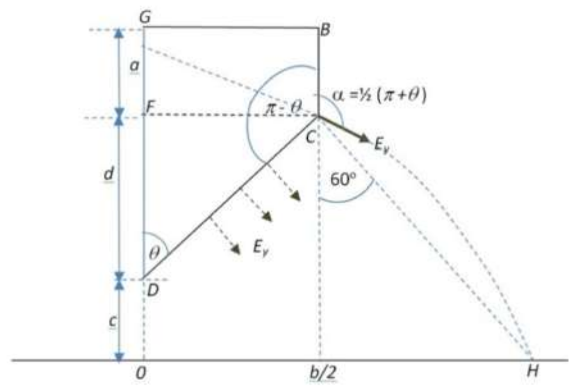

(a)

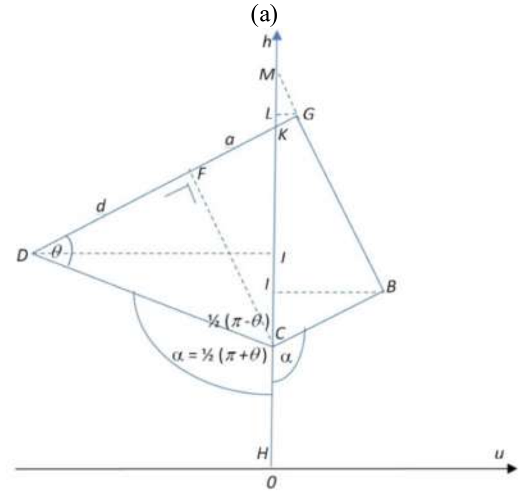

(b)

Figure 3. (a). The plasma outflows right obliquely from point *C*. The horizontal length of the plasma path on plate 2 is *l* sin 60^0, where *l* is the straight distance from the plasma path that exits from point *C* to the end of the *H* line, and the angle 60^0 is the mean angle of the observations. (b). The capacitance calculation model with a curved path *CH* is considered a straight line and functions as the vertical coordinate axis of variable *h* with the horizontal coordinate axis of variable *u*.

In the case of the CCP electrode, the sharper the electrode shape (the angle is getting taper), the plasma flow is also more excellent (which is indicated by the increasing value of *k*), so there is a relationship as $k \cong 1/\phi$, where ϕ is the acute angle at the end of the CCP electrode emitting plasma flow. If at point *C* which has an acute angle of 2θ and the multiplier factor of shape sharpness is k, then the magnitude of the shape sharpness factor at point C or E is equal to $k_1 = 2\theta k/(\pi-\theta)$.

The total capacitance in the case of plasma flow coming out of the right oblique electrode in Figure 3.a (with the depiction of the capacitance triangle in Figure 3.b) is,

$$C_2 = \left(\frac{2\theta}{\pi-\theta}\right)k\ C_{\mathrm{CBI}} + \left(\frac{2\theta}{\pi-\theta}\right)k\ C_{\mathrm{CDJ}} + \mathrm{C_{JDK}} + \mathrm{C_{IBM}} - \mathrm{C_{KGL}} - \mathrm{C_{LGM}}. \tag{9}$$

The multiplier factor k_1 is added to the capacitance-capacitance values of C_{CBI} and C_{CDJ} because the two electrodes are at the sharp end of the electrode at point C. The calculation of capacitance from C_{CBI} is based on the concept of the image in Figure 4,

By comparing the triangles and the same height limit from Figure 4, the values of v and h are obtained as,

$$v = \tan\left(\tfrac{1}{2}\theta\right)\left[d\sec\theta\cos\left(\tfrac{1}{2}\theta\right) - u\right],$$
$$h = 2(d+c) + u\tan\left(\tfrac{1}{2}\theta\right). \tag{10}$$

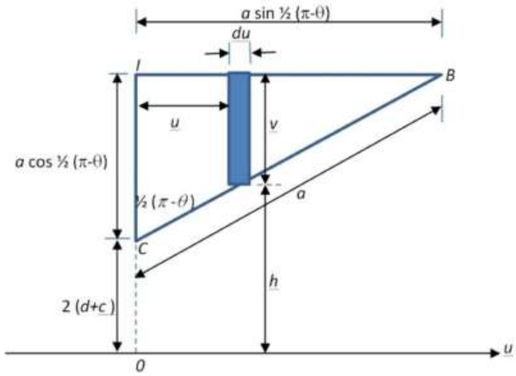

Figure 4. The concept of calculating the capacitance of an electrode C_{CBI}.

Through the formulation of the capacitance element and the boundary conditions of the variable u as,

$$dC_{CBI} = \varepsilon_0\, du \ln\left|\frac{v+h}{h}\right|, \quad 0 \le u \le a\cos\left(\tfrac{1}{2}\theta\right). \tag{11}$$

Table 1. Some capacitance boundary conditions for the triangular electrodes indexes name *CDJ*, *JDK*, *IBM*, *KGL* and *LGM*.

No.	Indexes name	v	h	boundary conditions of u
1.	*CDJ*	$d\sec\theta\sin\left(\tfrac{1}{2}\theta\right) - \tan\left(\tfrac{1}{2}\theta\right)u$	$2(d+c) + u\tan\left(\tfrac{1}{2}\theta\right)$	$-d\sec\theta\cos\left(\frac{1}{2}\theta\right) \le u \le 0$
2.	*JDK*	$d\sec\theta\sin\left(\tfrac{1}{2}\theta\right) - \tan\left(\tfrac{1}{2}\theta\right)u$	$2(d+c) + d\sec\theta\sin\left(\tfrac{1}{2}\theta\right)$	$-d\sec\theta\cos\left(\tfrac{1}{2}\theta\right) \le u \le 0$
3.	*IBM*	$a\cot\left(\tfrac{1}{2}\theta\right)\cos\left(\tfrac{1}{2}\theta\right) - u\cot\tfrac{1}{2}$	$2(d+c) + a\sin\left(\tfrac{1}{2}\theta\right)$	$0 \le u \le a\cos\left(\tfrac{1}{2}\theta\right)$
4.	*KGL*	$(a+d-d\sec\theta)\sin\left(\tfrac{1}{2}\theta\right)$ $-u\tan\left(\tfrac{1}{2}\theta\right)$	$2(d+c) + u\tan\left(\tfrac{1}{2}\theta\right)$ $+2d\sec\theta\sin\left(\tfrac{1}{2}\theta\right)$	$0 \le u \le 2(d+c) + 2d\sec\theta\sin\left(\tfrac{1}{2}\theta\right)$
5.	*LGM*	$\left[a\cos\left(\tfrac{1}{2}\theta\right) - u\right]\cot\left(\tfrac{1}{2}\theta\right)$ $-(d+d\sec\theta)\sin\left(\tfrac{1}{2}\theta\right)$	$2(d+c)+$ $(a+d+d\sec\theta)\sin\left(\tfrac{1}{2}\theta\right)$	$2(d+c) + a\sin\left(\tfrac{1}{2}\theta\right) + a\cos\left(\tfrac{1}{2}\theta\right)\cot\left(\tfrac{1}{2}\theta\right)$ $\le u \le 2(d+c) + (a+d+d\sec\theta)\sin\left(\tfrac{1}{2}\theta\right)$

Table 2. Some capacitance values for the triangular electrodes.

No.	Indexes name	The triangle capacitance value
1.	*CDJ*	$\varepsilon_0 d\sec\theta\cos\tfrac{1}{2}(\theta)\ln\left\|\frac{2(d+c)+d\sec\theta\sin\frac{1}{2}(\theta)}{2(d+c)-d\sec\theta\sin\frac{1}{2}(\theta)}\right\| + \frac{2\varepsilon_0(d+c)}{\tan\frac{1}{2}(\theta)}\ln\left\|\frac{2(d+c)-d\sec\theta\sin\frac{1}{2}(\theta)}{2(d+c)}\right\|$ $+\varepsilon_0 d\sec\theta\cos\tfrac{1}{2}(\theta)$
2.	*JDK*	$2\varepsilon_0 d\sec\theta\cos\tfrac{1}{2}(\theta)\ln\left\|3d\sec\theta\sin\left(\tfrac{1}{2}\theta\right)+2(d+c)\right\| - \varepsilon_0 d\sec\theta\cos\tfrac{1}{2}(\theta)\ln\left\|2d\sec\theta\sin\left(\tfrac{1}{2}\theta\right)+2(d+c)\right\|$ $+\left[2\varepsilon_0(d+c)\cot\left(\tfrac{1}{2}\theta\right)+\varepsilon_0 d\sec\theta\cos\left(\tfrac{1}{2}\theta\right)\right]\ln\left\|\frac{2d\sec\theta\sin\left(\frac{1}{2}\theta\right)+2(d+c)+d\sec\theta\sin\frac{1}{2}(\theta)}{d\sec\theta\sin\left(\frac{1}{2}\theta\right)+2(d+c)+d\sec\theta\sin\frac{1}{2}(\theta)}\right\|$ $-\varepsilon_0 d\sec\theta\cos\tfrac{1}{2}(\theta)\ln\left\|d\sec\theta\sin\tfrac{1}{2}(\theta)+2(d+c)\right\| - \varepsilon_0 d\sec\theta\cos\tfrac{1}{2}(\theta)$

3.	*IBM*	$\varepsilon_0\left[a\sin\tfrac{1}{2}(\theta)+2(d+c)\tan\tfrac{1}{2}(\theta)+a\sin\tfrac{1}{2}(\theta)\tan\tfrac{1}{2}(\theta)\right]\ln\left\|a\cos\tfrac{1}{2}(\theta)\cot\tfrac{1}{2}(\theta)+2(d+c)+a\sin\tfrac{1}{2}(\theta)\right\|$ $-\varepsilon_0\left[2(d+c)\tan\tfrac{1}{2}(\theta)+a\sin\tfrac{1}{2}(\theta)\tan\tfrac{1}{2}(\theta)\right]\ln\left\|2(d+c)+a\sin\tfrac{1}{2}(\theta)\right\|$ $-\varepsilon_0\, a\cos\tfrac{1}{2}(\theta)\ln\left\|\, 2(d+c)+a\sin\tfrac{1}{2}(\theta)\right\|-\varepsilon_0 a\cos\tfrac{1}{2}(\theta)$
4.	*KGL*	$\varepsilon_0\left[2(d+c)+2d\sec\theta\sin\tfrac{1}{2}\theta\right]\ln\left\|\,(a+d)\sin\left(\tfrac{1}{2}\theta\right)+2(d+c)+d\sec\theta\sin\left(\tfrac{1}{2}\theta\right)\right\|$ $+\left[2\varepsilon_0(d+c)\cot\left(\tfrac{1}{2}\theta\right)+2\varepsilon_0 d\sec\theta\cos\left(\tfrac{1}{2}\theta\right)\right]\ln\left\|2(d+c)+2d\sec\theta\sin\left(\tfrac{1}{2}\theta\right)\right\|$ $-\begin{bmatrix}2\varepsilon_0(d+c)\cot\left(\tfrac{1}{2}\theta\right)+2\varepsilon_0 d\sec\theta\cos\left(\tfrac{1}{2}\theta\right)\\ +2\varepsilon_0(d+c)+2\varepsilon_0 d\sec\theta\sin\tfrac{1}{2}\theta\end{bmatrix}\ln\begin{vmatrix}2d\sec\theta\sin\left(\tfrac{1}{2}\theta\right)+2(d+c)\tan\left(\tfrac{1}{2}\theta\right)\\ +2d\sec\theta\sin\tfrac{1}{2}\theta\tan\left(\tfrac{1}{2}\theta\right)+2(d+c)\end{vmatrix}$ $+2\varepsilon_0(d+c)+2\varepsilon_0 d\sec\theta\sin\tfrac{1}{2}\theta$
5.	*LGM*	$\varepsilon_0\begin{bmatrix}2(d+c)\tan\left(\tfrac{1}{2}\theta\right)+a\cos\left(\tfrac{1}{2}\theta\right)\\ +a\sin\left(\tfrac{1}{2}\theta\right)\tan\left(\tfrac{1}{2}\theta\right)\end{bmatrix}\ln\left\|\frac{2(d+c)+a\sin\left(\tfrac{1}{2}\theta\right)+a\cos\left(\tfrac{1}{2}\theta\right)\cot\left(\tfrac{1}{2}\theta\right)}{2(d+c)+(a+d+d\sec\theta)\sin\left(\tfrac{1}{2}\theta\right)}\right\|$ $+\varepsilon_0(d+d\sec\theta)\tan\left(\tfrac{1}{2}\theta\right)\sin\left(\tfrac{1}{2}\theta\right)-\varepsilon_0 a\cos\left(\tfrac{1}{2}\theta\right)$

We get the value of the capacitance C_{CBI} as,

$$\begin{aligned}C_{CBI} &= \varepsilon_0 a\cos\left(\tfrac{1}{2}\theta\right)\\ &-2\varepsilon_0(d+c)\cot\left(\tfrac{1}{2}\theta\right)\ln\left|\frac{2(d+c)+a\sin\left(\tfrac{1}{2}\theta\right)}{2(d+c)}\right|.\end{aligned} \tag{12}$$

The calculation of units along with other capacitance values from Eq. (9) can be seen in tables 1 and 2. Using Eqs. (9), (12) and table 2, then the capacitance part value is obtained in the case of plasma flow coming out of the right oblique direction of the electrode, as

$$\begin{aligned}C_2 = \left(\frac{2\theta}{\pi-\theta}\right)k&\left\{\begin{aligned}&\varepsilon_0 d\sec\theta\cos\tfrac{1}{2}(\theta)\ln\left|\frac{2(d+c)+d\sec\theta\sin\tfrac{1}{2}(\theta)}{2(d+c)-d\sec\theta\sin\tfrac{1}{2}(\theta)}\right|+\varepsilon_0 a\cos\left(\tfrac{1}{2}\theta\right)\\ &+2\varepsilon_0(d+c)\cot\left(\tfrac{1}{2}\theta\right)\ln\left|\frac{2(d+c)-d\sec\theta\sin\tfrac{1}{2}(\theta)}{2(d+c)+a\sin\left(\tfrac{1}{2}\theta\right)}\right|+\varepsilon_0 d\sec\theta\cos\tfrac{1}{2}(\theta)\end{aligned}\right\}\\
&-\varepsilon_0\left[2(d+c)\tan\tfrac{1}{2}(\theta)+a\sin\tfrac{1}{2}(\theta)\tan\tfrac{1}{2}(\theta)+a\cos\tfrac{1}{2}(\theta)\right]\ln\left|2(d+c)+a\sin\tfrac{1}{2}(\theta)\right|\\
&-\varepsilon_0\left[4(d+c)\cot\left(\tfrac{1}{2}\theta\right)+4d\sec\theta\cos\left(\tfrac{1}{2}\theta\right)\right]\ln\left|2d\sec\theta\sin\left(\tfrac{1}{2}\theta\right)+2(d+c)\right|\\
&+\varepsilon_0\left[2(d+c)\cot\left(\tfrac{1}{2}\theta\right)+3d\sec\theta\cos\tfrac{1}{2}(\theta)\right]\ln\left|3d\sec\theta\sin\left(\tfrac{1}{2}\theta\right)+2(d+c)\right|\\
&-\varepsilon_0 d\sec\theta\cos\tfrac{1}{2}(\theta)\ln\left|\,d\sec\theta\sin\tfrac{1}{2}(\theta)+2(d+c)\,\right|\\
&+\varepsilon_0\begin{bmatrix}2(d+c)\tan\left(\tfrac{1}{2}\theta\right)+a\sin\left(\tfrac{1}{2}\theta\right)\tan\left(\tfrac{1}{2}\theta\right)\\ +a\cos\left(\tfrac{1}{2}\theta\right)-2(d+c)-2d\sec\theta\sin\tfrac{1}{2}\theta\end{bmatrix}\ln\left|2(d+c)+(a+d+d\sec\theta)\sin\left(\tfrac{1}{2}\theta\right)\right|\\
&+\varepsilon_0\left[a\sin\tfrac{1}{2}(\theta)-a\cos\left(\tfrac{1}{2}\theta\right)\right]\ln\left|a\cos\tfrac{1}{2}(\theta)\cot\tfrac{1}{2}(\theta)+2(d+c)+a\sin\tfrac{1}{2}(\theta)\right|\\
&+\varepsilon_0\begin{bmatrix}2(d+c)\cot\left(\tfrac{1}{2}\theta\right)+2d\sec\theta\cos\left(\tfrac{1}{2}\theta\right)\\ +2(d+c)+2d\sec\theta\sin\tfrac{1}{2}\theta\end{bmatrix}\ln\begin{vmatrix}2(d+c)+2d\sec\theta\sin\left(\tfrac{1}{2}\theta\right)+2(d+c)\tan\left(\tfrac{1}{2}\theta\right)\\ +2d\sec\theta\sin\tfrac{1}{2}\theta\tan\left(\tfrac{1}{2}\theta\right)\end{vmatrix}\\
&-\varepsilon_0(d+d\sec\theta)\tan\left(\tfrac{1}{2}\theta\right)\sin\left(\tfrac{1}{2}\theta\right)-\varepsilon_0 d\sec\theta\cos\left(\tfrac{1}{2}\theta\right)-2\varepsilon_0(d+c)+2\varepsilon_0 d\sec\theta\sin\left(\tfrac{1}{2}\theta\right).\end{aligned} \tag{13}$$

By using the depiction symmetrical nature of the plasma flow of part half electrodes in the downward direction (Figure 2.b) and the right oblique direction (Figure 3.a) to the depiction total of the electrodes in Figure 2.a, then we get the total capacitance value of the electrode model with the CEM-P configuration is

$$C_{tot} = C_1 + 2C_2\ , \tag{14}$$

where C_1 and C_2 are the capacitance values in Eqs. (8) and (13), respectively.

The classical Gauss law concept is used to determine the electric current value of the electrode model with the CEM-P configuration. The amount of electric charge flowing between the two electrodes is equal to $q = C_{\mathrm{tot}}\,\Delta V$. The magnitude of the electric field in the air that is perpendicular downward (along the y axis) between two thin plates (plate thickness $\delta \cong 0.00015$ meters) at the position of the plates that are perpendicular to each other, as shown in Figure 1.a, can be written as [14,15]

$$E_y = \frac{q}{\varepsilon_0 (\Delta A)} = \frac{C_{tot}\ \Delta V}{\varepsilon_0\ (b\delta + \delta^2)}, \tag{15}$$

where the Gauss area is defined as $\Delta A = (b\delta + \delta^2)$ and the notation δ is defined as the thickness value of plate 1. The voltage difference $\Delta V = V - V_i$, where V is the applied voltage and V_i is the threshold voltage of the corona.

The total value of the electric current that leaves the electrode system with the CEM-P configuration using the concept of geometric calculations can be defined as [14,15]

$$I = -\frac{\mu_0}{\Delta V}\left(qE_y^{\ 2}\right)_{tot} = -\frac{\mu_0 \{C_{tot}\}^3}{\varepsilon_0^{\ 2}\left(b\delta + \delta^2\right)^2}(V - V_i)^2, \tag{16}$$

where $\varepsilon_0 = 8.854 \times 10^{-12}$ F m^{-1} and $\mu_0 = 4\pi \times 10^{-7}$ Hm^{-1}. Eq. (16) is the formulation of the electric current function I as a function of the voltage V that will characterize the (I-V) theoretical curve at the corona plasma discharge case. This study compared the (I-V) curve and the experimental data points. The sharpness factor of geometric shapes k (contained in the formula of C_{tot}), which is obtained fittingly through a comparison of the theory and experiment results, is the multiplication factor of the current in the corona plasma discharges concept when compared to the ordinary electronic circuit's.

3. EXPERIMENT TECHNIQUE

The electronic circuit arrangement of the corona plasma discharge equipment is shown in Figures 2.a and 2.b and consists of

1. The HV high-voltage source in the DC generator equipment (voltage 4 kV and frequency 25 kHz) is connected to the electrodes with the CEM-P configuration.
2. The electric current measuring instrument uses an analog Multimeter with SANWA brand (type YX-360TREB, voltage 220 V, and frequency 50/60 Hz), arranged in series with the main circuit.
3. The potential difference measuring instrument uses a digital multimeter with SANWA brand CD771.
4. HV probe equipment can convert the potential difference in kV into volts. The electric current that goes to the Voltmeter was passed through the HV probe (Maximum Voltage DC 40 kV DC, model number: AC 28 kV PD-28, serial number: 01605733).

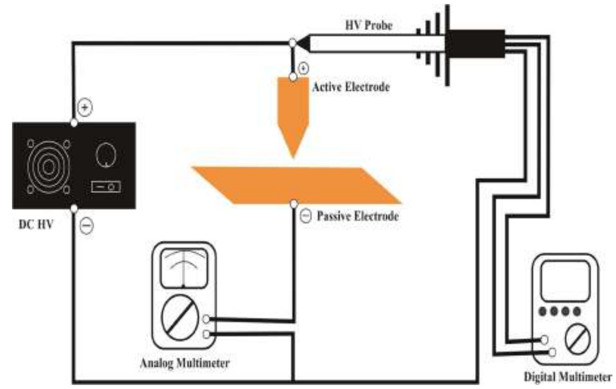

(a)

(b)

Figure 5. (a) and (b) show the circuit schematic and photos of the plasma discharge generator equipment for the CEM-P configuration model, respectively.

4. RESULTS OF SIMULATION AND EXPERIMENT

In the plasma discharge experiment of the CEM-P configuration model, the lower triangular ends of the active electrode have four different angle variations. In Figure 2.a, an active electrode section has several lengths and angles from the pentagon plate. There are several sizes of the same length of the active electrode variations, namely $a = 0.01$ meters, $b = 0.01$ meters and $\delta = 0.00015$ meters. While the different sizes (variations) lie in the values of the length d and a half- acute angle θ is,

a. The Electrode Model 1: $d = 0.010$ meters and $\theta = 26{,}57^{o}$
b. The Electrode Model 2: $d = 0.015$ meters and $\theta = 18.44^{o}$
c. The Electrode Model 3: $d = 0.025$ meters and $\theta = 11.31^{o}$
d. The Electrode Model 4: $d = 0.030$ meters and $\theta = 9.46^{o}$

Plasma discharge photos of the four electrode models can be seen in Figure 6,

Model 1

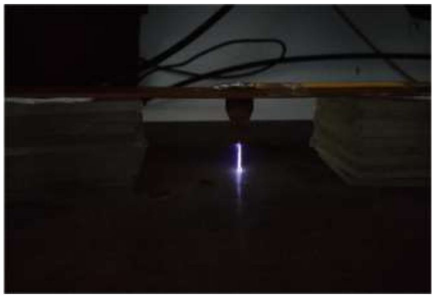

Model 2

Model 3

Model 4

Figure 6. The corona discharge photos of four electrode models.

The (*I*-*V*) characteristic graph of the corona discharge case for the CEM-P configuration model was made using the Python Graphical User Interface (*GUI*) Programming [23]. The graph is obtained from the numerical calculations in Eq. (16) for the appropriate value of *k*. Besides describing graphs and calculating the proper *k* value, this GUI program can also calculate graph error values consisting of standard deviation (*SD*) and t-tests. The explanation of the t-test and *SD* values in this study is

- The t-test value is a parameter that shows the degree of correspondence between the numerical simulation curve and the research data [23] for the (*I*-*V*) characteristic graph. The smaller the t-test value (which should be less than 0.05), the higher the level of conformity/accuracy between the two functions (simulation curve and research data).
- The value of *SD* (standard deviation) σ_{I} in the GUI program for this research comes from the distribution of the measured data up to order of power two of functions *V* in the polynomials [24]:

$$I = a_1 + a_2 V + a_3 V^2 \quad ; \quad \sigma_1 = \sqrt{\frac{\sum_j \left(I - A_1 - A_2 V_j - A_3 V_j^2 \right)^2}{(N-2)}}, \tag{17}$$

where a_1, a_2, and a_3 are constants that can be calculated. The values of A_1, A_2, and A_3 [24] are obtained through equation (18),

$$\begin{bmatrix} N & \sum V_j & \sum V_j^2 \\ \sum V_j & \sum V_j^2 & \sum V_j^3 \\ \sum V_j^2 & \sum V_j^3 & \sum V_j^4 \end{bmatrix} \begin{bmatrix} A_1 \\ A_2 \\ A_3 \end{bmatrix} = \begin{bmatrix} \sum I_j \\ \sum V_j I_j \\ \sum V_j^2 I_j \end{bmatrix}. \tag{18}$$

The *SD* formula in Eq. (17) is compatible with formula (16) to determine the degree of compatibility between the numerical simulation formula and the research data.

Two (*I*-*V*) characteristic graphs for each model (with the same angle of θ) are obtained from two variations of *c* values. The *k* factor value, *SD* value, and t-test value are also included in each graph. The display of the (*I*-*V*) characteristic graphs for the four-electrode models is presented in Figure 7.

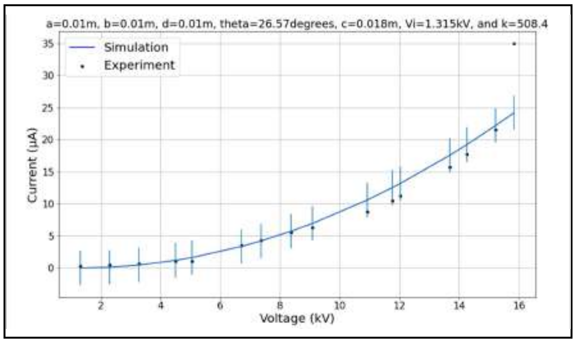

(a)

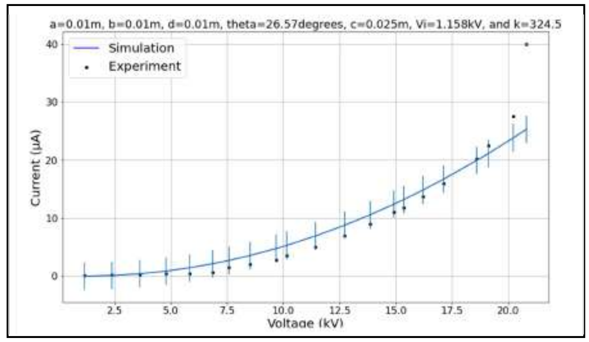

(b)

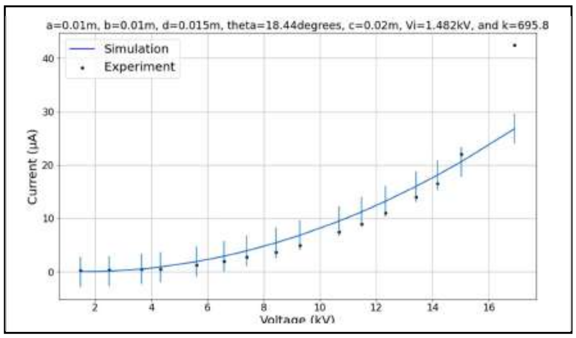

(c)

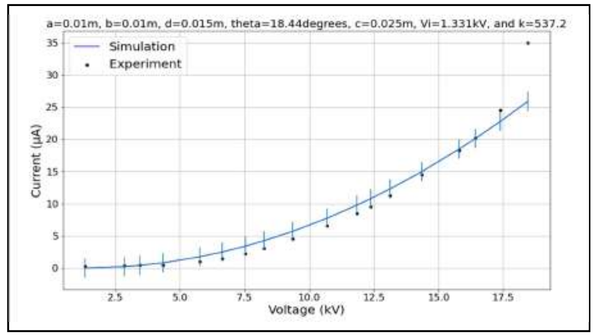

(d)

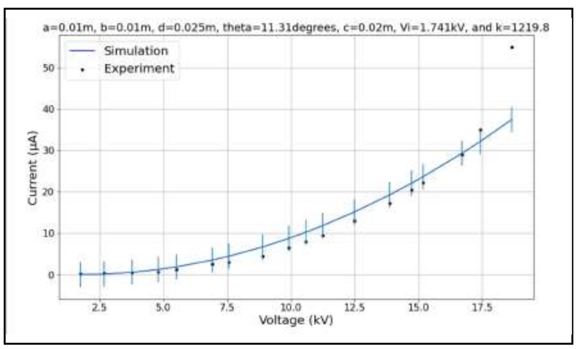

(e)

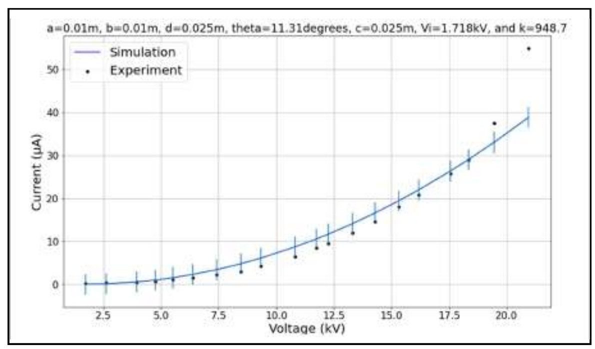

(f)

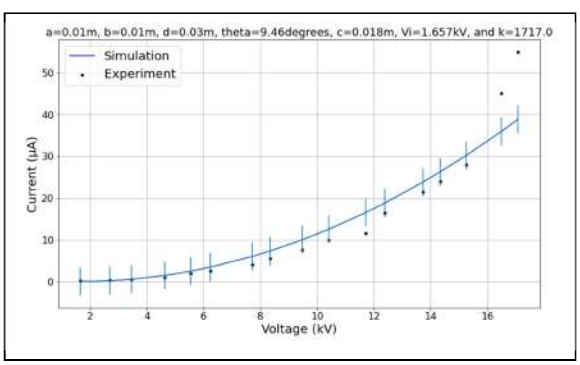

(g)

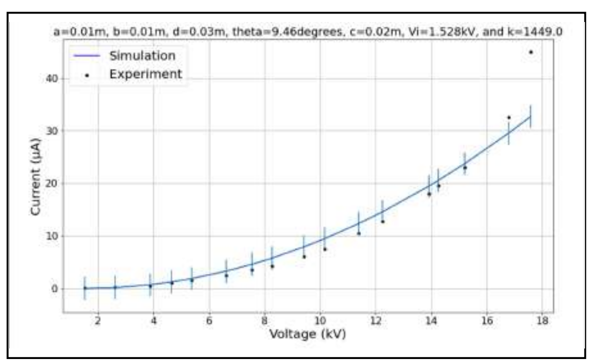

(h)

Figure 7. The (*I-V*) Characteristic graph of the corona plasma discharges with the CEM-P configuration at various angles θ and different distances c. (a) and (b) are graphs for Model 1 of distances c = 0.018 m and c = 0.025 m, respectively. (c) and (d) are graphs for Model 2 of distances c = 0.020 m and c = 0.025 m, respectively. (e) and (f) are graphs for Model 3 of distances c = 0.020 m and c = 0.025 m, respectively. (g) and (h) are graphs for Model 4 of distances c = 0.018 m and c = 0.020 m, respectively.

The calculation data for the factor *k*, the *SD* values, and the t-test values in Figure 7 are written in Table 3. On each graph in Figure 7, short vertical lines (*SVL*) connect the data points with the simulation curves. In Figure 7 also, we can manually calculate the values of the number of data points (*NDP*) and the number of tangent points (*NTP*) which is defined as the number of data points that intersect the simulation curve through the *SVL*, and the percentage of tangent points (*PTP*) which is the ratio between *NDP* to *NTP*. A list of the values of *NDP*, *NTP*, and *PTP* is also presented in table 3.

Table 3. Values of the factor *k*, *SD*, and t-test of the (*I-V*) characteristic functions graphs in Figure 7 for different values of *c*.

Model		*c* (m)	*k*	*SD*	t-test	Number of tangent points	Number of data points	Percentage of tangent points
1	$\theta = 26{,}57^{\circ}$	0.018	508.4	2.6831	0.0468	15	16	93.75 %
		0.025	324.5	2.3665	0.0399	19	21	90.48 %
2	$\theta = 18.44^{\circ}$	0.020	695.8	2.8317	0.0496	15	16	93.75 %
		0.025	537.2	1.4871	0.0448	17	18	94.44 %
3	$\theta = 11.31^{\circ}$	0.020	1219.8	3.0485	0.0475	17	18	94.44 %
		0.025	948.7	2.4341	0.0482	18	20	90.00 %
4	$\theta = 9.46^{\circ}$	0.018	1717.0	3.3546	0.0481	14	17	82.35 %
		0.020	1449.0	2.1841	0.0500	15	17	88.24 %

From the (*I-V*) characteristic graph in Figure 7 and from Table 3, which shows the *SD* and the t-test values, as well as from the calculation of the factor *k* based on the variation of the distance between the two electrodes of the *c*, turned out to produce several trends in cases that arise in this study including:

i. The fit between the line simulated curves with the experimental data points occurs in the low-current portion of the corona plasma discharge.
ii. The *SD* values are relatively large for all graphs, whose values vary between 1.4871-3.3546, and the t-test values for almost all graphs are still below 0.5 (except for the case of θ = 9.46° with *c* = 0.020). Similarly, the whole graph has relatively large *PTP* values (82.35 % – 94.44 %).
iii. For all variations of the electrodes model, we will see that if the models have a sharper half- acute angle θ, the values of the factor *k* will be greater.
iv. For the case of the same electrodes model, we get research results that the farther the distance between the two electrodes (the greater the value *c*), the values of the factor *k* will be smaller.

5. DISCUSSION

From various research results on the (*I-V*) characteristics of corona discharge such as [5,6,19] etc., the level of match between corona current vs voltage occurred only in the case of low current, not in the case of the sharply increasing current. So this study is the same as many cases of previous studies on the (*I-V*) characteristics of corona discharge.

We concluded that the degree of correspondence between the data points and the simulation curve (representing numerical calculation on the Eq. (16)) is relatively high. The statement is based on several measurable categories (use *GUI* programming result) for all graphs in Figure 7, such as

i. The values of PTP are relatively large (between 82.35 % – 94.44 %).
ii. The values of the t-test are almost less than 0.5.
iii. Although some factors do not support it, the *SD* values are relatively large (between 1.4871-3.3546). The large enough *SD* values mean that the *SVL* sizes are quite long [15].

The best graph in Figure 7 is a combination of low *SD* and t-test values and has a high PTP value, which is suitable for the case of Model 2 (θ= 18.44°) at *c* = 0.025 m.

The conclusion from the research results [16] is that the sharper the tip of the active electrode used in the case of corona discharge, the larger and brighter the flow of corona current will be. The factor *k* in this study is a multiplier factor of the corona current magnitude that emerges from the lower end of the sharp surface of the active electrode. The concept of the factor *k* is clear based on the research [16]. We conclude that the sharper the tip of the active electrode, the greater the value of the factor *k*.

Another result obtained in this study (in table 3) is that the greater the value of *c*, the smaller the value of the factor *k*. Figure 6 shows that this study's largest corona current is derived from the corona current coming out of the lower end of the active electrode or out of point *D* in Figure 2.a. The capacitance value of the area (ΔEDC) = 2 × area (ΔFDC) in Figure 2, which contains the current multiplier factor *k*, is part of the formulation of Eq. (8) is

$$C_{EDC} = \lim_{k \to \text{big value}} k \frac{\varepsilon_0 bc}{d}\left[\ln|c| - 1\right]. \tag{19}$$

The values of *b* and *d* in Eq. (18) are constant on the change variation of distance *c*. Suppose it is considered that the C_{EDC} capacitance value is close to a constant on the difference in the value of *c*. In Eq. (18), there is a tendency if the value of *c* is getting bigger it will make the value of *k* tend to be smaller, or vice versa if the value of *c* is getting smaller, then the value of *k* tends to be bigger.

6. CONCLUSION

The calculation results of the values of the fitting factor *k*, *SD* errors, and t-test in table 2 for the (*I-V*) characteristics case conclude that there is a high degree of conformity between numerical calculations and research data. This high degree of the agreement indicates that Eq. (16) is suitable as a general formulation of the (*I*-*V*) characteristics for the corona plasma discharge model with the Chisel Eye and Midpoint-Plane (CEM-P) electrode configuration. However, there may be deviations from the research results stemming from the negligence of the researchers' observations, the imprecision and asymmetry of the shape and position of the active electrode installation, energy leakage, and other problems that may occur from the physical properties of the corona discharge case.

ACKNOWLEDGMENT

The financials in this work get supported by non-tax revenue (PNBP), Diponegoro University, Semarang, Indonesia, with the schema of International Publication Research (RPI) in 2022. (No. 569-100/UN7.D2/PP/VII/2022).

REFERENCES

[1] Stambouli, A.B., Benallal, R., Oudini, N., Mesli, S.M., Tadjine, R. (2017). Control of Dual Frequency Capacitively Coupled Plasma via blocking capacitor and phase angle. European Physical Journal Applied Physics, 80: 10802. https://doi.org/10.1051/epjap/2017170180

[2] Tabares, F.L., Junkar, I. (2021). Cold plasma systems and their application in surface treatments for medicine. Molecules, 26(7). https://doi.org/10.3390/molecules26071903

[3] Saikia, P., Bhuyan, H., Escalona, M., Favre, M., Wyndham, E., Maze, J., Schulze, J. (2018). Study of dual radio frequency capacitively coupled plasma: an analytical treatment matched to an experiment. Plasma Sources Science and Technology, 27(1): 015014. https://doi.org/10.1088/1361-6595/aaa565

[4] Townsend, J.S. (1914) The potentials requires to maintain currents between coaxial cylinders. The London, Edinburgh, and Dublin Philosophical Magazine and Journal of Science, 28: 83-90. https://doi.org/10.1080/14786440708635186

[5] Robinson, M. (1967). The Corona Threshold for Coaxial Cylinders in Air at High Pressures. IEEE Transactions on Power Apparatus and Systems, Pas-86:185-189.

[6] Zheng, Y., Zhang, B., He, J. (2015). Current-voltage characteristics of dc corona discharges in air between coaxial cylinders. Physics of Plasmas, 22: 023501. https://doi.org/10.1063/1.4907234

[7] Guan, Y., Vaddi, R.S., Aliseda, A., Novosselov, I. (2018). Analytical model of electrohydrodynamic flow in corona discharge. Physics of Plasmas, 25: 083507. https://doi.org/10.1063/1.5029403

[8] Robinson, M. (1961) Movement of Air in the Electric Wind of the Corona Discharge. Transactions of the American Institute of Electrical Engineers, 80: 143-150. https://doi.org/10.1109/TCE.1961.6373091

[9] Abe, H., Yoneda, M., Fujiwara, N. (2008). Developments of Plasma Etching Technology for Fabricating Semiconductor Devices. Japanese Journal of Applied Physics, 47(3): 1435-1455. https://doi.org/10.1143/JJAP.47.1435

[10] Vidaurre, E.F.C., Achete, C.A., Gallo, F., Garciam D., Simão, R.A., Habert, A.C. (2002). Surface Modification of Polymeric Materials by Plasma Treatment. Materials Research, 5(1): 37-41. https://doi.org/10.1590/S1516-14392002000100006

[11] Anders, A. (2005). Plasma and Ion Sources in Large Area Coatings: A review. Surface and Coatings Technology, 200: 1893-1906. https://doi.org/10.1016/j.surfcoat.2005.08.018

[12] Schmidt, H., Sansonnens, L., Howling, A.A., Hollenstein, C., Elyaakoubi, M., Schmitt, J.P.M. (2004). Improving plasma uniformity using lens-shaped electrodes in a large area very high frequency reactor. Journal of Applied Physics, 95: 4559-4564. https://doi.org/10.1063/1.1690096

[13] Bouremel, Y., Li, J.M., Zhao, Z., Debiasi, M. (2013). Effects of AC Dielectric Barrier Discharge Plasma Actuator Location on Flow Separation and Airfoil Performance. Procedia Engineering, 67: 270-278. https://doi.org/10.1016/j.proeng.2013.12.026

[14] Wardaya, A.Y., Muhlisin, Z., Hudi, A., Suseno, J.E., Nur, M., Kinandana, A.W., Windarta, J. (2020). A study of line-plane configuration in the Corona discharge theory. The European Physical Journal Applied Physics, 89: 30801. https://doi.org/10.1051/epjap/2020200011

[15] Wardaya, A.Y., Muhlisin, Z., Suseno, J.E., Nur, M., Triadyaksa, P., Khumaeni, A., Sarwoko, E.A., Windarta, J., Hadi, S. (2022). The Current-Voltage Characteristics for Electrode Geometry Model of Positive DC Corona Discharge in Air. Gazi University Journal of Science, 35: 1140-1150. https://doi.org/10.35378/gujs.885345

[16] Dobranszky, J., Bernath, A., Marton, H.Z. (2008). Characterisation of the plasma shape of the TIG welding arc. International Journal of Microstructure and Materials Properties 3(1): 126-140. https://doi.org/10.1504/IJMMP.2008.016949

[17] Hua, X., Li, T., Wu, C., Zhou, D., Fan, G., Li, X., Cong, K., Yan, Z., Wu, Z. (2022). Novel physical treatments (Pulsed light and cold plasma) improve the quality of postharvest apricots after long-distance simulated transportation. Postharvest Biology and Technology, 194(159): 112098. https://doi.org/10.1016/j.postharvbio.2022.112098

[18] Bora, J., Khan, T., Mahnot, N.K. (2022). Cold Plasma Treatment Concerning Quality and Safety of Food: A Review. Current Research in Nutrition and Food Science, 10(2): 427–446. https://doi.org/10.12944/CRNFSJ.10.2.3

[19] Moreau, E., Benard, N., Alicalapa, F., Douyere, A. (2015). Electrohydrodynamic force produced by a corona discharge between a wire active electrode and several cylinder electrodes-Application to electric propulsion. Journal of Electrostatics, 76: 194-200. https://doi.org/10.1016/j.elstat.2015.05.025

[20] Giubbilini, P. (1988). The current‐voltage characteristics of point‐to‐ring corona. Journal of Applied Physics, 64: 3730-3732. https://doi.org/10.1063/1.341368

[21] Yamada, K. (2004). An empirical formula for negative corona discharge current in point-grid electrode geometry. Journal of Applied Physics, 96: 2472. https://doi.org/10.1063/1.1775301

[22] Ferreira, G.F.L., Oliveira Jr., O.N., Giacometti, J.A. (1986). Point‐to‐plane corona: Current‐voltage characteristics for positive and negative polarity with evidence of an electronic component. Journal of Applied Physics, 59: 3045-3049. https://doi.org/10.1063/1.336926

[23] Boslaugh, S. (2012). Statistics in a nutshell: A desktop quick reference, Second Edition. O'Reilly Media, Inc., USA. ISBN-13: 978-1449316822, ISBN-10: 1449316824.

[24] Taylor, J.R. (1997). An introduction to error analysis, the study of uncertainties in physical measurements, second edition. University Science Books, USA. ISBN 0-935702-42-3. ISBN 0-935702-75-X.

NOMENCLATURE

I	Electric current, Ampere
V	Voltage, Volt
a, b	width and length of the rectangular plate, meters.
d	width of the triangular plate, meters.
c	distance between the lower end of electrode active and electrode passive, meters.
SD	Standard Deviation
k, k_1	shape sharpness factor (dimensionless)
C	constant (the geometric function)
C_1, C_2, .. ,C_{tot}	Capacitance, Coulomb/Volt
q	electrical charge, Coulomb
$\boldsymbol{E}$	electric field, N/C
ΔA	area, m^2

Greek symbols

θ	half- acute angle, radian
δ	plate thickness, meters
σ	standard deviation
ε_0	vacuum permittivity, 8.854×10^{-12} F m^{-1}
μ_0	vacuum permeability, $4\pi \times 10^{-7}$ Hm^{-1}
ϕ	acute angle at the end of the CCP electrode emitting plasma flow

Subscripts

i	threshold/initial
j	sum index
tot	total
CBI, CDJ, JDK, IBM, KGL, LGM	triangular electrodes indexes name

Accept Submission

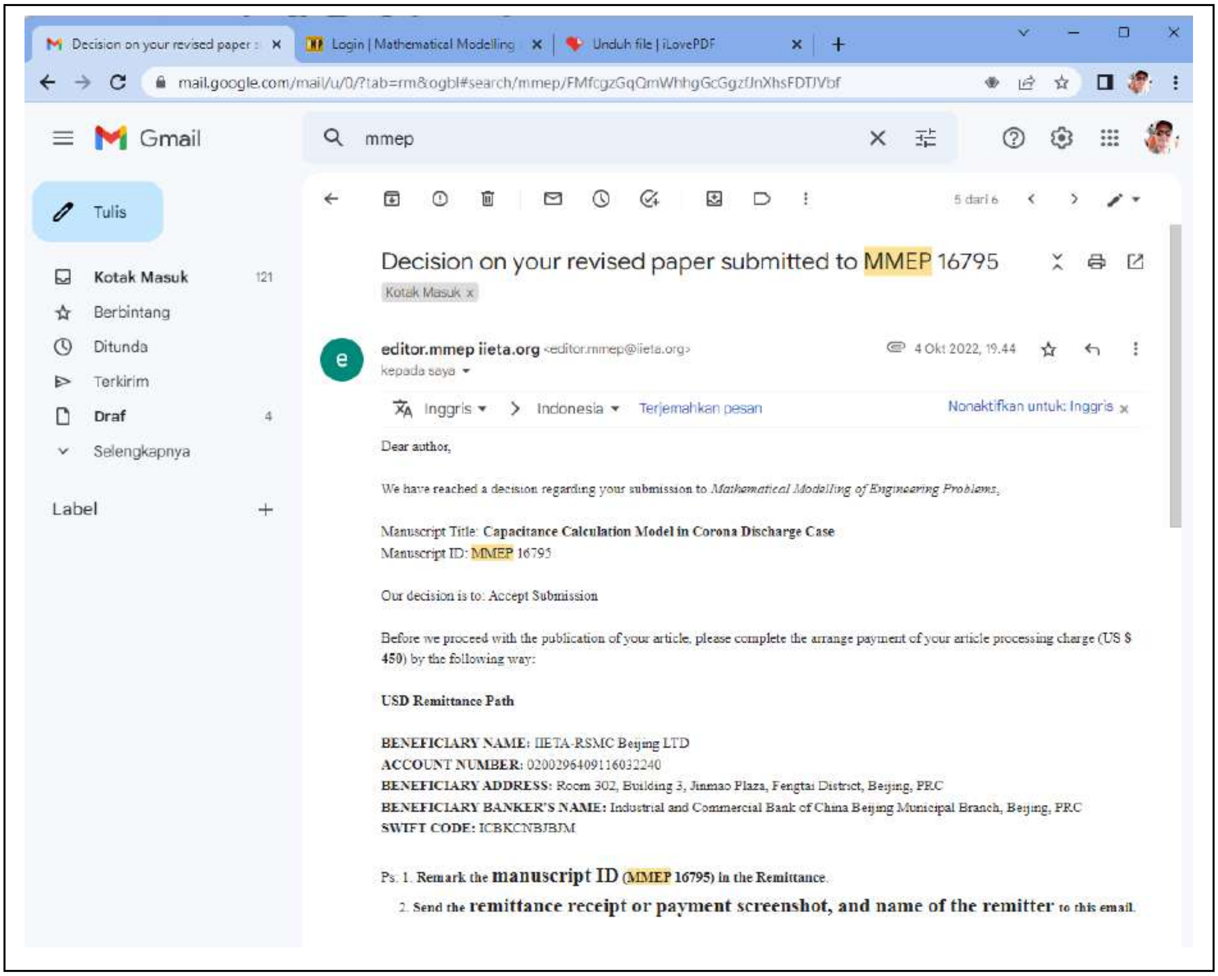
Decision on your revised paper submitted to MMEP 16795

editor.mmep iieta.org <editor.mmep@iieta.org>
kepada saya

4 Okt 2022, 19.44

Dear author,

We have reached a decision regarding your submission to *Mathematical Modelling of Engineering Problems*,

Manuscript Title: **Capacitance Calculation Model in Corona Discharge Case**
Manuscript ID: MMEP 16795

Our decision is to: Accept Submission

Before we proceed with the publication of your article, please complete the arrange payment of your article processing charge (US $ 450) by the following way:

USD Remittance Path

BENEFICIARY NAME: IIETA-RSMC Beijing LTD
ACCOUNT NUMBER: 0200296409116032240
BENEFICIARY ADDRESS: Room 302, Building 3, Jinmao Plaza, Fengtai District, Beijing, PRC
BENEFICIARY BANKER'S NAME: Industrial and Commercial Bank of China Beijing Municipal Branch, Beijing, PRC
SWIFT CODE: ICBKCNBJBJM

Ps. 1. **Remark the manuscript ID (MMEP 16795) in the Remittance.**

2. **Send the remittance receipt or payment screenshot, and name of the remitter to this email.**

If you have any questions, please do not hesitate to contact us.

Kind regards,

MMEP Editorial Board

Mathematical Modelling of Engineering Problems

http://www.iieta.org/Journals/MMEP

International Information and Engineering Technology Association (IIETA)

http://www.iieta.org/

IIETA International Information and Engineering Technology Association

Advancing the World of Information and Engineering

2 Lampiran • Dipindai dengan Gmail

Acceptance Lette...

IIETA Invoice-MM...

International Information & Engineering Technology Association
#2020, Scotia Place Tower One, 10060 Jasper Avenue, Edmonton,
AB T5J 3R8, Canada
Tel: +1 825 436 9306; Fax: +1 780 341 0600
www.iieta.org

IIETA International Information and Engineering Technology Association
Advancing the World of Information and Engineering

Acceptance Letter

Mathematical Modelling of Engineering Problems

October 4, 2022

Asep Yoyo Wardaya

Department of Physics, Faculty of Science and Mathematics, Diponegoro University
Semarang, Indonesia

Dear Asep Yoyo Wardaya, Zaenul Muhlisin, Jatmiko Endro Suseno, Charis Munajib, Susilo Hadi, Heri Sugito, Jaka Windarta

MS: Capacitance Calculation Model in Corona Discharge Case

I am pleased to inform you that as per the recommendation of the editorial board, your above-mentioned manuscript has been accepted for publication in Mathematical Modelling of Engineering Problems (ISSN 2369-0739).

Please note the following points, and ensure compliance:

1) Page Proofs of your paper will also be sent to you for minor corrections and approval.

2) Provide us with your E-mail ID for future correspondence.

3) Provide complete postal address with correct postal-code.

4) The corresponding author would receive a PDF of the published paper.

5) If your paper is found with plagiarism content after the release of Acceptance Letter, it will not be published in the Journal.

It is recommended that you cite this and other published works from International Information and Engineering Technology Association (www.iieta.org) in your papers to be published in other journals.

Yours sincerely,

INTERNATIONAL INFORMATION AND ENGINEERING TECHNOLOGY ASSOCIATION
IIETA
Seal
2013

Date: October 4, 2022
Place: Edmonton, Canada

International Information and Engineering Technology Association	**Invoice No.**	**20221004-16795**
Edmonton, AB T5J 3S4, Canada		

INVOICE

Customer		**Misc**	
Name	Asep Yoyo Wardaya	Date	4/10/2022
	Department of Physics, Faculty of Science and Mathematics, Diponegoro University	For	
City	Semarang Country Indonesia Post Code		
Phone			

Qty	Description	Unit Price	TOTAL
	INVOICE Publication fee for paper published in MMEP Title: Capacitance Calculation Model in Corona Discharge Case ID: 16795		USD 450.00
		Sub Total	USD 450.00
		Shipping	
	Tax Rate(S)	0.00%	USD -
		TOTAL	USD 450.00

Payment	Select One…
Comments	T/T advance payment USD$
Name	
CC #	
Expires	

Office Use Only

USD Remittance Path
BENEFICIARY NAME: IIETA-RSMC Beijing LTD
ACCOUNT NUMBER: 0200296409116032240
BENEFICIARY ADDRESS: Room 302, Building 3, Jinmao Plaza, Fengtai District, Beijing, PRC
BENEFICIARY BANKER'S NAME: Industrial and Commercial Bank of China Beijing Municipal Branch, Beijing, PRC
SWIFT CODE: ICBKCNBJBJM

Make all checks payable to **International Information and Engineering Technology Association**
Total due in 15 days. Overdue accounts subject to a service charge of 1% per month.

INTERNATIONAL INFORMATION AND ENGINEERING TECHNOLOGY ASSOCIATION
IIETA
Seal
2013

THANK YOU FOR YOUR BUSINESS!

Pembayaran Jurnal

5 dari 6

Acceptance Lette...

IIETA Invoice-MM...

Asep Wardaya <asepyoyowardayafisika@gmail.com>
kepada editor.mmep

6 Okt 2022, 12.43

Dear Editor

We have paid the processing fee of our article, which can be seen in the attachment where the remittance form says the purpose of the transaction is "Publication fee 16795 Asep Yoyo Wardaya", and the amount of the shipment is 450 USD. Thank you very much for your kindness.

Asep Yoyo Wardaya

Department of Physics, Faculty of Science and Mathematics, Diponegoro University, Semarang Indonesia

...

Satu lampiran • Dipindai dengan Gmail

Publication fee 16...

PT. BANK NEGARA INDONESIA (Persero), Tbk
CABANG : UNDIP SEMARANG

IBOC - Maintenance (S10)

Teller ID : 80414
Date : 06/10/2022
Time : 10:44:23

Sender's Reference:
:20:S10UDS00038322
Bank Operation Code:
:23B:CRED
Value Date/Currency/Interbank Settled Amount:
:32A:221006USD450,
Ordering Customer:
:50K:/0000000296571135
IYS SYABILLA RUSDA
AMBOKEMBANG RT 013 RW 006
PEKALONGAN INDONESIA
Ordering Institution:
:52A:BNINIDJAXXX
Account With Institution:
:57A:ICBKCNBJXXX
Beneficiary Customer:
:59:/0200296409116032240
IIETA RSMC BEIJING LTD
ROOM 302 BUILDING 3 JINMAO PLAZA
FENGTAI DISTRICT BEIJING PRC
CHINA SWIFT CODE ICBKCNBJBJMXXX
Remittance Information:
:70:INDUSTRIAL COMML BANK CHINA - BEIJ
INDUSTRIAL AND COMMERCIAL BANK OF
CHINA BEIJING MUNICIPAL BRANCH
BEIJING PRC ICBKCNBJXXX
Details Of Charges:
:71A:OUR
Sender to Receiver Information:
:72:PAYMENT OF PUBLICATION
FEE 16795 ASEP WARDAYA

BNI INDONESIA (PERSERO) Tbk KANTOR CAPEM TEMBALANG

BNI

BNI

REFERENCE : S10UDS00038322

NO. TRX. : 80414 900840 96962 TRAN 06/10/2022 10:35:24
NO. REK. : 000000296571135 IYS SYABILLA RUSDA
JUMLAH : IDR 419,625- 1568
261 - UNDIP SEMARANG

NO. TRX. : 80414 900840 96962 TRAN 06/10/2022 10:35:24
NO. REK. : 261360420801001 PENDAPATAN PROPISI KU
JUMLAH : IDR 35,000 1568
261 - UNDIP SEMARANG

NO. TRX. : 80414 900840 96962 TRAN 06/10/2022 10:35:24
NO. REK. : 261360482010001 Pendapatan Restitusi B
JUMLAH : IDR 384,625 1568
261 - UNDIP SEMARANG

NO. TRX. : 80414 900840 96962 TRAN 06/10/2022 10:35:24
NO. REK. : 000000296571135 IYS SYABILLA RUSDA
JUMLAH : IDR 6,923,250- 1568
261 - UNDIP SEMARANG

NO. TRX. : 80414 900840 96962 TRAN 06/10/2022 10:35:24
NO. REK. : 261840200101001 KU YAKIR
JUMLAH : USD 450 1568
261 - UNDIP SEMARANG

NEGARA INDONESIA (PERSERO) Tbk
BNI
CAPEM

BNI

Validasi:

Tanggal/ Date : 6-10-2022

Formulir Kiriman Uang
Remittance Application

SWIFT CODE = ICBKCNBJBJM

Penerima/ *Beneficiary* ☐ Penduduk/ *Resident* ☑ Bukan Penduduk/ *Non Resident*

Nama/ *Name* : IIETA - RSMC Beijing LTD

Alamat/ *Address* : Room 302, Building 3, Jinmao Plaza, Fengtai District, Beijing, PRC

Telepon/ *Phone* :

Kota/ *City* : Negara/ *Country* :

Bank Penerima/ *Beneficiary Bank* : Industrial and Commercial Bank of China Beijing Municipal Branch

Kota/ *City* : Beijing Negara/ *Country* : PRC

No. Rek./ *Acc. No.* : 0200296409116032240

Pengirim/ *Remitter* ☑ Penduduk/ *Resident* ☐ Bukan Penduduk/ *Non Resident*

Nama/ *Name* : IYS SYABILLA RUSDA

Nama Alias/ *Alias Name* :

No. ID KTP/SIM/ Passport/ KITAS : 3326141409900001

Alamat/ *Address* : Ambokembang RT 13 RW 06 Kedungwuni, Pekalongan

Telepon/ *Phone* : 085742022015

Kota/ *City* : Negara/ *Country* : Indonesia

Tujuan Transaksi (*Transaction Purpose*) : ....

Berita (*Message*) : Publication Fee 16795 Acep Yoyo Wardaya

Biaya dari bank koresponden dibebankan ke rekening/
Correspondent bank charges are for account of :
☐ Penerima/ *Beneficiary* ☐ Pengirim/ *Remitter* ☐ Sharing

Jenis Pengiriman/ *Type of Transfer* : ☐ LLG/ *Clearing* ☐ RTGS ☐ Draft ☑ SWIFT ☐ ....

Sumber Dana/ *Source of fund* :
☐ Tunai/ *Cash* ☐ Cek/ *BG No.* ....
☑ Debit Rek./ *Debit Acc. No.* ....

Mata Uang/ *Currency* : ☐ IDR ☑ USD ☐ ....

Jumlah Dana yang dikirim/ *Amount Transfer* :

Jumlah / *Amount*	Kurs/ *Rate*	Nilai/ *Total Amount*
450 USD	15.365	6.914.250

Biaya/ *Charge*	Valas/ *Amount in Foreign Exchange*	Kurs/ *Amount*	Nilai/ *Total Amount*
Komisi/ *Commission* Pengiriman/ *Handling* Bank Koresponden / *Correspondent Bank* KOM 25.000 UPK 364.625			
Jumlah Biaya / *Amount Charge* :			7.312.875
Total yang dibayarkan/ *Total Amount*			

Terbilang/ *Amount in Words* : Tujuh Juta tiga ratus empat puluh dua ribu delapan ratus tujuh puluh lima rupiah

Saya menyetujui sepenuhnya syarat-syarat yang tercantum pada halaman belakang formulir ini / *I unconditionally accept all the terms and conditions on the reverse form.*

PT BANK NEGARA INDONESIA (Persero) BNI KANTOR CAPEM TEMBALANG

Pejabat Bank/ *Bank Officer* Teller Pemohon/ *Applicant*

IYS Syabilla Rusda

KMU 1.0/PU/0711

Sah jika ada cetakan data komputer atau tanda tangan yang berwenang/ *The application form will be valid if there is a computerized validation or the authorized signature.*
- Transaksi oleh Walk In Customer (WIC) di atas Rp. 100 juta atau nilai yang setara dengan itu wajib mengisi form PMN (KYC)/ *Transaction by Walk In Customer amounting exceeds Rp. 100.000.000,- (one hundred million rupiahs) or equivalent value must fill in the PMN (KYC) form.*
- Transaksi oleh bukan penduduk di atas USD 10.000 atau ekuivalen wajib mengisi form LLD1 / *Transactional by non-resident amounting over US $ 10,000 or its equivalent must fill in the LLD 1 form.*

Lembar 1 & 2 : u/ Bank; Lembar 3 : u/ Nasabah

Copyright Transfer

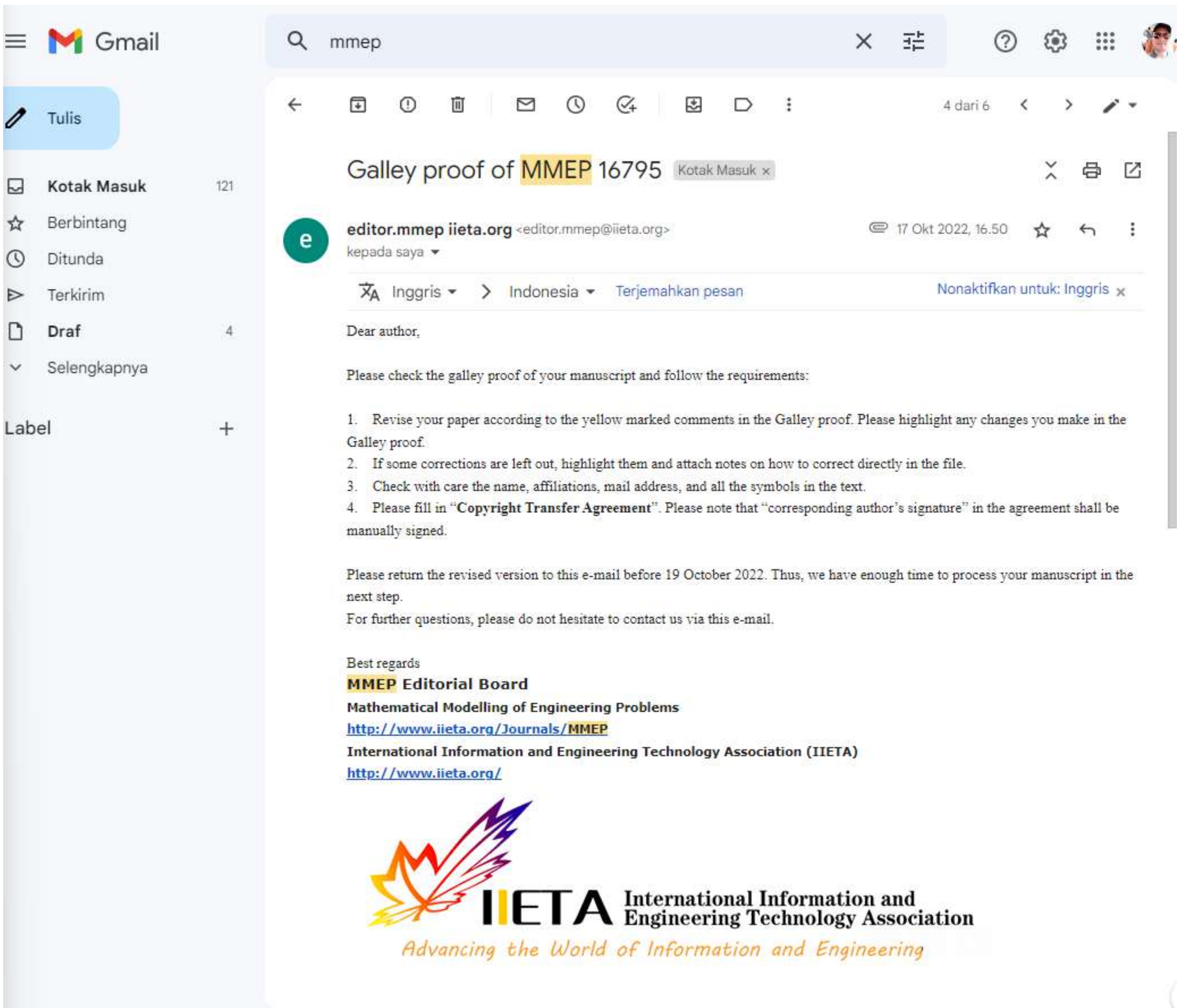
Gmail

mmep

Tulis

Kotak Masuk 121

Berbintang

Ditunda

Terkirim

Draf 4

Selengkapnya

Label

4 dari 6

Galley proof of MMEP 16795 Kotak Masuk ×

editor.mmep iieta.org <editor.mmep@iieta.org> 17 Okt 2022, 16.50

kepada saya

Inggris > Indonesia Terjemahkan pesan Nonaktifkan untuk: Inggris ×

Dear author,

Please check the galley proof of your manuscript and follow the requirements:

1. Revise your paper according to the yellow marked comments in the Galley proof. Please highlight any changes you make in the Galley proof.
2. If some corrections are left out, highlight them and attach notes on how to correct directly in the file.
3. Check with care the name, affiliations, mail address, and all the symbols in the text.
4. Please fill in "**Copyright Transfer Agreement**". Please note that "corresponding author's signature" in the agreement shall be manually signed.

Please return the revised version to this e-mail before 19 October 2022. Thus, we have enough time to process your manuscript in the next step.
For further questions, please do not hesitate to contact us via this e-mail.

Best regards
MMEP Editorial Board
Mathematical Modelling of Engineering Problems
http://www.iieta.org/Journals/MMEP
International Information and Engineering Technology Association (IIETA)
http://www.iieta.org/

IIETA International Information and Engineering Technology Association
Advancing the World of Information and Engineering

Copyright Transfer

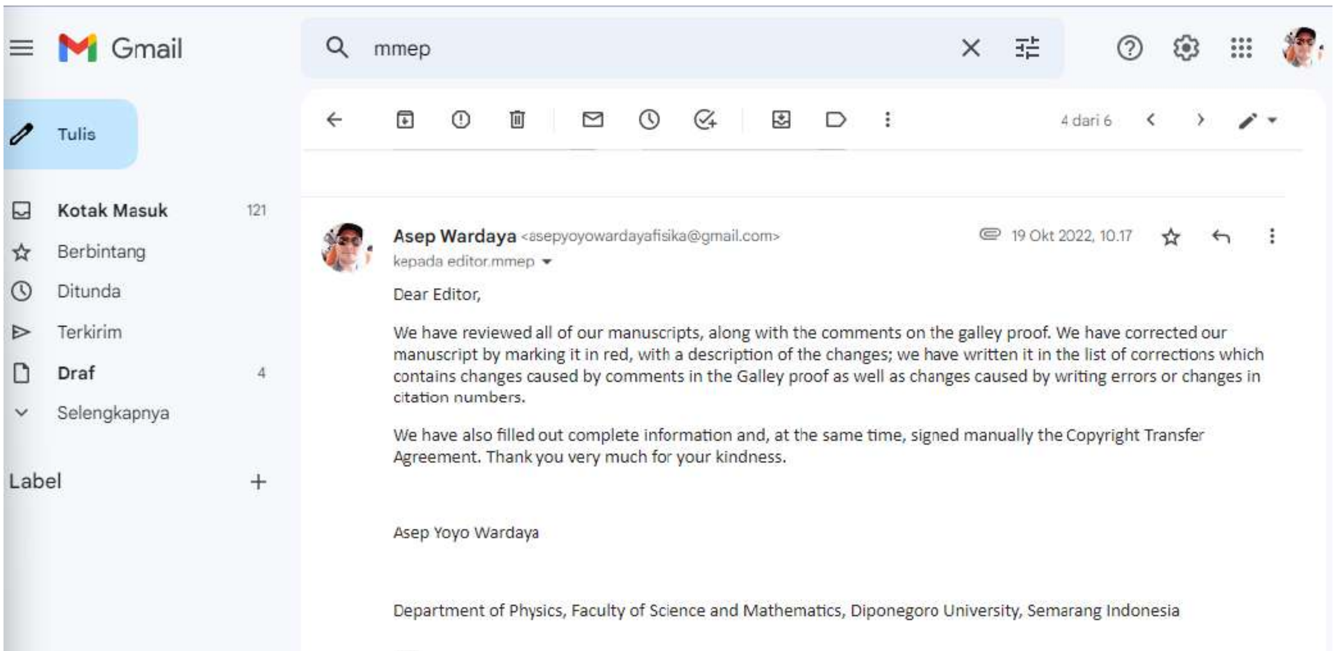

Asep Wardaya <asepyoyowardayafisika@gmail.com>
kepada editor.mmep

19 Okt 2022, 10.17

Dear Editor,

We have reviewed all of our manuscripts, along with the comments on the galley proof. We have corrected our manuscript by marking it in red, with a description of the changes; we have written it in the list of corrections which contains changes caused by comments in the Galley proof as well as changes caused by writing errors or changes in citation numbers.

We have also filled out complete information and, at the same time, signed manually the Copyright Transfer Agreement. Thank you very much for your kindness.

Asep Yoyo Wardaya

Department of Physics, Faculty of Science and Mathematics, Diponegoro University, Semarang Indonesia

Copyright Transfer Agreement

Please read the terms of this agreement, and send back a scanned copy of the signed original.

Article entitled:

Capacitance Calculation Model in Corona Discharge Case

Author/s:

Asep Yoyo Wardaya, Zaenul Muhlisin, Jatmiko Endro Suseno, Charis Munajib, Susilo Hadi, Her

Corresponding author (if more than one author):

Asep Yoyo Wardaya

Journal Name:

Mathematical Modelling of Engineering Problems

Publisher:

International Information and Engineering Technology Association

1. Copyright Assignment

The author hereby grants the Publisher the exclusive right to reproduce and distribute the article for commercial use in any other reproductions of similar nature, effective upon acceptance for publication.

2. Author's Warranties

The author warrants that the article is original, written by stated author/s, has not been published before and it will not be submitted anywhere else for publication prior to acceptance/rejection by the Publisher, contains no unlawful statements, does not infringe the rights of others, is subject to copyright that is vested exclusively in the author and free of any third party rights, and that any necessary written permissions to quote from other sources have been obtained by the author/s.

3. User rights

This article, if accepted, will be an open access article distributed under the terms and conditions of the Creative Commons Attribution License (http://creativecommons.org/licenses/by/4.0/). Publisher will insert the following note at the end of the published text: © 2022 by the authors; licensee IIETA, Edmonton, Canada. This article is an open-access article distributed under the terms and conditions of the Creative Commons Attribution License (http://creativecommons.org/licenses/by/4.0/).

4. Rights of Authors

Authors retain the following rights:

- all proprietary rights relating to the article, other than the rights mentioned in 1. Copyright Assignment, such as patent rights,
- the right to use the substance of the article in future own works, including lectures and books,
- the right to reproduce this article for own purposes, provided the copies are not offered for sale.

An author may self-archive an author-created version of his/her article on his/her own website and or in his/her institutional repository. He/she may also deposit this version on his/her funder's or funder's designated repository at the funder's request or as a result of a legal obligation, provided it is not made publicly available until 12 months after official publication. Furthermore, the author may only post his/her version provided acknowledgement is given to the original source of publication and a link is inserted to the published article on http://www.iieta.org. The link must be accompanied by the following text: "The original publication is available also at http://www.iieta.org". He/she may use the Publisher's PDF version, which is posted on http://www.iieta.org, for the purpose of self-archiving or deposit. Any other use of the article requires permission from the Publisher.

5. Co-Authorship

If the article was prepared jointly with other authors, the signatory of this form warrants that he/she has been authorized by all co-authors to sign this agreement on their behalf, and agrees to inform his/her co-authors of the terms of this agreement.

IIETA International Information and Engineering Technology Association

Advancing the World of Information and Engineering

6. Publication Fee

Please refer to the Instructions for Authors of each IIETA journal for whether the journal charges a publication fee and, if yes, how much the journal charges in publication.

7. Termination

This agreement can be terminated by the author or the Publisher upon two months' notice where the other party has materially breached this agreement and failed to remedy such breach within a month of being given the terminating party's notice requesting such breach to be remedied. No breach or violation of this agreement will cause this agreement or any license granted in it to terminate automatically or affect the definition of the Publisher. After the lapse of forty (40) years of the date of this agreement, this agreement can be terminated without cause by the author or the Publisher upon two years' notice. The author and the Publisher may agree to terminate this agreement at any time. This agreement or any license granted in it cannot be terminated otherwise than in accordance with this section 6.

8. Royalties

This agreement entitles the author to no royalties or other fees. To such extent as legally permissible, the author waives his or her right to collect royalties relative to the article in respect of any use of the article by the Publisher or its sublicensee.

9. Miscellaneous

The Publisher will publish the article (or have it published) in the Journal, if the article's editorial process is successfully completed and the Publisher or its sublicense has become obligated to have the article published. The Publisher may conform the article to a style of punctuation, spelling, capitalization and usage that it deems appropriate. The author acknowledges that the article may be published so that it will be publicly accessible and such access will be free of charge for the readers. The Publisher will be allowed to sublicense the rights that are licensed to it under this agreement. This agreement will be governed by the laws of Canada.

10. Scope of the Commercial License

The exclusive right and license granted under this agreement to the Publisher for commercial use is as follows:

a. to prepare, reproduce, manufacture, publish, distribute, exhibit, advertise, promote, license and sub- license printed and electronic copies of the article, through the Internet and other means of data transmission now known or later to be developed; the foregoing will include abstracts, bibliographic information, illustrations, pictures, indexes and subject headings and other proprietary materials contained in the article,

b. to exercise, license, and sub-license others to exercise subsidiary and other rights in the article, including the right to photocopy, scan or reproduce copies thereof, to reproduce excerpts from the article in other works, and to reproduce copies of the article as part of compilations with other works, including collections of materials made for use in classes for instructional purposes, customized works, electronic databases, document delivery, and other information services, and publish, distribute, exhibit and license the same.

Where this agreement refers to a license granted to the Publisher in this agreement as exclusive, the author commits not only to refrain from granting such license to a third party but also to refrain from exercising the right that is the subject of such license otherwise than by performing this agreement.

The Publisher will be entitled to enforce in respect of third parties, to such extent as permitted by law, the rights licensed to it under this agreement.

Corresponding author's signature:

....

Name printed:

Asep Yoyo Wardaya

Date:

October 18, 2022

List of corrections

No	Comment	Correction	chapter and paragraph (revised manuscript)
1.	Comment [CG1]: Please add the zip code after the city.	[1]Department of Physics, Faculty of Science and Mathematics, Diponegoro University, Semarang 50275, Indonesia [2]M1 Physique, Faculté de sciences, Université d'Aix-Marseille, Marseille 13331, France [3]Department of Electrical Engineering, Faculty of Engineering, Diponegoro University, Semarang 50275, Indonesia	Title
2.	Comment [CG2]: Please make sure figure 5 is mentioned in the text.	The electronic circuit arrangement of the corona plasma discharge equipment is shown in Figures 5 (a) and 5 (b) and consists of: (There is an error in writing the numbering of figures in the early manuscript)	3. EXPERIMENT TECHNIQUE (First paragraph)
3.	Comment [CG3]: Please cite a paper from MMEP.	The capacitance function in the corona discharge is different from the capacitance function in the case of ordinary electricity [23, 24].	2. MATHEMATICAL MODELS (Second paragraph)
		[23] Katuri, R., Gorantla, S. (2018). Analysis of math function based controller for a smooth transition between battery and ultracapacitor. Mathematical Modelling of Engineering Problems, 5(4): 386-394. https://doi.org/10.18280/mmep.050416 [24] Sreedhar, T., Ramana, N.V. (2020). Impact of Distribution Network Reconfiguration and Optimal Capacitor Placement under Wheeling Transactions. Mathematical Modelling of Engineering Problems, 7(1): 113-118. https://doi.org/10.18280/mmep.070114	REFERENCES

Permintaan Check the Final Proof

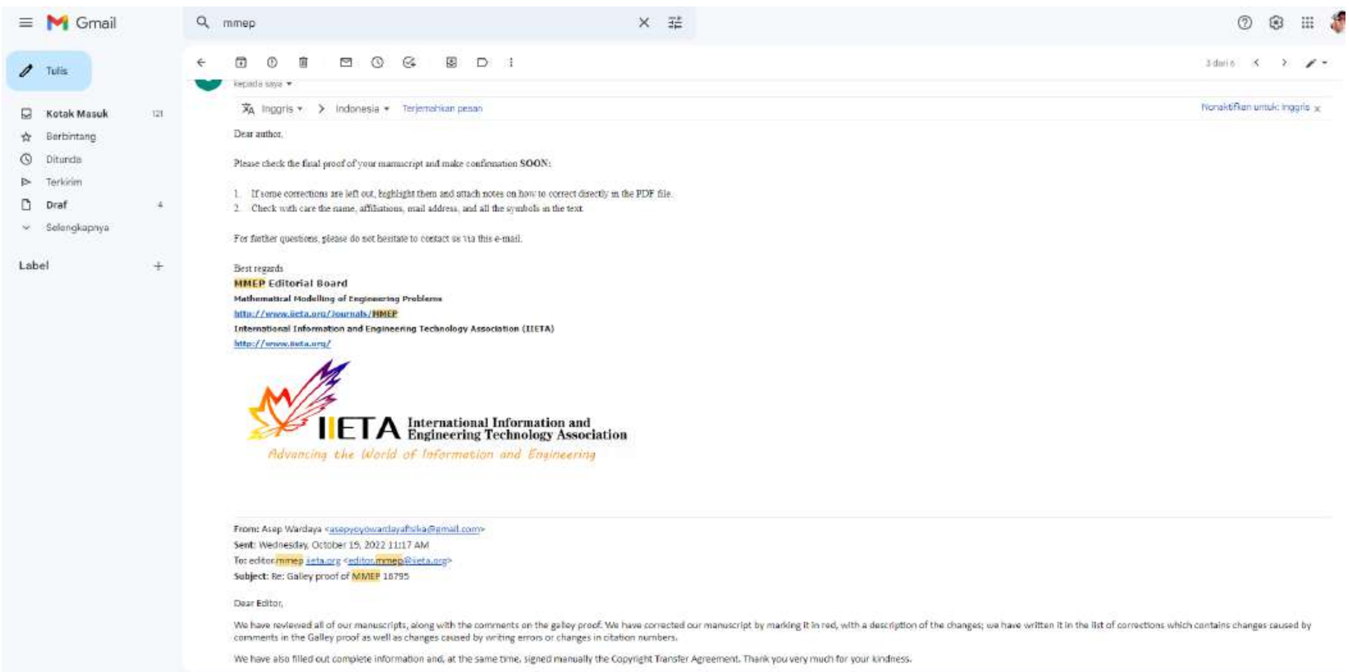

Dear author,

Please check the final proof of your manuscript and make confirmation **SOON**:

1. If some corrections are left out, highlight them and attach notes on how to correct directly in the PDF file.
2. Check with care the name, affiliations, mail address, and all the symbols in the text.

For further questions, please do not hesitate to contact us via this e-mail.

Best regards
MMEP Editorial Board
Mathematical Modelling of Engineering Problems
http://www.iieta.org/Journals/MMEP
International Information and Engineering Technology Association (IIETA)
http://www.iieta.org/

IIETA International Information and Engineering Technology Association
Advancing the World of Information and Engineering

From: Asep Wardaya <asepyoyowardayafisika@gmail.com>
Sent: Wednesday, October 19, 2022 11:17 AM
To: editor.mmep iieta.org <editor.mmep@iieta.org>
Subject: Re: Galley proof of MMEP 16795

Dear Editor,

We have reviewed all of our manuscripts, along with the comments on the galley proof. We have corrected our manuscript by marking it in red, with a description of the changes; we have written it in the list of corrections which contains changes caused by comments in the Galley proof as well as changes caused by writing errors or changes in citation numbers.

We have also filled out complete information and, at the same time, signed manually the Copyright Transfer Agreement. Thank you very much for your kindness.

Pernyataan sudah mengecel Final Proof

Asep Wardaya <asepyoyowardayafisika@gmail.com> 20 Okt 2022, 06.15

kepada editor.mmep

Dear Editor,

We have checked all the writings of The Final proof of MMEP 16795 file. It turns out that there are some minor writing errors that we noted in the word file with the title list of final corrections, and we marked the writing in red i the Final proof of MMEP 16795 revision file, which is the Final proof of MMEP 16795 file with the addition of the re marker. Thank you very much for your kindness.

Asep Yoyo Wardaya

Department of Physics, Faculty of Science and Mathematics, Diponegoro University, Semarang Indonesia

•••

2 Lampiran • Dipindai dengan Gmail

Final proof of MM...

List of correction...

Koreksi Final

List of corrections final

No	The Final manuscript	Correction on the Final manuscript	chapter and paragraph (revised manuscript)
1.	M1 Physique, Facult é de sciences, Université d'Aix-Marseille	M1 Physique, Faculté de sciences, Université d'Aix-Marseille (Writing Facult é becomes Faculté)	Title (address)
2.	…the total ABCDE plate (i.e., GBCDF plate) is shown in Figure 3a	…..the total ABCDE plate (i.e., GBCDF plate) is shown in Figure 3 (a)	2. MATHEMATICAL MODELS (9th paragraph)
3	and the notation δ is defined as the thickness value of plate 1	and the notation δ is defined as the thickness value of the active electrode	2. MATHEMATICAL MODELS (17th paragraph)
4	The values of b and d in Eq. (18) are constant on the change variation of distance c. Suppose it is considered that the CEDC capacitance value is close to a constant on the difference in the value of c. In Eq. (18), there is a tendency……	The values of b and d in Eq. (19) are constant on the change variation of distance c. Suppose it is considered that the C_{EDC} capacitance value is close to a constant on the difference in the value of c. In Eq. (19), there is a tendency….	5. DISCUSSION (last paragraph)
5	The calculation results of the values of the fitting factor k, SD errors, and t-test in Table 2 for the (I-V) characteristics case…..	The calculation results of the values of the fitting factor k, SD errors, and t-test in Table 3 for the (I-V) characteristics case…..	6. CONCLUSIONS (First paragraph)

International Information and Engineering Technology Association
Advancing the World of Information and Engineering

Mathematical Modelling of Engineering Problems
Vol. 9, No. 5, October, 2022, pp. 1161-1171
Journal homepage: http://iieta.org/journals/mmep

Capacitance Calculation Model in Corona Discharge Case

Asep Yoyo Wardaya[1*], Zaenul Muhlisin[1], Jatmiko Endro Suseno[1], Charis Munajib[1], Susilo Hadi[2], Heri Sugito[1], Jaka Windarta[3]

[1] Department of Physics, Faculty of Science and Mathematics, Diponegoro University, Semarang 50275, Indonesia
[2] M1 Physique, Facult é de Sciences, Université d'Aix-Marseille, Marseille 13331, France
[3] Department of Electrical Engineering, Faculty of Engineering, Diponegoro University, Semarang 50275, Indonesia

Corresponding Author Email: asepyoyowardayafisika@gmail.com

https://doi.org/10.18280/mmep.090501

Received: 17 August 2022
Accepted: 4 October 2022

Keywords:
corona discharge, (I-V) characteristics, CEM-P, shape sharpness factor, python GUI programming

ABSTRACT

The (*I-V*) characteristic pattern of the corona discharge case is very different from the pattern of ordinary electric circuits, so it is interesting to investigate. Several previous studies involved the concept of Maxwell's equations on several physical case models such as coaxial cylinder, electrohydrodynamic, and the electric wind. In this study, we use a capacitance calculation model for positive dc corona discharge in air, especially in calculating the (*I-V*) current-voltage characteristics of an electrode configuration model, often referred to as capacitively coupled plasma (CCP). The configuration model comprises active and passive electrodes, with the active electrode in the form of a pentagonal with the sharp end (in the middle) facing downwards in an upright position. The passive electrode under the active electrode has a large rectangular shape in a lying place. This configuration model is named The Chisel Eye and Midpoint-Plane (CEM-P). The analytical calculation of the (*I-V*) characteristics uses the geometric properties of the active electrode, which will produce a large corona current flow at the pointed electrode. These properties in analytical calculation manifest with the emergence of the corona flow multiplication factor at the sharp active electrode's integration boundary condition called the shape sharpness factor k. The Python GUI Programming simulation program makes graphic simulations, Standard Deviation (*SD*), t-tests, and calculating the factor *k* (fitting curve value) between numerical calculations and research data. The values of the *SD*, the t-tests, and the Percentage of tangent points meet the requirements for a high level of accuracy for the four CEM-P configuration models of the (*I-V*) characteristics simulation graph with the graph has a relatively large percentage of tangent points values (82.35% – 94.44%).

1. INTRODUCTION

The development of cold plasma technology had a positive impact on the industry, especially for use in electronic equipment with plasma temperatures that are not too high but produce a high enough technological leap through an equipment model called capacitively coupled plasma (CCP) [1]. Cold plasma is characterised by the temperature of the heavy species (particles and neutral ions) close to room temperature (25℃-100℃). This condition becomes important when irradiating materials sensitive to high temperatures [2], such as those used in CCP equipment or materials radiated by the CCP equipment.

The CCP model uses the concept of corona plasma discharge with an electrode configuration consisting of an active electrode in a vertical position and a passive electrode in a horizontal position (under the active electrode). The active electrode has a sharp-shaped surface towards the bottom. The passive electrode has a large surface to accommodate all the plasma flow from the active electrode. The CCP equipment is similar to the capacitance equipment with the position of the two electrodes perpendicular to each other [3]. If the CCP equipment connects to a dc voltage source, it can produce a corona plasma discharge under the appropriate voltage conditions.

The (*I-V*) current-voltage characteristic in the corona plasma discharge is an exciting research topic. This topic involves a variety of physical properties that cause Townsend's low current to appear, followed by a reasonably high current increase in corona discharge and arc discharge events [4]. Various studies explain the characteristic current-voltage phenomenon in the corona discharge, including the coaxial cylinders model [5, 6], the electro-hydrodynamics model [7], and the Electric Wind model [8]. Similarly, the application of CCP equipment has helped the development of research in other fields or used for industries such as ultra-large-scale integrated circuit (ULSI) fabrication [9], surface modification of polymeric materials [10], Large-area coating [11], lens-shaped electrodes [12], AC dielectric barrier discharges [13], etc.

In 2020, Wardaya et al. [14] make another form of the (I-V) characteristic related to the geometric function of the CCP electrode model. The geometric part has also been discussed [8] to compare the corona current function and the voltage's square function. In the research [14, 15], the geometric part comes from the modified capacitance function by adding a multiplier factor k to the sharp surface of the active electrode. The value of factor k came from the suitability factor between the analytical formulation and the experimental results (curve fitting value). The factor k is the shape sharpness factor, which came from calculating the capacitance through the insertion of the integration limit on the part of the active electrode with a sharp surface. The ideal value of k will be higher if the shape of the active electrode is more tapered. The presence of the factor k came from the research results from Dobranszky et al. [16], who proved that the pointed tip of the active electrode (with a variety of sharpness angles and different materials) would look the plasma discharge brighter and more significant.

This research discusses the calculation of the (*I-V*) characteristic of positive dc corona discharge in the air (the CCP model) using The Chisel Eye and Midpoint-Plane (CEM-P) electrodes configuration models. Zheng et al. [6], Guan et al. [7], Robinson [8] uses the electric field concept from Maxwell's equation applied to the coaxial cylinder model, the continuity equation of electrohydrodynamic, and the electric wind, respectively. This study does not use a physical approach from Maxwell's equations but a geometric approach from the active electrode tip of the capacitor, which gives rise to the shape sharpness factor of k [14, 15]. Wardaya et al. [14] used an active electrode tip approach in the form of a sharp line, Wardaya et al. [15] using a sharp semicircular active electrode shape with pointed left and right sides. This study uses the tip of the active electrode as a sharp and pointed triangle. The pointed angle at the tip of the active electrode is $\phi=2\theta$. This study uses variations in the angle θ not found [14, 15] and variations in the distance between the two electrodes. This study is significant. We will be able to calculate the variation of electric current and plasma discharge required from the electrode model (*CCP* equipment) only by using the given voltage variation and variations in the length and angle of sharpness of the active electrode at a specific value of k. This method is more practical than considering physical effects, such as the effect of using Maxwell's equations on plasma discharge.

The CEM-P electrode produces corona plasma under atmospheric conditions. Corona plasma is a form of cold plasma that produces reactive oxygen-nitrogen species (RONS) in atmospheric conditions. In industrial interests, RONS can be used to improve post-harvest quality [17], food quality and safety management [18] and so on.

The research results are a graph of the current-voltage characteristics of the corona plasma discharge with a high degree of correspondence between numerical calculations and experimental data (82.35% - 94.44%). The value of the research errors includes standard deviation values between 1.4871-3.3546 and t-test values which are almost all below the value of 0.5 (only one research data with a t-test value=0.5). This (CEM-P) electrode configuration model uses four variations of the sharp angle at the tip of the active electrode ($\phi = 2\theta$) and two variations of the distance between the active and passive electrodes for any given θ value. The value of the resulting corona discharge current is a function of the voltage difference ΔV, the angle and geometric size of the active electrode, and the distance between the active and passive electrodes.

These electrodes model consists of a pair of electrodes positioned perpendicular to each other in the air. These electrodes couple consist of an active electrode shaped like a Pentagonal thin plate, and the mid-sharp end is directed downward in a vertical position. In contrast, a passive electrode is horizontally shaped under the active electrode.

The paper's layout has a structure through the following chapters:

a. Abstract contains a brief explanation of the background, research objectives, research methods, and research results.
b. Introduction contains the background and importance of this research on technological and industrial developments, the background of previous research, research methods, research objectives, research gaps, reasons, and motivations for research.
c. Mathematical model contains a detailed explanation physically and mathematically that relates the concept of electric current formulation from plasma discharge with other variables such as voltage and capacitance value. The capacitance value is determined by the length measurements of the electrode components and the value of k.
d. The technical experiment explains the electronic circuits and equipment used in this research.
e. Results of Simulation and Experiments explain the study of four different sizes of electrode models through the depiction of the (*I-V*) characteristic graphs and their uncertainty errors related to the degree of correspondence between numerical calculations and research data.
f. Discussion contains a discussion of the analysis of the (*I-V*) characteristic graph and the value of the error based on physical and mathematical reasons.
g. Conclusion contains a discussion about the feasibility level of this study based on the research results and discussions that have been presented previously.
h. Acknowledgment and References.

2. MATHEMATICAL MODELS

The (*I-V*) characteristic model in the case of corona plasma discharge expressed in terms of the current function as a function of the square of V has two equations. The first form of this model is as follows:

$$I = CV\left(V - V_i\right) \tag{1}$$

where, I is the corona plasma current, V is the applied voltage, V_i is the initial voltage, and C is the constant. Some of the proponents of the Eq. (1) model include [5, 8, 19-21]. The form of the constant C in Eq. (1) is a function of geometry [8]. The next model of the (*I-V*) characteristic, as proposed [7, 14, 15, 22], has the equation form as:

$$I = C\left(V - V_i\right)^2 \tag{2}$$

This study will use the Eq. (2) model as a reference in the calculation of the (*I-V*) characteristic model, with constant C being a geometric function of the capacitance as proposed by [14, 15]. The capacitance function in the corona discharge is different from the capacitance function in the case of ordinary electricity [23, 24]. The electrode active of the CEM-P configuration has a pentagonal shape. The width and length of the rectangular plate are a and b, respectively, while the width and sharp angle of the triangular plate are d and 2θ, respectively. In comparison, the thickness of the electrode active is skinny ($\delta \cong 0.00015$ meters). The distance between the lower end of electrode active and electrode passive is equal to c. The Electrode passive has a rectangular plane configuration with a big area to accommodate all the flow of electric plasma flux from the electrode active to the electrode passive. If a dc voltage difference of V between the two electrodes is attached, then a corona plasma discharge event can be created, producing an electric current. The electrode scheme with the CEM-P configuration is found in Figure 1 (a).

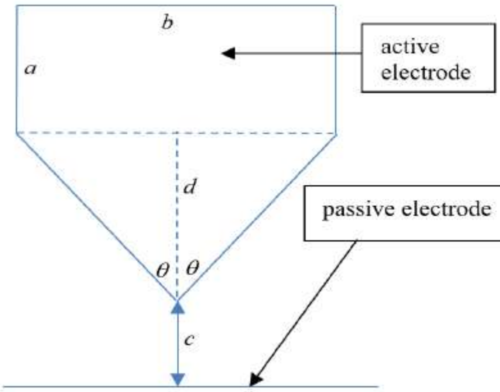

(a)

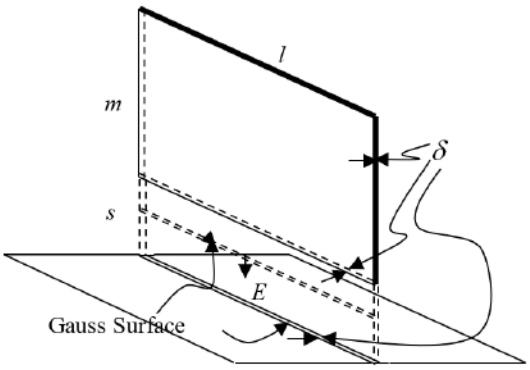

(b)

Figure 1. The electrode model Illustration for (a) the CEM-P configuration, (b) the L-P Configuration [14, 15]

Figure 1 (a) is a two-dimensional representation of the CEM-P electrode configuration model. According to geometric calculations, the most significant plasma flow will come out from the lower center end of the pointed active electrode. Furthermore, a smaller stream of plasma will come out of the pointed end of the electrode on both sides of the active electrode. In comparison, the most negligible flow will come out of the sharp lower triangular surface of the active electrode. A passive electrode will accommodate all the plasma flow under the active electrode. For the calculation of the capacitance model of the active electrode system, it has two conditions, namely:

a. For plasma flow straight down, the pentagon-shaped capacitance calculation is transformed into rectangular and triangular capacitances.

b. For the plasma flow coming out of the left and right sides of the active electrode, the capacitance value will be calculated using the integration technique of the capacitance elements.

Before calculating the capacitance value of the electrode model with the CEM-P configuration, a simpler electrode model is needed as the basis for calculating the CEM-P configuration model, namely the electrode model with the Line-Plane (*L-P*) configuration [14, 15]. This electrode model consists of two rectangular plates in a mutually perpendicular position in the air. The active electrode has the area of the rectangle as lm (l and m are the lengths and width values of the plate, respectively) in a vertical position above the passive electrode, which is in a horizontal position. These plates have a thin thickness δ, and the distance between the two plates is s, as shown in Figure 1 (b).

The total capacitance value of the electrode model with the *L-P* configuration [14, 15], can be written as:

$$C_{LP} = \varepsilon_0 \, l \ln \left| \frac{m+s}{s} \right| \tag{3}$$

where, ε_0 is the vacuum permittivity. By using formulation (3), we can derive the formulation of the capacitance element from the electrode model with the CEM-P configuration as shown in Figure 2 (a).

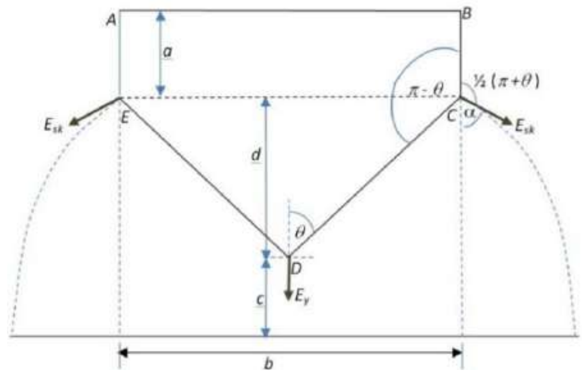

(a)

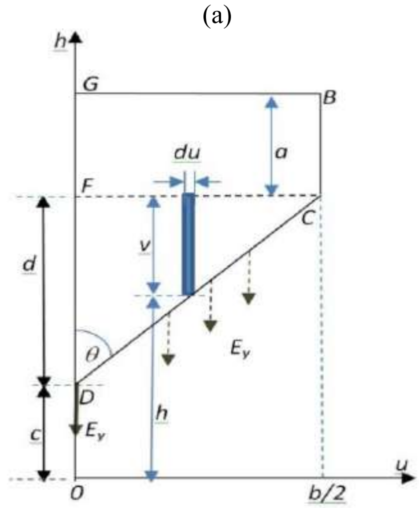

(b)

Figure 2. (a) Calculation of the corona plasma discharge electrode's capacitance with the CEM-P configuration has three plasma flows: the lower oblique of the right and left; and straight downward, (b) The plasma flows are calculated straight down, taking only half the right part of the plate. The enormous plasma flow is the one coming out of point D

Figure 2 (a) shows the CEM-P electrode configuration model with plate 1 in the shape of an *ABCDE* five-angle plate in an upright position to plate 2, lying horizontally. In this study, the plasma flow was thought to have multiple flow directions that were visible out of some of the sharp surfaces of the electrodes. The flow direction is straight down (seen clearly out of point D) and towards the left oblique (seen at point E), and oblique to the right (seen at point C). Figure 2 (b) shows the calculation model of the plasma flow, which is specifically directed downward by taking half part of the electrode because it has a symmetrical character between the right and left sides of the *ABCDE* five-angle plate.

The *ABCDE* five-angle plate can be divided into two symmetrical plate areas, where half of the *ABCDE* plate consists of a *GBCF* rectangular plate and an *FDC* triangle. By adopting the Eq. (3) in Figure 2 (b), the capacitance calculation of the *GBCF* rectangular plate electrode will produce a value:

$$C_{1A} = \varepsilon_0 \left(\frac{b}{2}\right) \ln \left| \frac{a+c+d}{c+d} \right| \tag{4}$$

To calculate the electrode capacitance value of the *FDC* triangular plate, we can make a comparison of the *FDC* triangular plate elements with the Eq. (3) so that the value of the capacitance element along with the boundary condition of variable u is obtained as:

$$dC_{1B} = \varepsilon_0 \, du \ln \left| \frac{v+h}{h} \right| ; \; 0 \le u \le \tfrac{1}{2} b \tag{5}$$

where, there is a relationship:

$$d+c=v+h \text{ and } \; v = \frac{2ud}{b} \tag{6}$$

The variables v and h in Eq. (5) can be made as a function of u using Eq. (6). The capacitance value calculating results of the FDC triangle plate in Eq. (5) through the concept of integration is:

$$\begin{aligned} C_{1B} = &\left\{ \varepsilon_0 \frac{b}{2d}(c+d) - \varepsilon_0 \frac{bc}{2d} \ln|c+d| \right\} \\ &+ \left\{ c\varepsilon_0 \frac{b}{2d} \ln|c| - c\varepsilon_0 \frac{b}{2d} \right\}. \end{aligned} \tag{7}$$

From the comparison of Figures 2 (a) and 2 (b), the *ABCDE* plate's capacitance value is two times that of the *GBCDF* plate. However, if the multiplier factor k is entered in the sharp surface around point D or at the limit condition u=0 in Figure 2 (b), then the capacitance value involving the *ABCDE* plate in the plasma flow downward is:

$$\begin{aligned} C_1 = &\varepsilon_0 \, b \ln \left| \frac{a+c+d}{c+d} \right| + \frac{\varepsilon_0 b}{d} \left[c+d - c \ln|c+d| \right] \\ &+ \lim_{k \to \text{big value}} k \frac{\varepsilon_0 bc}{d} \left[\ln|c| - 1 \right]. \end{aligned} \tag{8}$$

In the case of plasma flow out of the left and right oblique directions (points E and C) from the *ABCDE* plate in Figure 2 (a), then plasma flow depiction for the case half the portion of the total *ABCDE* plate (i.e., *GBCDF* plate) is shown in Figure 3(a). From point C in the GBCDF plate, we assumed that there is a plasma flow that is curved at an angle of 60° (considered the mean angle of the observations) so that in the end, the plasma flow reaches the second plate (the passive electrode). The concept of plasma flow from the *GBCDF* plate in Figure 3 (a) will be easier to calculate if a simplification is made with the plate position on the *u-h* coordinate axis, respectively, on the horizontal and vertical coordinate axes as shown in Figure 3 (b). Point C on the *GBCDF* plate is the tip of the sharp electrode surface that delivers a more significant amount of plasma than any other surface.

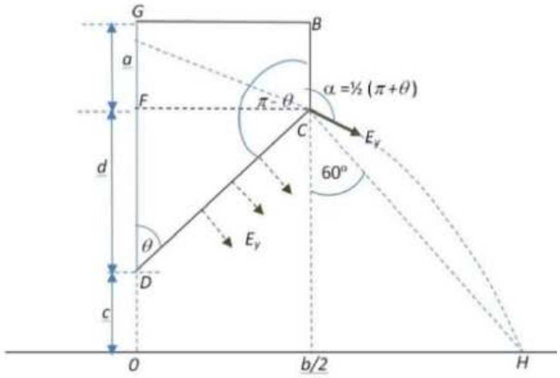

(a)

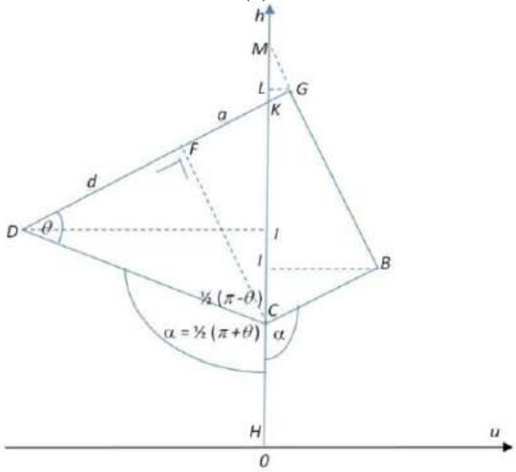

(b)

Figure 3. (a) The plasma outflows right obliquely from point C. The horizontal length of the plasma path on plate 2 is l sin 60°, where l is the straight distance from the plasma path that exits from point C to the end of the H line, and the angle 60° is the mean angle of the observations, (b) The capacitance calculation model with a curved path *CH* is considered a straight line and functions as the vertical coordinate axis of variable h with the horizontal coordinate axis of variable u

In the case of the CCP electrode, the sharper the electrode shape (the angle is getting taper), the plasma flow is also more excellent (which is indicated by the increasing value of k), so there is a relationship as $k \cong 1/\phi$, where ϕ is the acute angle at the end of the CCP electrode emitting plasma flow. If at point C which has an acute angle of 2θ and the multiplier factor of shape sharpness is k, then the magnitude of the shape sharpness factor at point C or E is equal to $k_1=2\theta k/(\pi-\theta)$.

The total capacitance in the case of plasma flow coming out of the right oblique electrode in Figure 3 (a) (with the depiction of the capacitance triangle in Figure 3 (b) is:

$$\begin{aligned} C_2 = &\left(\frac{2\theta}{\pi-\theta}\right) k \; C_{CBI} + \left(\frac{2\theta}{\pi-\theta}\right) k \; C_{CDJ} \\ &+ C_{JDK} + C_{IBM} - C_{KGL} - C_{LGM}. \end{aligned} \tag{9}$$

The multiplier factor k_1 is added to the capacitance-capacitance values of C_{CBI} and C_{CDJ} because the two electrodes are at the sharp end of the electrode at point C. The calculation of capacitance from C_{CBI} is based on the concept of the image in Figure 4.

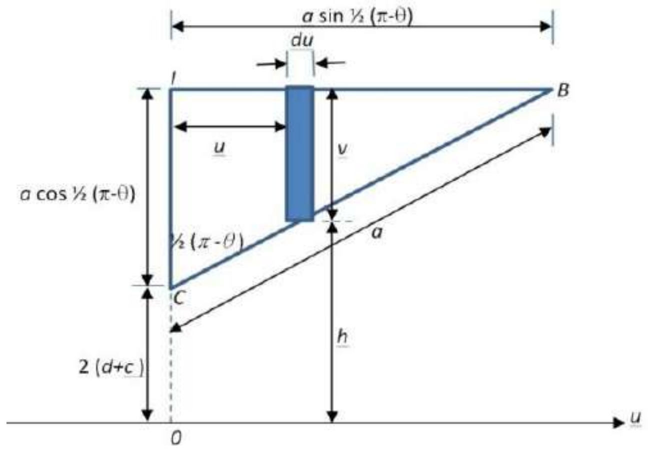

Figure 4. The concept of calculating the capacitance of an electrode C_{CBI}

By comparing the triangles and the same height limit from Figure 4, the values of v and h are obtained as:

$$\begin{aligned} v &= \tan\left(\tfrac{1}{2}\theta\right)\left[d\sec\theta\cos\left(\tfrac{1}{2}\theta\right)-u\right], \\ h &= 2(d+c)+u\tan\left(\tfrac{1}{2}\theta\right). \end{aligned} \tag{10}$$

Through the formulation of the capacitance element and the boundary conditions of the variable u as:

$$dC_{CBI} = \varepsilon_0\, du \ln\left|\frac{v+h}{h}\right|,\ 0 \le u \le a\cos\left(\tfrac{1}{2}\theta\right). \tag{11}$$

We get the value of the capacitance C_{CBI} as:

$$\begin{aligned} C_{CBI} &= \varepsilon_0 a\cos\left(\tfrac{1}{2}\theta\right) \\ &\quad -2\varepsilon_0(d+c)\cot\left(\tfrac{1}{2}\theta\right)\ln\left|\frac{2(d+c)+a\sin\left(\tfrac{1}{2}\theta\right)}{2(d+c)}\right|. \end{aligned} \tag{12}$$

The calculation of units along with other capacitance values from Eq. (9) can be seen in Tables 1 and 2. Using Eqns. (9), (12) and Table 2, then the capacitance part value is obtained in the case of plasma flow coming out of the right oblique direction of the electrode, as:

$$\begin{aligned} C_2 = \left(\frac{2\theta}{\pi-\theta}\right)k &\left\{\begin{aligned} &\varepsilon_0 d\sec\theta\cos\tfrac{1}{2}(\theta)\ln\left|\frac{2(d+c)+d\sec\theta\sin\tfrac{1}{2}(\theta)}{2(d+c)-d\sec\theta\sin\tfrac{1}{2}(\theta)}\right| + \varepsilon_0 a\cos\left(\tfrac{1}{2}\theta\right) \\ &+2\varepsilon_0(d+c)\cot\left(\tfrac{1}{2}\theta\right)\ln\left|\frac{2(d+c)-d\sec\theta\sin\tfrac{1}{2}(\theta)}{2(d+c)+a\sin\left(\tfrac{1}{2}\theta\right)}\right| + \varepsilon_0 d\sec\theta\cos\tfrac{1}{2}(\theta) \end{aligned}\right\} \\ &-\varepsilon_0\left[2(d+c)\tan\tfrac{1}{2}(\theta)+a\sin\tfrac{1}{2}(\theta)\tan\tfrac{1}{2}(\theta)+a\cos\tfrac{1}{2}(\theta)\right]\ln\left|2(d+c)+a\sin\tfrac{1}{2}(\theta)\right| \\ &-\varepsilon_0\left[4(d+c)\cot\left(\tfrac{1}{2}\theta\right)+4d\sec\theta\cos\left(\tfrac{1}{2}\theta\right)\right]\ln\left|2d\sec\theta\sin\left(\tfrac{1}{2}\theta\right)+2(d+c)\right| \\ &+\varepsilon_0\left[2(d+c)\cot\left(\tfrac{1}{2}\theta\right)+3d\sec\theta\cos\tfrac{1}{2}(\theta)\right]\ln\left|3d\sec\theta\sin\left(\tfrac{1}{2}\theta\right)+2(d+c)\right| \\ &-\varepsilon_0 d\sec\theta\cos\tfrac{1}{2}(\theta)\ln\left|d\sec\theta\sin\tfrac{1}{2}(\theta)+2(d+c)\right| \\ &+\varepsilon_0\left[\begin{aligned}&2(d+c)\tan\left(\tfrac{1}{2}\theta\right)+a\sin\left(\tfrac{1}{2}\theta\right)\tan\left(\tfrac{1}{2}\theta\right) \\ &+a\cos\left(\tfrac{1}{2}\theta\right)-2(d+c)-2d\sec\theta\sin\tfrac{1}{2}\theta\end{aligned}\right]\ln\left|2(d+c)+(a+d+d\sec\theta)\sin\left(\tfrac{1}{2}\theta\right)\right| \\ &+\varepsilon_0\left[a\sin\tfrac{1}{2}(\theta)-a\cos\left(\tfrac{1}{2}\theta\right)\right]\ln\left|a\cos\tfrac{1}{2}(\theta)\cot\tfrac{1}{2}(\theta)+2(d+c)+a\sin\tfrac{1}{2}(\theta)\right| \\ &+\varepsilon_0\left[\begin{aligned}&2(d+c)\cot\left(\tfrac{1}{2}\theta\right)+2d\sec\theta\cos\left(\tfrac{1}{2}\theta\right) \\ &+2(d+c)+2d\sec\theta\sin\tfrac{1}{2}\theta\end{aligned}\right]\ln\left|\begin{aligned}&2(d+c)+2d\sec\theta\sin\left(\tfrac{1}{2}\theta\right)+2(d+c)\tan\left(\tfrac{1}{2}\theta\right) \\ &+2d\sec\theta\sin\tfrac{1}{2}\theta\tan\left(\tfrac{1}{2}\theta\right)\end{aligned}\right| \\ &-\varepsilon_0(d+d\sec\theta)\tan\left(\tfrac{1}{2}\theta\right)\sin\left(\tfrac{1}{2}\theta\right)-\varepsilon_0 d\sec\theta\cos\left(\tfrac{1}{2}\theta\right)-2\varepsilon_0(d+c)+2\varepsilon_0 d\sec\theta\sin\left(\tfrac{1}{2}\theta\right) \end{aligned} \tag{13}$$

Table 1. Some capacitance boundary conditions for the triangular electrodes indexes name *CDJ*, *JDK*, *IBM*, *KGL* and *LGM*

No.	Indexes name	v	h	Boundary conditions of u
1	*CDJ*	$d\sec\theta\sin\left(\tfrac{1}{2}\theta\right)-\tan\left(\tfrac{1}{2}\theta\right)u$	$2(d+c)+u\tan\left(\tfrac{1}{2}\theta\right)$	$-d\sec\theta\cos\left(\frac{1}{2}\theta\right)\le u\le 0$
2	*JDK*	$d\sec\theta\sin\left(\tfrac{1}{2}\theta\right)-\tan\left(\tfrac{1}{2}\theta\right)u$	$2(d+c)+d\sec\theta\sin\left(\tfrac{1}{2}\theta\right)$	$-d\sec\theta\cos\left(\tfrac{1}{2}\theta\right)\le u\le 0$
3	*IBM*	$a\cot\left(\tfrac{1}{2}\theta\right)\cos\left(\tfrac{1}{2}\theta\right)-u\cot\tfrac{1}{2}(\theta)$	$2(d+c)+a\sin\left(\tfrac{1}{2}\theta\right)$	$0\le u\le a\cos\left(\tfrac{1}{2}\theta\right)$
4	*KGL*	$(a+d-d\sec\theta)\sin\left(\tfrac{1}{2}\theta\right)$ $-u\tan\left(\tfrac{1}{2}\theta\right)$	$2(d+c)+u\tan\left(\tfrac{1}{2}\theta\right)$ $+2d\sec\theta\sin\left(\tfrac{1}{2}\theta\right)$	$0\le u\le 2(d+c)+2d\sec\theta\sin\left(\tfrac{1}{2}\theta\right)$
5	*LGM*	$\left[a\cos\left(\tfrac{1}{2}\theta\right)-u\right]\cot\left(\tfrac{1}{2}\theta\right)$ $-(d+d\sec\theta)\sin\left(\tfrac{1}{2}\theta\right)$	$2(d+c)+$ $(a+d+d\sec\theta)\sin\left(\tfrac{1}{2}\theta\right)$	$2(d+c)+a\sin\left(\tfrac{1}{2}\theta\right)+a\cos\left(\tfrac{1}{2}\theta\right)\cot\left(\tfrac{1}{2}\theta\right)$ $\le u\le 2(d+c)+(a+d+d\sec\theta)\sin\left(\tfrac{1}{2}\theta\right)$

Table 2. Some capacitance values for the triangular electrodes

No.	Indexes name	The triangle capacitance value
1	*CDJ*	$\begin{aligned} &\varepsilon_0 d\sec\theta\cos\tfrac{1}{2}(\theta)\ln\left\lvert\frac{2(d+c)+d\sec\theta\sin\tfrac{1}{2}(\theta)}{2(d+c)-d\sec\theta\sin\tfrac{1}{2}(\theta)}\right\rvert+\frac{2\varepsilon_0(d+c)}{\tan\tfrac{1}{2}(\theta)}\ln\left\lvert\frac{2(d+c)-d\sec\theta\sin\tfrac{1}{2}(\theta)}{2(d+c)}\right\rvert \\ &+\varepsilon_0 d\sec\theta\cos\tfrac{1}{2}(\theta) \end{aligned}$
2	*JDK*	$\begin{aligned} &2\varepsilon_0 d\sec\theta\cos\tfrac{1}{2}(\theta)\ln\left\lvert 3d\sec\theta\sin\left(\tfrac{1}{2}\theta\right)+2(d+c)\right\rvert-\varepsilon_0 d\sec\theta\cos\tfrac{1}{2}(\theta)\ln\left\lvert 2d\sec\theta\sin\left(\tfrac{1}{2}\theta\right)+2(d+c)\right\rvert \\ &+\left[2\varepsilon_0(d+c)\cot\left(\tfrac{1}{2}\theta\right)+\varepsilon_0 d\sec\theta\cos\left(\tfrac{1}{2}\theta\right)\right]\ln\left\lvert\frac{2d\sec\theta\sin\left(\tfrac{1}{2}\theta\right)+2(d+c)+d\sec\theta\sin\tfrac{1}{2}(\theta)}{d\sec\theta\sin\left(\tfrac{1}{2}\theta\right)+2(d+c)+d\sec\theta\sin\tfrac{1}{2}(\theta)}\right\rvert \\ &-\varepsilon_0 d\sec\theta\cos\tfrac{1}{2}(\theta)\ln\left\lvert d\sec\theta\sin\tfrac{1}{2}(\theta)+2(d+c)\right\rvert-\varepsilon_0 d\sec\theta\cos\tfrac{1}{2}(\theta) \end{aligned}$
3	*IBM*	$\begin{aligned} &\varepsilon_0\left[a\sin\tfrac{1}{2}(\theta)+2(d+c)\tan\tfrac{1}{2}(\theta)+a\sin\tfrac{1}{2}(\theta)\tan\tfrac{1}{2}(\theta)\right]\ln\left\lvert a\cos\tfrac{1}{2}(\theta)\cot\tfrac{1}{2}(\theta)+2(d+c)+a\sin\tfrac{1}{2}(\theta)\right\rvert \\ &-\varepsilon_0\left[2(d+c)\tan\tfrac{1}{2}(\theta)+a\sin\tfrac{1}{2}(\theta)\tan\tfrac{1}{2}(\theta)\right]\ln\left\lvert 2(d+c)+a\sin\tfrac{1}{2}(\theta)\right\rvert \\ &-\varepsilon_0\, a\cos\tfrac{1}{2}(\theta)\ln\left\lvert 2(d+c)+a\sin\tfrac{1}{2}(\theta)\right\rvert-\varepsilon_0 a\cos\tfrac{1}{2}(\theta) \end{aligned}$
4	*KGL*	$\begin{aligned} &\varepsilon_0\left[2(d+c)+2d\sec\theta\sin\tfrac{1}{2}\theta\right]\ln\left\lvert(a+d)\sin\left(\tfrac{1}{2}\theta\right)+2(d+c)+d\sec\theta\sin\left(\tfrac{1}{2}\theta\right)\right\rvert \\ &+\left[2\varepsilon_0(d+c)\cot\left(\tfrac{1}{2}\theta\right)+2\varepsilon_0 d\sec\theta\cos\left(\tfrac{1}{2}\theta\right)\right]\ln\left\lvert 2(d+c)+2d\sec\theta\sin\left(\tfrac{1}{2}\theta\right)\right\rvert \\ &-\begin{bmatrix}2\varepsilon_0(d+c)\cot\left(\tfrac{1}{2}\theta\right)+2\varepsilon_0 d\sec\theta\cos\left(\tfrac{1}{2}\theta\right) \\ +2\varepsilon_0(d+c)+2\varepsilon_0 d\sec\theta\sin\tfrac{1}{2}\theta\end{bmatrix}\ln\begin{vmatrix}2d\sec\theta\sin\left(\tfrac{1}{2}\theta\right)+2(d+c)\tan\left(\tfrac{1}{2}\theta\right) \\ +2d\sec\theta\sin\tfrac{1}{2}\theta\tan\left(\tfrac{1}{2}\theta\right)+2(d+c)\end{vmatrix} \\ &+2\varepsilon_0(d+c)+2\varepsilon_0 d\sec\theta\sin\tfrac{1}{2}\theta \end{aligned}$
5	*LGM*	$\begin{aligned} &\varepsilon_0\begin{bmatrix}2(d+c)\tan\left(\tfrac{1}{2}\theta\right)+a\cos\left(\tfrac{1}{2}\theta\right) \\ +a\sin\left(\tfrac{1}{2}\theta\right)\tan\left(\tfrac{1}{2}\theta\right)\end{bmatrix}\ln\left\lvert\frac{2(d+c)+a\sin\left(\tfrac{1}{2}\theta\right)+a\cos\left(\tfrac{1}{2}\theta\right)\cot\left(\tfrac{1}{2}\theta\right)}{2(d+c)+(a+d+d\sec\theta)\sin\left(\tfrac{1}{2}\theta\right)}\right\rvert \\ &+\varepsilon_0(d+d\sec\theta)\tan\left(\tfrac{1}{2}\theta\right)\sin\left(\tfrac{1}{2}\theta\right)-\varepsilon_0 a\cos\left(\tfrac{1}{2}\theta\right) \end{aligned}$

By using the depiction symmetrical nature of the plasma flow of part half electrodes in the downward direction (Figure 2 (b)) and the right oblique direction (Figure 3 (a)) to the depiction total of the electrodes in Figure 2 (a), then we get the total capacitance value of the electrode model with the CEM-P configuration is:

$$C_{tot} = C_1 + 2C_2 \tag{14}$$

where, C_1 and C_2 are the capacitance values in Eqns. (8) and (13), respectively.

The classical Gauss law concept is used to determine the electric current value of the electrode model with the CEM-P configuration. The amount of electric charge flowing between the two electrodes is equal to $q=C_{tot}\,\Delta V$. The magnitude of the electric field in the air that is perpendicular downward (along the y axis) between two thin plates (plate thickness $\delta \cong 0.00015$ meters) at the position of the plates that are perpendicular to each other, as shown in Figure 1 (a), can be written as [14, 15]:

$$E_y = \frac{q}{\varepsilon_0(\Delta A)} = \frac{C_{tot}\,\Delta V}{\varepsilon_0\left(b\delta+\delta^2\right)} \tag{15}$$

where, the Gauss area is defined as $\Delta A=(b\delta+\delta^2)$ and the notation δ is defined as the thickness value of the active electrode. The voltage difference $\Delta V=V-V_i$, where V is the applied voltage and V_i is the threshold voltage of the corona.

The total value of the electric current that leaves the electrode system with the CEM-P configuration using the concept of geometric calculations can be defined [14, 15]:

$$I = -\frac{\mu_0}{\Delta V}\left(qE_y{}^2\right)_{tot} = -\frac{\mu_0\left\{C_{tot}\right\}^3}{\varepsilon_0{}^2\left(b\delta+\delta^2\right)^2}\left(V-V_i\right)^2, \tag{16}$$

where, $\varepsilon_0=8.854\times10^{-12}$ F m^{-1} and $\mu_0=4\pi\times10^{-7}$ Hm^{-1}. Eq. (16) is the formulation of the electric current function I as a function of the voltage V that will characterize the (I-V) theoretical curve at the corona plasma discharge case. This study compared the (I-V) curve and the experimental data points. The sharpness factor of geometric shapes k (contained in the formula of C_{tot}), which is obtained fittingly through a comparison of the theory and experiment results, is the multiplication factor of the current in the corona plasma discharges concept when compared to the ordinary electronic circuit's.

3. EXPERIMENT TECHNIQUE

The electronic circuit arrangement of the corona plasma discharge equipment is shown in Figures 5 (a) and 5 (b) and consists of:

1. The HV high-voltage source in the DC generator equipment (voltage 4 kV and frequency 25 kHz) is connected to the electrodes with the CEM-P configuration.
2. The electric current measuring instrument uses an analog Multimeter with SANWA brand (type YX-360TREB,

voltage 220 V, and frequency 50/60 Hz), arranged in series with the main circuit.
3. The potential difference measuring instrument uses a digital multimeter with SANWA brand CD771.
4. HV probe equipment can convert the potential difference in kV into volts. The electric current that goes to the Voltmeter was passed through the HV probe (Maximum Voltage DC 40 kV DC, model number: AC 28 kV PD-28, serial number: 01605733).

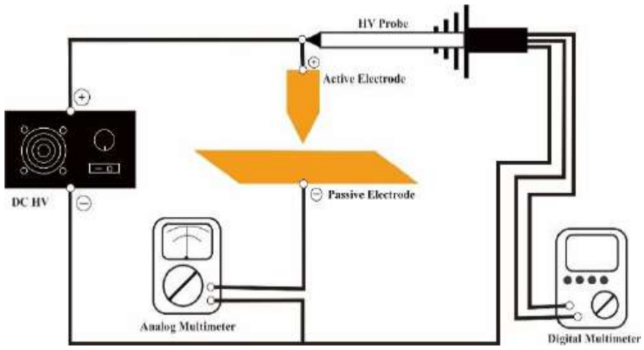

(a)


(b)

Figure 5. (a) and (b) show the circuit schematic and photos of the plasma discharge generator equipment for the CEM-P configuration model, respectively

4. RESULTS OF SIMULATION AND EXPERIMENT

In the plasma discharge experiment of the CEM-P configuration model, the lower triangular ends of the active electrode have four different angle variations. In Figure 2 (a), an active electrode section has several lengths and angles from the pentagon plate. There are several sizes of the same length of the active electrode variations, namely a=0.01 meters, b=0.01 meters and δ=0.00015 meters. While the different sizes (variations) lie in the values of the length d and a half- acute angle θ is:

a. The Electrode Model 1: d=0.010 meters and θ=26,57°
b. The Electrode Model 2: d=0.015 meters and θ=18.44°
c. The Electrode Model 3: d =0.025 meters and θ=11.31°
d. The Electrode Model 4: d=0.030 meters and θ=9.46°

Plasma discharge photos of the four electrode models can be seen in Figure 6.

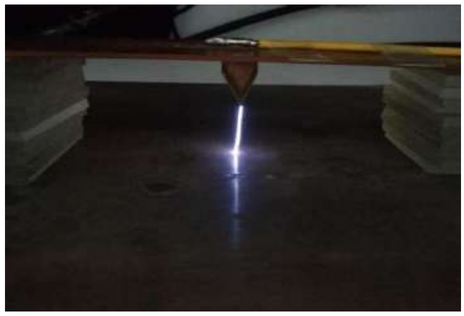
(a) Model 1


(b) Model 2

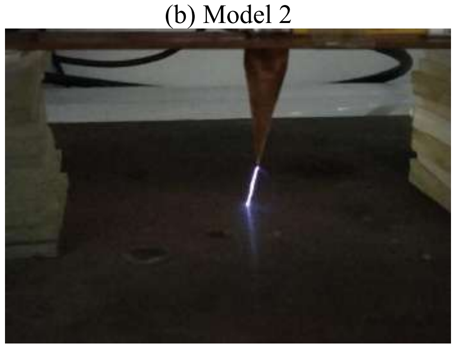
(c) Model 3

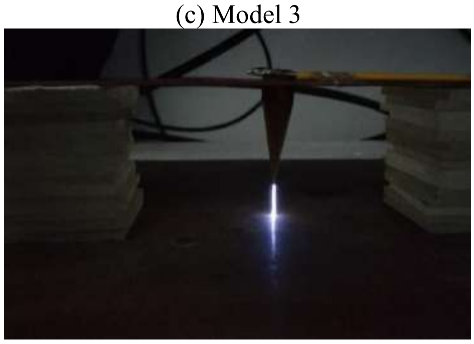
(d) Model 4

Figure 6. The corona discharge photos of four electrode models

The (I-V) characteristic graph of the corona discharge case for the CEM-P configuration model was made using the Python Graphical User Interface (*GUI*) Programming [25]. The graph is obtained from the numerical calculations in Eq. (16) for the appropriate value of k. Besides describing graphs and calculating the proper k value, this GUI program can also calculate graph error values consisting of standard deviation (*SD*) and t-tests. The explanation of the t-test and *SD* values in this study is:

• The t-test value is a parameter that shows the degree of correspondence between the numerical simulation curve and the research data [25] for the (I-V) characteristic graph. The smaller the t-test value (which should be less than 0.05), the higher the level of conformity/accuracy between the two functions (simulation curve and research data).

• The value of *SD* (standard deviation) σ_I in the GUI program for this research comes from the distribution of the measured data up to order of power two of functions *V* in the polynomials [26]:

$$I = a_1 + a_2 V + a_3 V^2 \quad ; \quad \sigma_I = \sqrt{\frac{\sum_j \left(I - A_1 - A_2 V_j - A_3 V_j^2\right)^2}{(N-2)}}, \tag{17}$$

where, a_1, a_2, and a_3 are constants that can be calculated. The values of A_1, A_2, and A_3 [26] are obtained through Eq. (18):

$$\begin{bmatrix} N & \sum V_j & \sum V_j^2 \\ \sum V_j & \sum V_j^2 & \sum V_j^3 \\ \sum V_j^2 & \sum V_j^3 & \sum V_j^4 \end{bmatrix} \begin{bmatrix} A_1 \\ A_2 \\ A_3 \end{bmatrix} = \begin{bmatrix} \sum I_j \\ \sum V_j I_j \\ \sum V_j^2 I_j \end{bmatrix} \tag{18}$$

The *SD* formula in Eq. (17) is compatible with formula (16) to determine the degree of compatibility between the numerical simulation formula and the research data.

Two (*I-V*) characteristic graphs for each model (with the same angle of θ) are obtained from two variations of *c* values. The *k* factor value, *SD* value, and t-test value are also included in each graph. The display of the (*I-V*) characteristic graphs for the four-electrode models is presented in Figure 7.

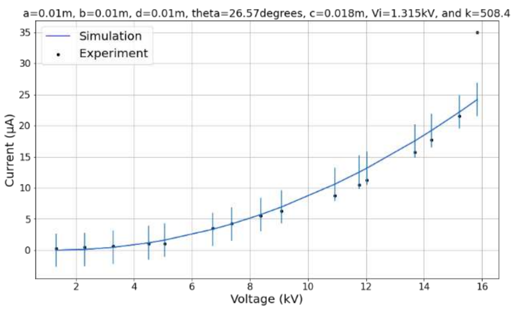

(a)

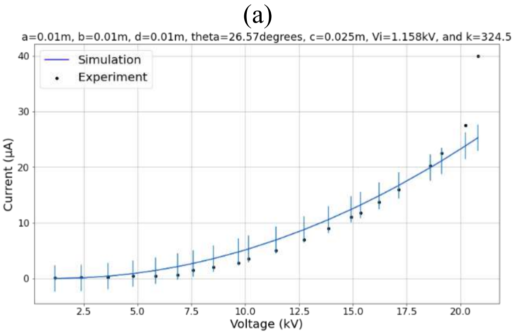

(b)

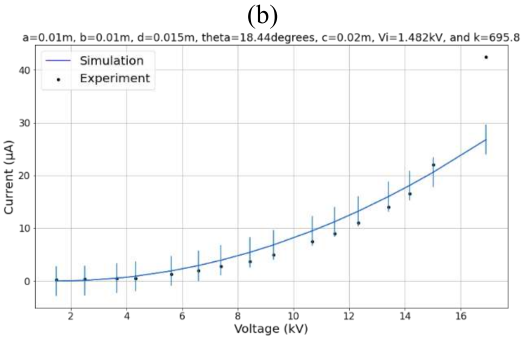

(c)

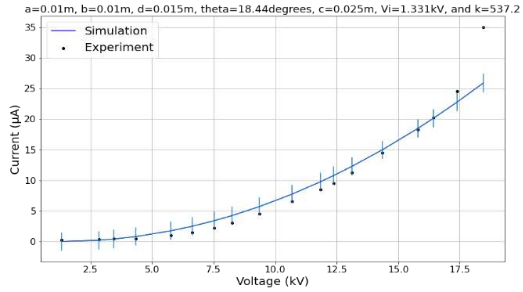

(d)

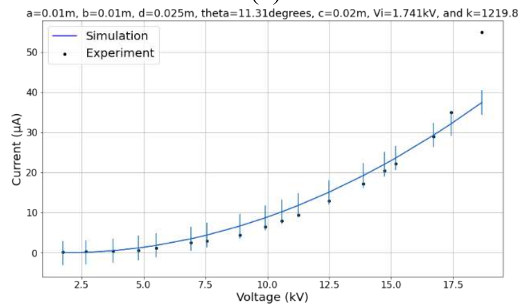

(e)

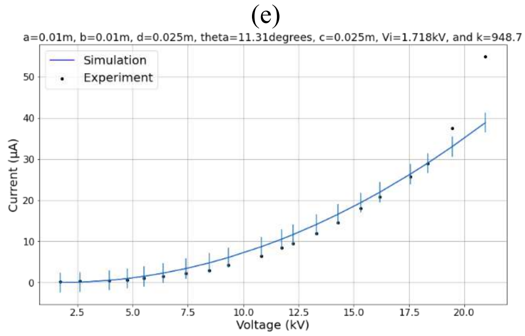

(f)

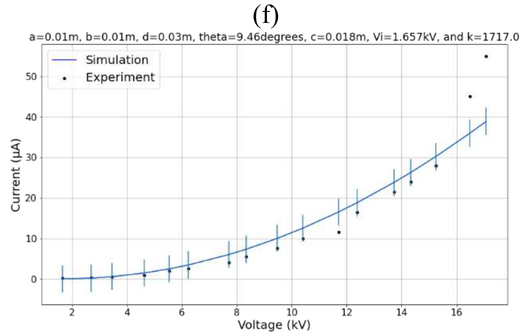

(g)

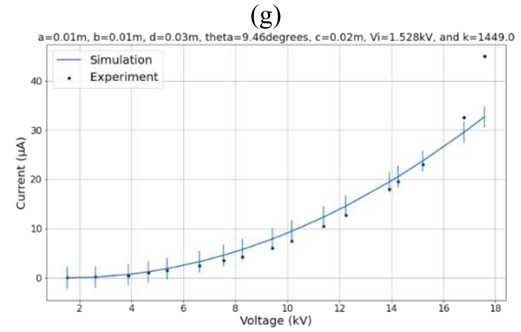

(h)

Figure 7. The (*I-V*) Characteristic graph of the corona plasma discharges with the CEM-P configuration at various angles θ and different distances *c*, (a) and (b) are graphs for Model 1 of distances *c*=0.018 m and *c*=0.025 m, respectively (c) and (d) are graphs for Model 2 of distances *c*=0.020 m and *c*=0.025 m, respectively, (e) and (f) are graphs for Model 3 of distances *c*=0.020 m and *c*=0.025 m, respectively, (g) and (h) are graphs for Model 4 of distances *c* = 0.018 m and *c*=0.020 m, respectively

The calculation data for the factor *k*, the *SD* values, and the t-test values in Figure 7 are written in Table 3. On each graph in Figure 7, short vertical lines (*SVL*) connect the data points with the simulation curves. In Figure 7 also, we can manually calculate the values of the number of data points (*NDP*) and the number of tangent points (*NTP*) which is defined as the number of data points that intersect the simulation curve through the *SVL*, and the percentage of tangent points (*PTP*) which is the ratio between *NDP* to *NTP*. A list of the values of *NDP*, *NTP*, and *PTP* is also presented in Table 3.

Table 3. Values of the factor *k, SD,* and t-test of the (*I-V*) characteristic functions graphs in Figure 7 for different values of *c*

Model		c (m)	k	SD	t-test	Number of tangent points	Number of data points	Percentage of tangent points
1	θ=26,57°	0.018	508.4	2.6831	0.0468	15	16	93.75%
		0.025	324.5	2.3665	0.0399	19	21	90.48%
2	θ=18.44°	0.020	695.8	2.8317	0.0496	15	16	93.75%
		0.025	537.2	1.4871	0.0448	17	18	94.44%
3	θ=11.31°	0.020	1219.8	3.0485	0.0475	17	18	94.44%
		0.025	948.7	2.4341	0.0482	18	20	90.00%
4	θ=9.46°	0.018	1717.0	3.3546	0.0481	14	17	82.35%
		0.020	1449.0	2.1841	0.0500	15	17	88.24%

From the (*I-V*) characteristic graph in Figure 7 and from Table 3, which shows the *SD* and the t-test values, as well as from the calculation of the factor *k* based on the variation of the distance between the two electrodes of the *c*, turned out to produce several trends in cases that arise in this study including:

i. The fit between the line simulated curves with the experimental data points occurs in the low-current portion of the corona plasma discharge.
ii. The *SD* values are relatively large for all graphs, whose values vary between 1.4871-3.3546, and the t-test values for almost all graphs are still below 0.5 (except for the case of θ=9.46° with *c*=0.020). Similarly, the whole graph has relatively large *PTP* values (82.35% - 94.44%).
iii. For all variations of the electrodes model, we will see that if the models have a sharper half- acute angle θ, the values of the factor *k* will be greater.
iv. For the case of the same electrodes model, we get research results that the farther the distance between the two electrodes (the greater the value *c*), the values of the factor *k* will be smaller.

5. DISCUSSION

From various research results on the (*I-V*) characteristics of corona discharge such as [5, 6, 19] etc., the level of match between corona current vs voltage occurred only in the case of low current, not in the case of the sharply increasing current. So this study is the same as many cases of previous studies on the (*I-V*) characteristics of corona discharge.

We concluded that the degree of correspondence between the data points and the simulation curve (representing numerical calculation on the Eq. (16)) is relatively high. The statement is based on several measurable categories (use *GUI* programming result) for all graphs in Figure 7, such as:

i. The values of PTP are relatively large (between 82.35% - 94.44%).
ii. The values of the t-test are almost less than 0.5.
iii. Although some factors do not support it, the *SD* values are relatively large (between 1.4871 - 3.3546). The large enough *SD* values mean that the *SVL* sizes are quite long [15].

The best graph in Figure 7 is a combination of low *SD* and t-test values and has a high PTP value, which is suitable for the case of Model 2 (θ=18.44°) at *c*=0.025 m.

The conclusion from the research results [16] is that the sharper the tip of the active electrode used in the case of corona discharge, the larger and brighter the flow of corona current will be. The factor *k* in this study is a multiplier factor of the corona current magnitude that emerges from the lower end of the sharp surface of the active electrode. The concept of the factor *k* is clear based on the research [16]. We conclude that the sharper the tip of the active electrode, the greater the value of the factor *k*.

Another result obtained in this study (in Table 3) is that the greater the value of *c*, the smaller the value of the factor *k*. Figure 6 shows that this study's largest corona current is derived from the corona current coming out of the lower end of the active electrode or out of point *D* in Figure 2 (a). The capacitance value of the area (ΔEDC) = 2×area (Δ *FDC*) in Figure 2, which contains the current multiplier factor *k*, is part of the formulation of Eq. (8) is:

$$C_{EDC} = \lim_{k \to \text{big value}} k \frac{\varepsilon_0 bc}{d}\left[\ln|c| - 1\right]. \tag{19}$$

The values of b and d in Eq. (19) are constant on the change variation of distance c. Suppose it is considered that the C_{EDC} capacitance value is close to a constant on the difference in the value of *c*. In Eq. (19), there is a tendency if the value of c is getting bigger it will make the value of k tend to be smaller, or vice versa if the value of *c* is getting smaller, then the value of *k* tends to be bigger.

6. CONCLUSIONS

The calculation results of the values of the fitting factor *k*, *SD* errors, and t-test in Table 3 for the (*I-V*) characteristics case conclude that there is a high degree of conformity between numerical calculations and research data. This high degree of the agreement indicates that Eq. (16) is suitable as a general formulation of the (*I-V*) characteristics for the corona plasma discharge model with the Chisel Eye and Midpoint-Plane (CEM-P) electrode configuration. However, there may be deviations from the research results stemming from the negligence of the researchers' observations, the imprecision and asymmetry of the shape and position of the active electrode installation, energy leakage, and other problems that may occur from the physical properties of the corona discharge case.

ACKNOWLEDGMENT

The financials in this work get supported by non-tax revenue (PNBP), Diponegoro University, Semarang, Indonesia, with the schema of International Publication Research (RPI) in 2022. (No. 569-100/UN7.D2/PP/VII/2022).

REFERENCES

[1] Stambouli, A.B., Benallal, R., Oudini, N., Mesli, S.M., Tadjine, R. (2017). Control of dual frequency capacitively coupled plasma via blocking capacitor and phase angle. European Physical Journal Applied Physics, 80: 10802. https://doi.org/10.1051/epjap/2017170180

[2] Tabares, F.L., Junkar, I. (2021). Cold plasma systems and their application in surface treatments for medicine. Molecules, 26(7). https://doi.org/10.3390/molecules26071903

[3] Saikia, P., Bhuyan, H., Escalona, M., Favre, M., Wyndham, E., Maze, J., Schulze, J. (2018). Study of dual radio frequency capacitively coupled plasma: An analytical treatment matched to an experiment. Plasma Sources Science and Technology, 27(1): 015014. https://doi.org/10.1088/1361-6595/aaa565

[4] Townsend, J.S. (1914). The potentials requires to maintain currents between coaxial cylinders. The London, Edinburgh, and Dublin Philosophical Magazine and Journal of Science, 28: 83-90. https://doi.org/10.1080/14786440708635186

[5] Robinson, M. (1967). The corona threshold for coaxial cylinders in air at high pressures. IEEE Transactions on Power Apparatus and Systems, Pas-86: 185-189. https://doi.org/10.1109/TPAS.1967.291834

[6] Zheng, Y., Zhang, B., He, J. (2015). Current-voltage characteristics of dc corona discharges in air between coaxial cylinders. Physics of Plasmas, 22: 023501. https://doi.org/10.1063/1.4907234

[7] Guan, Y., Vaddi, R.S., Aliseda, A., Novosselov, I. (2018). Analytical model of electrohydrodynamic flow in corona discharge. Physics of Plasmas, 25: 083507. https://doi.org/10.1063/1.5029403

[8] Robinson, M. (1961). Movement of air in the electric wind of the corona discharge. Transactions of the American Institute of Electrical Engineers, 80: 143-150. https://doi.org/10.1109/TCE.1961.6373091

[9] Abe, H., Yoneda, M., Fujiwara, N. (2008). Developments of plasma etching technology for fabricating semiconductor devices. Japanese Journal of Applied Physics, 47(3): 1435-1455. https://doi.org/10.1143/JJAP.47.1435

[10] Vidaurre, E.F.C., Achete, C.A., Gallo, F., Garciam D., Simão, R.A., Habert, A.C. (2002). Surface modification of polymeric materials by plasma treatment. Materials Research, 5(1): 37-41. https://doi.org/10.1590/S1516-14392002000100006

[11] Anders, A. (2005). Plasma and ion sources in large area coatings: A review. Surface and Coatings Technology, 200: 1893-1906. https://doi.org/10.1016/j.surfcoat.2005.08.018

[12] Schmidt, H., Sansonnens, L., Howling, A.A., Hollenstein, C., Elyaakoubi, M., Schmitt, J.P.M. (2004). Improving plasma uniformity using lens-shaped electrodes in a large area very high frequency reactor. Journal of Applied Physics, 95: 4559-4564. https://doi.org/10.1063/1.1690096

[13] Bouremel, Y., Li, J.M., Zhao, Z., Debiasi, M. (2013). Effects of AC dielectric barrier discharge plasma actuator location on flow separation and airfoil performance. Procedia Engineering, 67: 270-278. https://doi.org/10.1016/j.proeng.2013.12.026

[14] Wardaya, A.Y., Muhlisin, Z., Hudi, A., Suseno, J.E., Nur, M., Kinandana, A.W., Windarta, J. (2020). A study of line-plane configuration in the Corona discharge theory. The European Physical Journal Applied Physics, 89: 30801. https://doi.org/10.1051/epjap/2020200011

[15] Wardaya, A.Y., Muhlisin, Z., Suseno, J.E., Nur, M., Triadyaksa, P., Khumaeni, A., Sarwoko, E.A., Windarta, J., Hadi, S. (2022). The current-voltage characteristics for electrode geometry model of positive DC corona discharge in air. Gazi University Journal of Science, 35: 1140-1150. https://doi.org/10.35378/gujs.885345

[16] Dobranszky, J., Bernath, A., Marton, H.Z. (2008). Characterisation of the plasma shape of the TIG welding arc. International Journal of Microstructure and Materials Properties, 3(1): 126-140. https://doi.org/10.1504/IJMMP.2008.016949

[17] Hua, X., Li, T., Wu, C., Zhou, D., Fan, G., Li, X., Cong, K., Yan, Z., Wu, Z. (2022). Novel physical treatments (Pulsed light and cold plasma) improve the quality of postharvest apricots after long-distance simulated transportation. Postharvest Biology and Technology, 194(159): 112098. https://doi.org/10.1016/j.postharvbio.2022.112098

[18] Bora, J., Khan, T., Mahnot, N.K. (2022). Cold plasma treatment concerning quality and safety of food: A Review. Current Research in Nutrition and Food Science, 10(2): 427-446. https://doi.org/10.12944/CRNFSJ.10.2.3

[19] Moreau, E., Benard, N., Alicalapa, F., Douyere, A. (2015). Electrohydrodynamic force produced by a corona discharge between a wire active electrode and several cylinder electrodes-Application to electric propulsion. Journal of Electrostatics, 76: 194-200. https://doi.org/10.1016/j.elstat.2015.05.025

[20] Giubbilini, P. (1988). The current-voltage characteristics of point-to-ring corona. Journal of Applied Physics, 64: 3730-3732. https://doi.org/ 10.1063/1.341368

[21] Yamada, K. (2004). An empirical formula for negative corona discharge current in point-grid electrode geometry. Journal of Applied Physics, 96: 2472. https://doi.org/10.1063/1.1775301

[22] Ferreira, G.F.L., Oliveira Jr., O.N., Giacometti, J.A. (1986). Point-to-plane corona: Current-voltage characteristics for positive and negative polarity with evidence of an electronic component. Journal of Applied Physics, 59: 3045-3049. https://doi.org/10.1063/1.336926

[23] Katuri, R., Gorantla, S. (2018). Analysis of math function based controller for a smooth transition between battery and ultracapacitor. Mathematical Modelling of

Engineering Problems, 5(4): 386-394. https://doi.org/10.18280/mmep.050416
[24] Sreedhar, T., Ramana, N.V. (2020). Impact of distribution network reconfiguration and optimal capacitor placement under wheeling transactions. Mathematical Modelling of Engineering Problems, 7(1): 113-118. https://doi.org/10.18280/mmep.070114
[25] Boslaugh, S. (2012). Statistics in a Nutshell: A Desktop Quick Reference. Second Edition. O'Reilly Media, Inc., USA. ISBN-13: 978-1449316822, ISBN-10: 1449316824.
[26] Taylor, J.R. (1997). An Introduction to Error Analysis, the Study of Uncertainties in Physical Measurements. Second Edition. University Science Books, USA. ISBN 0-935702-42-3.

NOMENCLATURE

I	Electric current, Ampere
V	Voltage, Volt
a, b	width and length of the rectangular plate, meters
d	width of the triangular plate, meters
c	distance between the lower end of electrode active and electrode passive, meters
SD	Standard Deviation
k, k_1	shape sharpness factor (dimensionless)
C	constant (the geometric function)
C_1, C_2, ... , C_{tot}	Capacitance, Coulomb/Volt
q	electrical charge, Coulomb
E	electric field, N/C
ΔA	area, m^2

Greek symbols

θ	half- acute angle, radian
δ	plate thickness, meters
σ	standard deviation
ε_0	vacuum permittivity, 8.854×10^{-12} F m^{-1}
μ_0	vacuum permeability, $4\pi\times10^{-7}$ Hm^{-1}
ϕ	acute angle at the end of the CCP electrode emitting plasma flow

Subscripts

i	threshold/initial
j	sum index
tot	total
CBI CDJ JDK IBM KGL LGM	triangular electrodes indexes name